

**Entwicklung und Anwendung neuer analytischer  
Methoden zur schnellen Bestimmung von kurzlebigen  
Radiumisotopen und Radon im grundwasser-  
beeinflussten Milieu der Ostsee**



Dissertation  
zur Erlangung des Doktorgrades  
der Mathematisch-Naturwissenschaftlichen Fakultät  
der Christian-Albrechts-Universität  
zu Kiel

vorgelegt von

**Stefan Purkl**

Kiel 2002

Referent: \_\_\_\_\_

Korreferent: \_\_\_\_\_

Tag der mündlichen Prüfung: \_\_\_\_\_

Zum Druck genehmigt: Kiel, den \_\_\_\_\_

Der Dekan

Hiermit erkläre ich an Eides statt, dass die vorliegende Abhandlung, abgesehen der Beratung durch meine akademischen Lehrer, nach Inhalt und Form meine eigene Arbeit darstellt.

---

Stefan Purkl

## Inhaltsverzeichnis

<b>Einleitung und Zielsetzung.....</b>	<b>1</b>
EINLEITUNG.....	1
ZIELSETZUNG UND KONZEPTION.....	4
LITERATUR.....	5
<b>Kapitel I: Neue analytische Methoden Teil 1.....</b>	<b>8</b>
<b>Solid-Phase Extraction Using Empore™ Radium Rad Disks to Separate Radium from Thorium</b>	
ABSTRACT.....	9
INTRODUCTION.....	9
EXPERIMENTAL SETUP.....	11
Instrumentation.....	11
Tracers and Reference Materials.....	12
Chemical Separation Procedures.....	13
Spectrometry.....	15
RESULTS AND DISCUSSION.....	20
Separation of Ra from Th.....	20
Intercomparison of Ra Measurements.....	22
SUMMARY AND CONCLUSIONS.....	23
REFERENCES .....	24
<b>Kapitel II. Neue analytische Methoden Teil 2.....</b>	<b>25</b>
<b>A Rapid Method for a-Spectrometric Analysis of Radium Isotopes in Natural Waters Using Ion-Selective Membrane Technology</b>	
ABSTRACT.....	26
INTRODUCTION.....	26
CHEMICAL PROCEDURES.....	27
Flow Diagram for Sample Preparation.....	27
Procedure for Ion-Selective Extraction of Ra via Membrane Technology.....	27
Low Pressure Column-Chromatography.....	28
Electrodeposition from Ethanolic Solution.....	29
α-Spectrometric Analysis .....	30
RESULTS AND DISCUSSION.....	33
Ra Determination Using a $^{229}\text{Th}/^{225}\text{Ra}$ Standard Solution.....	33
Ra Stripping Using Adapted EDTA-Mixtures.....	35
Separation of Disturbing Matrix Composition Using Low Pressure Column-Chromatography....	36
Production of Homogenous α-Sources in Presence of Ba .....	36
High Rn Retention in Thin Deposits.....	38
SUMMARY .....	43
REFERENCES .....	44

---

<b>Kapitel III. Radium und Radon als natürliche Tracer .....</b>	<b>46</b>
<b>Determination of Radium Isotopes and <math>^{222}\text{Rn}</math> in a Groundwater Affected</b>	
<b>Coastal Area of the Baltic Sea and the Underlying Sub-Sea Floor Aquifer</b>	
ABSTRACT.....	47
INTRODUCTION.....	47
LOCATION AND SAMPLING.....	50
SIMULTANEOUS DETERMINATION OF Ra ISOTOPES.....	52
$^{222}\text{Rn}$ MEASUREMENT USING A PORTABLE LS-COUNTER.....	53
Principle.....	53
Analytical Procedure.....	54
RESULTS.....	55
ANALYSIS OF SMALL-SCALE COASTAL MIXING PROCESSES .....	58
Modelling of Vertical Dispersive Mixing.....	58
Modelling of Horizontal Dispersive Mixing .....	61
Simple Two-Box Model for Groundwater Discharge.....	63
SUMMARY AND CONCLUSION.....	65
REFERENCES .....	66
<b>Kapitel IV. Neuanmeldung zum Gebrauchsmuster .....</b>	<b>68</b>
<b>Vorrichtung zur Extraktion von Stoffen von einer Membran</b>	
<b>Zusammenfassung .....</b>	<b>77</b>
<b>Anhang .....</b>	<b>78</b>
$\alpha$ -SPEKTROMETRIE.....	78
BERECHNUNG VON MITTELWERTEN UND UNSICHERHEITEN .....	85
URKUNDE ÜBER DIE EINTRAGUNG DES GEBRAUCHSMUSTERS.....	88
LITERATUR .....	89

# Einleitung und Zielsetzung

## 1.1. Einleitung

Weltweit sind in verschiedenen Küstenregionen (Nordamerika [1], Mittelamerika [2] Australien [3], Indien [4], Europa [5]) submarine Grundwasseraustritte beobachtet worden. Im Zusammenhang mit Karstsystemen kennt man gut charakterisierte submarinen Quellen [6], während an den Küsten von Nord- und Ostsee teilweise fokussierte [7], aber auch diffuse Austritte beobachtet werden. Trotz geringer Flussraten kann auch dieser diffuse Austritt, integriert über die Fläche, Auswirkungen auf das küstennahe Milieu haben. Große Mengen an Nährstoffen, Metallen, organischen Verbindungen und anorganischem Kohlenstoff können so in die Küstenzone eingetragen werden [8]. Kalkulationen, dass der direkte submarine Eintrag 40 % [9] des Flusswassereintrags in den Ozean beträgt, sind möglicherweise zu hoch [10, 11]. Autoren wie Zektser and Loaiciga [12] berichten von Einträgen in der Größenordnung von weniger als 10 %. Auch wenn der Einfluss auf den Wasserhaushalt nicht die herausragende Gewichtung besitzen sollte, so werden in stark besiedelten Küstenregionen etwaige Schadstoffe über sehr kurze Transportwege eingetragen und führen damit unmittelbar zur Beeinträchtigung der Küstenzone.

Bollinger und Moore [13] und Cable et al. [14] haben gezeigt, dass Radiumisotope ( $^{223}\text{Ra}$ ,  $^{224}\text{Ra}$ ,  $^{226}\text{Ra}$ ,  $^{228}\text{Ra}$ ) und Radon ( $^{222}\text{Rn}$ ) aufgrund ihrer Anreicherung im Grundwasser grundsätzlich als natürliche Tracer geeignet sind und zur Identifizierung und Quantifizierung von Fluidaustritten herangezogen werden können. Der bisherige Mangel an schnellen und sensitiven Analyseverfahren bedingt aber, dass Parameter, die Mobilität und Transport der verwendeten Radionuklide bestimmen und damit eine präzisere Quantifizierung erlauben, nicht ausreichend verstanden sind. Um küstennahe Mischungsprozesse von Grund- und Meerwasser im Bereich von  $10^0$  von  $10^3 \text{ m}$  zu untersuchen benötigt man möglichst kurzlebige Nuklide mit Halbwertszeiten ( $T_{1/2}$ ) in der Größenordnung von Tagen [15].

Die Analyse dieser Prozesse mit Radiumisotopen und  $^{222}\text{Rn}$  als Tracer, stellt vor allem im Falle der kurzlebigen Radiumisotope  $^{223}\text{Ra}$  ( $T_{1/2} = 11,43 \text{ d}$ ) und  $^{224}\text{Ra}$  ( $T_{1/2} = 3,66 \text{ d}$ ) hohe Anforderungen an die verwendete Analytik. Für die Radiumbestimmung muss der Analyt zunächst aufkonzentriert werden. Das etablierte Anreicherungsverfahren über Mangandioxidfilter wird seit den 70er Jahren verwendet [16], ist aber sehr unspezifisch für Radium. Neben Radium wird unter anderem auch Thorium an die sorptive Oberfläche gebunden und führt, je länger der Zeitraum zwischen Probennahme und Messung ist, durch die Nachbildung kurzlebiger Zerfallsprodukte zu großen Messunsicherheiten. Die Bestimmung der Radiumisotope erfolgte dann zumeist  $\gamma$ -spektrometrisch [17]. Aufgrund der geringen Empfindlichkeit, (hoher Nulleffekt durch terrestrische und kosmische Strahlung) musste der Analyt allerdings vorher aus großen Probevolumina angereichert werden. So wurden bei den ersten Messungen von  $^{224}\text{Ra}$  in den Buchten von Delaware und Winyah [18] Mengen von ca. 500 l verwendet.

Die Bestimmung von kurzlebigen Radiumisotopen mittels Emanationstechnik [19], über die gasförmigen Zerfallsprodukte  $^{219}\text{Rn}$  und  $^{220}\text{Rn}$  stellt eine wesentliche messtechnische Verbesserung dar. Der Einbau elektronischer Komponenten [20] in das System berücksichtigt die Zerfallscharakteristik von  $^{220}\text{Rn}$  und  $^{219}\text{Rn}$  und ermöglicht so eine Unterscheidung der Mutternuklide  $^{224}\text{Ra}$  und  $^{223}\text{Ra}$ . Auch die Nulleffektzählraten der verwendeten  $\alpha$ -Szintillationszelle von  $10^{-2}$  bis  $10^{-3}$  Ereignisse pro Sekunde reduzieren sich, die Nachweisgrenzen sinken dadurch entsprechend. Das System muss allerdings durch Standardmessungen immer wieder kalibriert und die Messbedingungen für jede Messung gleichgehalten werden. Da während der Bestimmung Helium als Trägergas durch den Manganfilter zirkuliert und eine Änderungen im Feuchtigkeitsgehalt [21] bewirkt, ist die Einstellung dieser Standardbedingungen jedoch schwierig. Um die Gesamteffektivität der Methode (Anreicherung und Messung) zu bestimmen, müssen an einer Probe Mehrfachmessungen der langlebigen Radiumisotope durchgeführt werden. Der zeitliche Aufwand erhöht sich. Die Verwendung eines internen Standards ist nicht möglich.

Es gibt methodische Ansätze alle vier Radiumisotope simultan über energieaufgelöste  $\alpha$ -Spektrometrie zu bestimmen [22, 23]. Durch die Verwendung eines internen Standards, hier  $^{225}\text{Ra}$ , entfallen Mehrfachmessungen und Unsicherheiten bei der Kalibrierung des Messsystems. Außerdem stellt die  $\alpha$ -Spektrometrie aufgrund des geringen Untergrunds ( $7 \cdot 10^{-5}$  Ereignisse pro Sekunde im Energiebereich 3-8 MeV) eine besonders empfindliche Messmethode dar und erlaubt bei Messzeiten von 5000 min ein Detektionslimit von 0,2 mBq [24]. Aufwendige nasschemische Anreicherungsverfahren und die Vielzahl der benötigten Aufarbeitungsschritte

führen allerdings dazu, dass diese Methode für die Bestimmung der kurzlebigen Radiumisotope in küstennahem Meerwasser bis jetzt kaum Anwendung findet.

Entwicklungen der 90er Jahre auf dem Gebiet der Molekülerkennungstechnologie eröffnen nun neue Wege, Radium, trotz hoher Salzfracht, einfach, effizient und sehr spezifisch anzureichern [25]. Mittels ionenselektiver Membrane kann der Analyt durch enorm schnelle Extraktionskinetik mit 400 bis 4000 höheren Durchflußraten [26] aus salpetersaurer Lösung extrahiert werden. Diese neu entwickelten Membrane bestehen aus einer Teflonmatrix, auf der Kronen-Ether kovalent gebunden aufgebracht sind [27]. Kronen-Ether sind 20-25 Atome enthaltende Makrozyklen, die durch Käfiggröße und Substituenten auf  $\text{Ra}^{2+}$  als Analyten abgestimmt sind.

Die weitere Analytik kann so ausgerichtet werden, dass eine Messung des Analyten über energieaufgelöste  $\alpha$ -Spektrometrie schnell und einfach durchführbar sein sollte. Durch die Kombination der radiumselektiven Membrantechnik mit der Sensitivität der  $\alpha$ -Spektrometrie wird das Probevolumen minimiert und der apparative und zeitliche Aufwand reduziert. Neben den geochemischen Vorteilen von Radium als Tracer für submarine Grundwasseraustritte, ergibt sich so die geforderte einfache, schnelle und präzise Messbarkeit der Radiumisotope.

## 1.2. Zielsetzung und Konzeption

Der Schwerpunkt dieser Arbeit liegt in der Entwicklung eines neuen  $\alpha$ -spektrometrischen Verfahrens zur simultanen, sensitiven und schnellen Bestimmung von Radiumisotopen. Zusammen mit einer optimierten Technik zur Messung von  $^{222}\text{Rn}$  soll in Anwendung der Analyseverfahren in einem vom submarinen Grundwassereintrag beeinflussten Küstengebiet deren Leistungsfähigkeit aufgezeigt werden. Durch die Etablierung einer praktikablen Methodik soll diese Arbeit einen Beitrag zum Verständnis über den Transport der verwendeten natürlichen Tracer leisten.

### Kapitel I: Neue analytische Methoden Teil 1

Im Rahmen dieser Arbeit sollen die Untersuchungen zeigen, ob ionenselektive Membrane eine effektive Anreicherung von Radium aus wässrigen Medien ermöglichen und die gleichzeitige Abtrennung störender Matrixkomponenten erlauben. Die Bestimmung von Trennungsfaktoren für Thorium gestattet eine Einschätzung, ob sich die Verwendung dieser Extraktionstechnik für die  $\alpha$ -spektrometrische Bestimmung von Radium eignet.

### Kapitel II: Neue analytische Methoden Teil 2

Für die  $\alpha$ -spektrometrische Bestimmung von kurzlebigen Radiumisotopen müssen die entsprechenden Analyseschritte so optimiert werden, dass die Aufbereitung der wässrigen Proben innerhalb weniger Stunden erfolgen kann. Vor allem für die Radiumbestimmung in Proben mit hoher Salzfracht ist die Verwendung eines internen Standards zu fordern. Für die Radiumextraktion über ionenselektive Membrane wird daher erstmals mit  $^{225}\text{Ra}$  als interner Standard gearbeitet und führt durch Reduktion zeitaufwendiger Separationsmethoden und das Wegfallen von externen Kalibrierungen zu dem geforderten hohen Probendurchsatz.

### Kapitel III: Radium und Radon als natürliche Tracer

Konzentrationsbestimmungen der Tracer  $^{223}\text{Ra}$ ,  $^{224}\text{Ra}$ ,  $^{226}\text{Ra}$ ,  $^{228}\text{Ra}$  und  $^{222}\text{Rn}$  in der Wassersäule der Eckernförder Bucht (Westliche Ostsee) und in dem einflussnehmenden Grundwasserleiter sollen Aufschluss über das Verhalten und die Bewegung der Tracer geben. Über einfache Ansätze zur Modellierung der Felddaten kann so ein besseres Verständnis für die Parameter gewonnen werden, die den Transport der Tracer steuern.

### Kapitel IV: Neuanmeldung zum Gebrauchsmuster

Die Anmeldung zum Gebrauchsmuster sollen die technischen Anforderungen, Eigenschaften und Ausführung der verwendeten Apparatur zur Extraktion von Radium aus wässrigen Medien dokumentieren. Die gewerbliche Verfügbarkeit ist Voraussetzung für die Etablierung einer neuen Methodik.

## Literatur

- [1] J. M. Krest, W. S. Moore, Rama;  $^{226}\text{Ra}$  and  $^{228}\text{Ra}$  in the mixing zones of the Mississippi and Atchafalaya rivers: indicators of groundwater input; *Marine Chemistry*; **64** (1999) 129-152.
- [2] J. E. Cable, W. C. Burnett, J. P. Chanton, G. L. Weatherly; Estimating groundwater discharge into the northeastern Gulf of Mexico using radon-222; *Earth and Planetary Science Letters*; **144** (1996), 591-604.
- [3] R. E. Johannes, C. J. Hearn; The effect of submarine groundwater discharge on nutrient and salinity regimes in a coastal lagoon off Perth, Western Australia; *Estuarine, Coastal and Shelf Science*; **21** (1985) 789-800.
- [4] W. S. Moore; High fluxes of radium and barium from the mouth of the Ganges-Brahmaputra River during low river discharge suggest a large groundwater source; *Earth and Planetary Science Letters*; **150** (1997) 141-150.
- [5] I. Bussmann, E. Suess; Groundwater seepage in Eckernförde Bay (Western Baltic Sea): effect on methane and salinity distribution of the water column; *Continental Shelf Research*; **18** (1998) 1795-1806.
- [6] F. A. Kohout, G. W. Leve, F.T. Manheim; Red Snapper Sink and ground water flow off Shore of southeastern Florida; In Proceedings of the 12th International Congress: Karst Hydrology; International Association of Geohydrological Memoirs; **12** (1977) 193.
- [7] A. Kandriche, F. Werner; Freshwater-induced pockmarks in Bay of Eckernförde, Western Baltic; *Proceedings of the Third Marine Geological Conference "The Baltic"*; (1995) 155-164.
- [8] T. M. Church; An underground route for the water cycle; *Nature*; **380** 579-580.
- [9] W. S. Moore; Large groundwater inputs to coastal waters revealed by  $^{226}\text{Ra}$  enrichments; *Nature*; **380** (1996) 612-614.
- [10] P. L. Younger, W. S. Moore, T. M. Church; Submarine groundwater discharge: discussion and reply; *Nature*; **382** (1996) 121-122.
- [11] L. Li, D. A. Barry, F. Stagnitti, J. Y. Parlange; Submarine groundwater discharge and associated chemical input to a coastal sea; *Water Resources Research*; **35** (1999) 3253-3259.

- [12] I. S. Zektser, H. A. Loaiciga; Ground water fluxes in the global hydrologic cycle: past, present and future; *Journal of Hydrology*; **144** (1993) 405-427.
- [13] Rama, W. S. Moore; Using the radium quartet for evaluating groundwater input and water exchange in salt marshes. *Geochimica et Cosmochimica Acta*, **60** (1996) 4645-4652.
- [14] J. E. Cable, G. C. Bugna, W. C. Burnett, J. P. Chanton; Application of  $^{222}\text{Rn}$  and  $\text{CH}_4$  for assessment of groundwater discharge to the coastal ocean; *Limnology and Oceanography*; **41** (1996) 1347-1353.
- [15] W. S. Moore; Ages of continental shelf waters determined from  $^{223}\text{Ra}$  and  $^{224}\text{Ra}$ ; *Journal of Geophysical Research*; **105** (2000) 22117-22122.
- [16] W. S. Moore; D. F. Reid; Extraction of radium from natural waters using manganese-impregnated acrylic fibers; *Journal of Geophysical Research*; **78** (1973) 8880-8886.
- [17] R. J., Elsinger, P. T. King, W. S. Moore;  $^{224}\text{Ra}$  in natural waters measured by  $\gamma$ -ray spectrometry; *Analytica Chemica Acta*; **144** (1982) 227-281.
- [18] R. J. Elsinger, W. S. Moore;  $^{224}\text{Ra}$ ,  $^{228}\text{Ra}$ ,  $^{226}\text{Ra}$  in Winyah Bay and Delaware Bay; *Earth and Planetary Science Letters*; **64** (1983), 430-436.
- [19] Rama, J. F. Todd, J. L. Butts, W. S. Moore; A new method for the rapid measurement of  $^{224}\text{Ra}$  in natural waters; *Marine Chemistry*; **22** (1987) 43-54.
- [20] W. S. Moore, R. Arnold; Measurement of  $^{223}\text{Ra}$  and  $^{224}\text{Ra}$  in coastal waters using a delayed coincidence counter; *Journal of Geophysical Research*; **101** (1996) 1321-1329.
- [21] Y. Sun, T. Torgersen; The effects of water content and Mn-fiber surface conditions on  $^{224}\text{Ra}$  measurement by  $^{220}\text{Rn}$  emanation; *Marine Chemistry*; **62** (1998) 299-306.
- [22] S. A. Short; Measurement of all Radium isotopes at environmental levels on a single electrodeposited source; *Nuclear Instruments and Methods in Physics Research*; **17** (1986) 540-544.
- [23] G. J. Hancock, P. Martin; Determination of Ra in environmental samples by  $\alpha$ -particle spectrometry; *International Journal of Applied Radiation and Isotopes*; **42** (1991) 63-69.
- [24] M. Yamamoto, K. Komura; Determination of low-level  $^{226}\text{Ra}$  in environmental water samples by alpha-ray Spectrometry; *Radiochimica Acta*; **46** (1980) 137-142.

- [25] G. L. Goken, R. L. Bruening, K. E. Krakowiak, R. M. Izatt; In Metal-ion separation and preconcentration: Progress and opportunities; A.H, Bond, M.L, Dietz, R.D, Rogers (Eds.); ACS Symposium Series 716; Washington, D.C. (1999) pp. 251-259.
- [26] R. M. Izatt, J. S. Bradshaw, R. L. Bruening; Accomplishment of difficult chemical separations using solid phase extraction; Pure & Applied Chemistry; **68** (1996) 1237-1241.
- [27] A. Durecova; Contribution to the simultaneous determination of  $^{228}\text{Ra}$  and  $^{226}\text{Ra}$  by 3M's Empore<sup>TM</sup> Radium Rad Disks; Journal of Radioanalytical and Nuclear Chemistry; **223** (1997) 225-228.

## **Kapitel I: Neue analytische Methoden Teil 1**

# **Solid-Phase Extraction Using Empore<sup>TM</sup> Radium Rad Disks to Separate Radium from Thorium**

**Stefan Purkl and Anton Eisenhauer**

## Abstract

A new method is presented for rapid and selective enrichment of radium (Ra) in natural samples using  $^{225}\text{Ra}$  as a chemical yield tracer. The new technique allows a complete separation of the target nuclide from the sample matrix with high separation factors for thorium (Th) and uranium (U). The use of Empore<sup>TM</sup> Radium Rad Disks combines the easy handling of column chromatography with the high selectivity and rapid extraction kinetics of solvent extraction chromatography. Following this new chemical approach, eluats are obtained which are well suited for  $\alpha$ -spectrometric analysis of Ra, Th and U.

## 1. Introduction

Independent of the method chosen to determine Ra its concentrations in natural waters normally requires a pre-concentration before chemical analysis. There are already numerous procedures published like Ba- or Pb-coprecipitation [1,2], adsorption onto  $\text{MnO}_2$ -films [3] and  $\text{MnO}_2$ -fibres [4] as well as the use of cation exchange resins [5] or solvent extraction techniques [6]. Methods including coprecipitation or adsorption suffer from low specificity of the reagents being used whereas preconcentration via cation exchange is time-consuming due to low reaction kinetics. In contrast, solvent extraction using crown ethers achieve high selectivity for Ra and show rapid extraction kinetics. However, their disadvantage is that the number of practicable measurement methods following the preconcentration procedure is reduced and furthermore the sample volume that can be processed is restricted.

The development of macrocyclic and chelating ligands that are enmeshed in a matrix of PTFE fibrils offers new ways for metal-ion separation. These ligands are able to selectively recognise the ionic radius, shape and electrical charge of a certain target ion. The ligands are connected covalently with a spacer to silica gel representing the solid phase support. The spacer has the important function of allowing the ligand to be immersed in the aqueous phase. The stable covalent bonding prevents dissolution in the used medium [7]. The silica gel particles, with a diameter of less than 10  $\mu\text{m}$ , are enmeshed in a fibrous PTFE-matrix (Fig. 1). Comprising  $90 \pm 2\%$  of so-called AnaLig particles, the membrane can be considered as a short column (500  $\mu\text{m}$ ) that is more compact than a typical solid phase extraction column. Due to the large concentration of active sites, high flow rates can be attained, exceeding those of typical column systems and can be up to 4000 times [8] those of ion-exchange. Adjusting the flow-rate to 50 ml/min, rapid and quantitative sample extraction can be achieved.

Membranes preferentially complexing Ra are marketed under the name “3M Empore<sup>TM</sup> Radium Rad Disks”. The new membrane technique combines the easy handling of column chromatography with the high selectivity and rapid extraction kinetics of solvent extraction chromatography.

A few methods have already been reported in the literature using this membrane technique to determine Ra [9,10,11] in aqueous samples. However, none of these use internal standards to control the chemical yield of the analytical steps prior to radiometric measurement. Thus, the composition of the sample has to be well known because high Ba<sup>2+</sup>, Sr<sup>2+</sup>, Pb<sup>2+</sup> or K<sup>+</sup> ion concentrations may cause interferences. In order to assure 100 % extraction efficiency, the volume of the aqueous sample that can be processed has to be restricted. Thus repeated calibration measurements are requested under fully reproducible conditions.

In this study we present a new method which overcomes these problems by using <sup>225</sup>Ra and <sup>229</sup>Th as a the yield tracer. This study shows that after adding the yield tracer and passing the nitric acidic solution through the Empore system, a quantitative separation of <sup>225</sup>Ra from the parent nuclide is achieved. Within a single step, a rapid preconcentration of the analyte and the separation of the stipulated yield tracer from its parent Th is performed. As the most sensitive radiometric method,  $\alpha$ -spectrometry has been chosen for Ra determination. Chemical yield is determined via the  $\alpha$ -line of <sup>217</sup>At (7.067 MeV), which is a daughter of <sup>225</sup>Ra. Using an internal standard in combination with  $\alpha$ -spectrometry, the membrane approach with its easy handling and high selectivity, is less restricted in terms of sample volume as well as sample composition and becomes more accurate without time-consuming repeated calibration measurements. The new method is applied onto a Ra solution assayed by an international laboratory intercomparison.

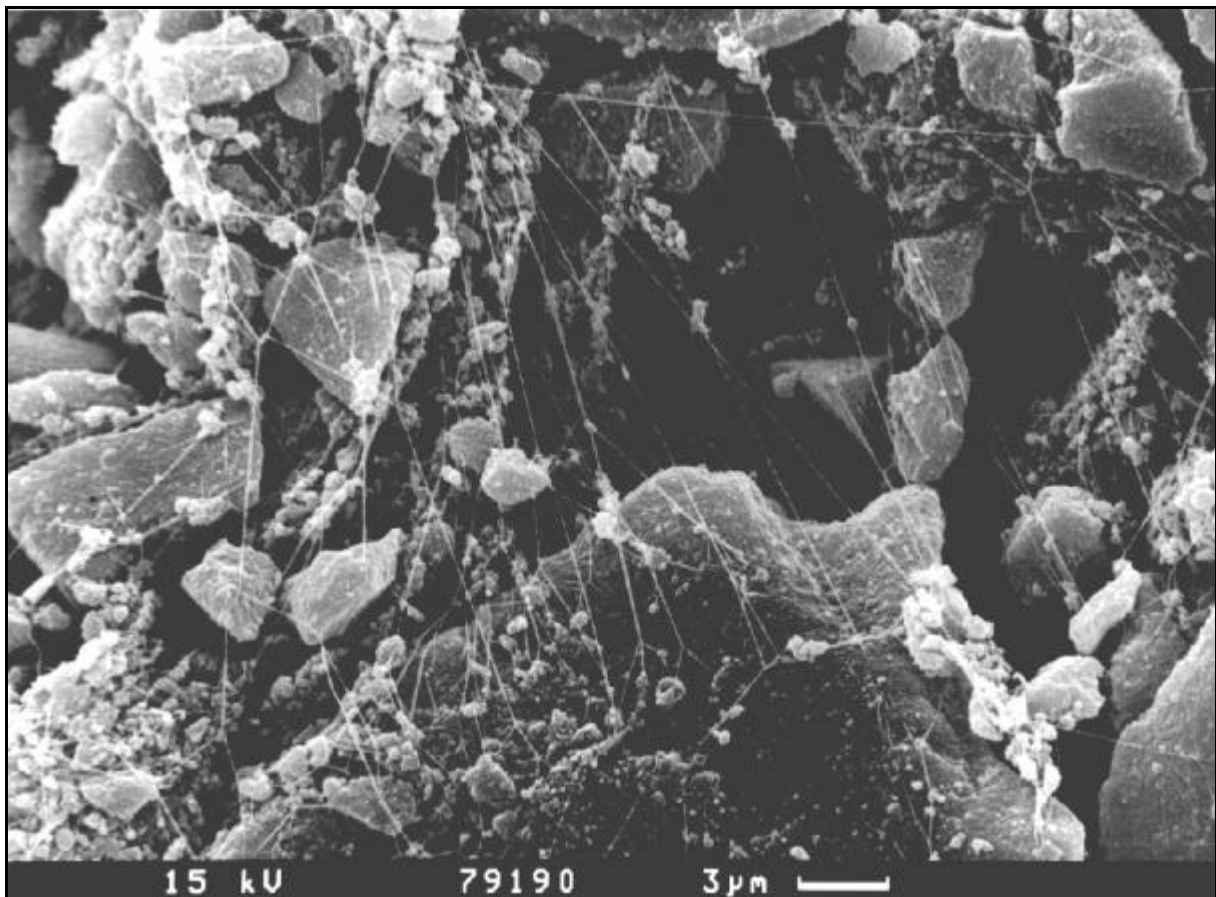


Fig. 1: Electron microscope photograph of a 3M Empore<sup>TM</sup> Radium Rad Disk. AnaLig<sup>TM</sup> particles, crown ethers covalently bond to a silica gel support, are enmeshed in a fibrous PTFE-matrix.

## 2. Experimental Setup

### 2.1. Instrumentation

$\gamma$ -ray counting was done with an n-type, planar, HPGe low-energy photon detector. The active area was 2000 mm<sup>2</sup> and the crystal depth was 10 mm. Energy resolution at 6.4 keV and 1330 keV was 8 keV and 1.9 keV respectively. The Be window thickness of 0.5 mm allows optimal counting conditions for low-energy  $\gamma$ -ray emitters.

The  $\alpha$ -particle spectroscopy system used consists of an octal  $\alpha$ -spectrometer, OCTÈTE<sup>TM</sup> PC (EG&G ORTEC, Oak Ridge) and eight independent ion-implanted silicon ULTRA<sup>TM</sup>  $\alpha$ -detectors with 450 mm<sup>2</sup> active area, guaranteed resolution of 20 keV (Full-Width-at-Half-Maximum, FWHM) and an especially low background of 1-6 counts/d. The operating pressure was 20-25 Pa and the source/detector distance was chosen as 16 mm.

## 2.2. Tracers and Reference Materials

### 2.2.1. Ra and Th Separation Study

The  $^{229}\text{Th}$  tracer used to determine the retention of Th onto the Ra extractive disks was obtained from Harwell, Oxfordshire. Reference data for measurements, date 17.06.87, give  $^{228}\text{Th}$  0.42 % of  $^{229}\text{Th}$  determined via  $\alpha$ -activity. The  $^{228}\text{Th}$  impurities are negligible because after dilution the 8 M nitric acid solution was stored away for about 13 years. Before use radioactive equilibrium between  $^{229}\text{Th}$  and  $^{225}\text{Ra}$  was verified. This was done after evaporation with an infra-red lamp onto a stainless steel disc followed by counting of the sample in an  $\alpha$ -spectrometer. Equilibrium was checked by the measurement of  $^{225}\text{Ac}$ ,  $^{221}\text{Fr}$  and  $^{217}\text{At}$  which are the  $\alpha$ -emitting daughters of  $^{225}\text{Ra}$ .

$^{228}\text{Th}$  tracer later added to the extracted solution was calibrated against the  $^{229}\text{Th}$  standard in a separate measurement in order to achieve internal consistency. The tracer is assumed to be in equilibrium with its parent  $^{232}\text{U}$ , nevertheless the use one week after calibration excludes erratic results due to ingrowth of Th.

### 2.2.2. Laboratory Intercomparison

Groundwater samples containing  $^{226}\text{Ra}$  were distributed by the Laboratory of Natural Radiation, Radiation and Nuclear Safety Authority (STUK), Helsinki, and sent to 20 laboratories in 15 different countries [12]. The water samples were conserved with  $\text{HNO}_3$  and  $\text{HCl}$  respectively. Assayed volume differs and depends on the method of measurement.

Analysed samples were  $\text{HCl}$  conditioned and thus acidified with conc.  $\text{HNO}_3$  in order to obtain a nitric acid solution of 2 mol/l. Due to the sensitivity of  $\alpha$ -spectrometry, only small sample volumes of 5 ml and 10 ml are necessary to obtain satisfactory results with relative uncertainty lower than 5 % (1  $\sigma$ ).

In this study, the  $^{229}\text{Th}/^{225}\text{Ra}$  tracer activities are prepared from a  $^{229}\text{Th}$  stock solution obtained from the National Institute of Standards and Technology. (NIST, Gaithersburg, SRM No.4328B). After dilution, the tracer activity corresponds to  $348.9 \pm 3.5 \text{ mBq/g}$ .

## 2.3. Chemical Separation Procedures

The flow diagram in Fig. 2 schematically shows the chronological sequence of the individual separation steps and summarizes the involved spectrometric methods. Details for each step are given below.

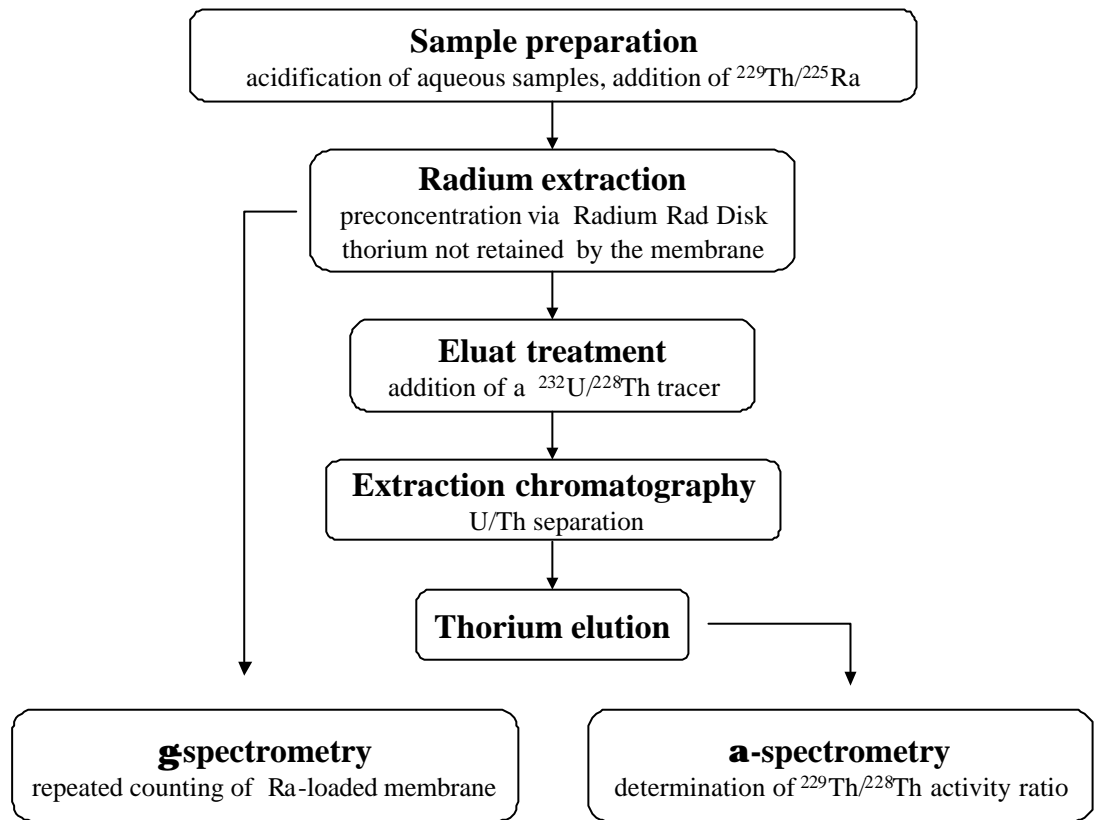


Fig. 2: Flow diagram illustrating the analytical steps and the spectrometric methods involved to verify quantitative separation of  $^{229}\text{Th}$  and  $^{225}\text{Ra}$  using Radium Rad Disks.

### 2.3.1. Preconcentration of Ra and Separation from Th via Ion-Selective Extraction Disks

Concentrated HNO<sub>3</sub> is added to deionised water to raise the HNO<sub>3</sub> concentration to 2 mol/l. Then a <sup>229</sup>Th-solution containing <sup>225</sup>Ra in radioactive equilibrium is added and the sample is heated to boiling. After cooling down, a homogeneous distribution of tracer activities in the solution is ensured.

Prior to sample processing, the Radium Rad disk is conditioned using 20 ml of 2 mol/l HNO<sub>3</sub> under a gentle vacuum. The sample is extracted in a 47 mm diameter vacuum filter apparatus (Roth, Karlsruhe) adjusting the flow rate to 50 ml/min. The Ra-loaded membrane is washed with three 20 ml aliquots of 2 mol/l HNO<sub>3</sub>. After drying overnight, the disk is measured periodically in a  $\gamma$ -ray counting system.

### 2.3.2. Procedure for Eluat Processing

The eluats from the extraction procedure are combined in a Teflon® beaker yielding about 750 ml HNO<sub>3</sub> acidic solution. The amount of <sup>232</sup>U and <sup>228</sup>Th tracer activities added corresponds to those of <sup>229</sup>Th activity levels, expected in the solution. <sup>228</sup>Th is used to control the chemical yield of the procedure, which is necessary to quantify the amount of <sup>229</sup>Th that passed through the membrane. The chemical procedure described below requires a reduced volume of 10 ml of 1 mol/l HNO<sub>3</sub>.

The column material for the extraction chromatography is produced by mixing of “Reversed-Phase-Material Chromabond NO<sub>2</sub>” (Macherey-Nagel, Düren) and trioctylphosphin (TOPO) (Merck, Darmstadt) in a weight proportion of five to one in the presence of CHCl<sub>3</sub> as solvent. CHCl<sub>3</sub> has to be quantitatively removed via evaporation before the material can be used.

350 mg of the prepared material is poured into a Teflon® column with 5 mm inner diameter. 5 ml of HNO<sub>3</sub> (1 mol/l) is used for conditioning the column. The sample is extracted under gentle vacuum in order to attain a flow rate of 1 ml/min. After successive washings with 10 ml of HNO<sub>3</sub> (1 mol/l), 10 ml of a 10 % (mass to volume) solution of ascorbic acid in HNO<sub>3</sub> (1 mol/l) and 10 ml deionised water Th is eluted using 5 ml of H<sub>2</sub>SO<sub>4</sub> (0.8 mol/l) and 5 ml of deionised water. The U-fraction remains on the column and, if required, could also be eluted with a saturated (NH<sub>4</sub>)<sub>2</sub>CO<sub>3</sub> solution. Details for analysis are given in [13].

For  $\alpha$ -spectrometric assay, 1 g (NH<sub>4</sub>)<sub>2</sub>SO<sub>4</sub> is added to the collected Th fraction [14] and the pH-value is adjusted to 2.5 using NH<sub>4</sub>OH [15]. After transferring the solution obtained into an

appropriate electrodeposition cell, Th is plated onto a polished stainless steel planchette and flamed to assure fixation.

## 2.4. Spectrometry

### 2.4.1. $\alpha$ -Spectrometric Determination of $^{229}\text{Th}$ in the Eluat

The amount of  $^{229}\text{Th}$  is evaluated using  $\alpha$ -lines in the energy region between 4.730 MeV and 5.052 MeV. The chemical yield is calculated by analysing those  $\alpha$ -lines of  $^{228}\text{Th}$  at 5.423 MeV and 5.340 MeV. Due to good  $\alpha$ -energy resolution (17.3 keV, FWHM), the presence of  $^{232}\text{U}$  (5.320 MeV and 5.263 MeV) could be excluded by monitoring the peak at 5.263 MeV. Direct counting after sample preparation minimises the ingrowth of  $^{224}\text{Ra}$  (5.686 MeV and 5.445 MeV) into the  $^{228}\text{Th}$  peak at 5.423 MeV. The residual could be calculated and stripped from the region via analysis of the well-separated peak at 5.686 MeV.

### 2.4.2. $\gamma$ -Spectrometric Determination of $^{229}\text{Th}$ on the Ra Extractive Disk

Due to low  $\gamma$ -ray intensities of  $^{229}\text{Th}$  (4.4 % at 193.5 keV and 2.8 % at 210.9 keV) residual Th that remains on the Ra-loaded membrane is determined by analysing the decay of its daughter  $^{225}\text{Ra}$ . The photopeak at 40.0 keV with an easily detectable  $\gamma$ -transition probability of 30.0 % was used. Within the time interval of 103 days (close to 7 half-lives) 10 successively performed measurements were conducted. During the whole time the disk was attached in a defined counting geometry.

Searching for the initial activity ratio of  $^{229}\text{Th}$  and  $^{225}\text{Ra}$  ( $A_{\text{Th}} / A_{\text{Ra}}^0$ ) at time  $t_0$  after sample extraction, the acquired  $\gamma$ -spectrometric data are used as follows:

Counts measured using the  $^{225}\text{Ra}$  photopeak ( $E_{\text{Ra,tot}}$ ) consist of those supported by Th ( $E_{\text{Ra,s}}$ ) in radioactive equilibrium with its daughter and of unsupported  $^{225}\text{Ra}$  ( $E_{\text{Ra,us}}$ ):

$$E_{\text{Ra,tot}} = E_{\text{Ra,s}} + E_{\text{Ra,us}} \quad (1)$$

The counts resulting from Th decay-fed and correspondingly constant  $^{225}\text{Ra}$  activity ( $A_{\text{Ra,s}}$ ) within one measuring period ( $\Delta$ ) are given by:

$$E_{\text{Ra,s}} = A_{\text{Ra,s}} \Delta_t \quad (2)$$

Taking into account that the activity of unsupported  $^{225}\text{Ra}$  ( $A_{\text{Ra},\text{us}}$ ) is time dependent,  $E_{\text{Ra},\text{us}}$  can be calculated by using the law of radioactive decay and integrating over the measuring period, starting at counting time  $t_1$ :

$$E_{\text{Ra},\text{us}} = A_{\text{Ra},\text{us}}^0 e^{-I_{225}(t_1-t_0)} \int_{t_1}^{t_1+\Delta_t} e^{-I_{225}(t-t_1)} dt \quad (3)$$

$A_{\text{Ra},\text{us}}^0$  = unsupported  $^{225}\text{Ra}$  activity at time  $t_0$  (Bq)

$\lambda_{225}$  = decay constant of  $^{225}\text{Ra}$  (1/s)

Solving the integral, putting expression (2) and (3) in (1), and rearranging by using  $A_{\text{Ra}}^0 = A_{\text{Ra,s}} + A_{\text{Ra},\text{us}}^0$  the following term is obtained:

$$\frac{E_{\text{Ra,tot}}}{\Delta_t} = A_{\text{Ra},\text{us}}^0 \left( \frac{e^{-I_{225}(t_1-t_0)} (1 - e^{-I_{225}\Delta_t})}{I_{225}\Delta_t} - 1 \right) + A_{\text{Ra}}^0 \quad (4)$$

$A_{\text{Ra}}^0$  and  $A_{\text{Ra},\text{us}}^0$  could be determined by plotting  $\frac{E_{\text{Ra,tot}}}{\Delta_t}$  versus  $\frac{e^{-I_{225}(t_1-t_0)} (1 - e^{-I_{225}\Delta_t})}{I_{225}\Delta_t} - 1$  and

linear fitting of the spectrometric data. The desired activity ratio of Th to Ra at time  $t_0$  after sample extraction is then given by:

$$\frac{A_{\text{Th}}}{A_{\text{Ra}}^0} = \frac{A_{\text{Ra}}^0 - A_{\text{Ra},\text{us}}^0}{A_{\text{Ra}}^0} \quad (5)$$

### 2.4.3. Determination of Ra via $\alpha$ -Spectrometry

After elution of the enriched radium sample, followed by a low pressure column chromatography step to change the matrix and eliminate of disturbing elements, a thin  $\alpha$ -source is prepared via electrodeposition. The chemical yield ( $k$ ) is determined by using  $^{217}\text{At}$ , an  $\alpha$ -emitting daughter of  $^{225}\text{Ra}$  and comparing measured counts  $E_{\text{me}}$  in the  $^{217}\text{At}$  peak region with calculated, maximal detectable, counts  $E_{\text{max}}$  ( $k = E_{\text{me}}/E_{\text{max}}$ ). Depending on the tracer activities  $A_{^{225}\text{Ra}}^0$  initially used, the counts  $E_{\text{max}}$  are calculated by considering decay of unsupported  $^{225}\text{Ra}$  after extraction at time  $t_0$  as well as ingrowth of  $^{225}\text{Ac}$  ( $T_{1/2} = 10.0$  d) during the column chromatography at time  $t_1$  and integrating over the counting period  $\Delta_t$ . Time  $t_2$  marks the start of counting. Counts  $E_{\text{me}}$  observed in the well-resolved  $^{217}\text{At}$  peak region are measured with an efficiency  $\epsilon$  via an energy and efficiency calibrated semiconductor  $\alpha$ -detector.

The correspond chemical yield in percent is given by:

$$k = \frac{100 E_{\text{me}}}{\epsilon A_{^{225}\text{Ra}}^0 e^{-\lambda_{^{225}\text{Ra}}(t_1-t_0)} \frac{\lambda_{^{225}\text{Ac}}}{\lambda_{^{225}\text{Ac}} - \lambda_{^{225}\text{Ra}}} \int_{t_2}^{t_2 + \Delta_t} (e^{-\lambda_{^{225}\text{Ra}}(t-t_1)} - e^{-\lambda_{^{225}\text{Ac}}(t-t_1)})} \quad (6)$$

$E_{\text{me}}$  = measured counts in the  $^{217}\text{At}$  peak region

$\epsilon$  = geometrical efficiency of the  $\alpha$ -detector

$A_{^{225}\text{Ra}}^0$  = initial  $^{225}\text{Ra}$  activity (Bq)

$\lambda_{^{225}\text{Ra}}$  = decay constant of  $^{225}\text{Ra}$  (1/s)

$\lambda_{^{225}\text{Ac}}$  = decay constant of  $^{225}\text{Ac}$  (1/s)

$t_0$  = time of separation from Th (s)

$t_1$  = time of  $^{225}\text{Ac}$  build-up(s)

$t_2$  = start of counting (s)

$\Delta_t$  = counting period (s)

Fig. 3 and Fig. 4 show  $\alpha$ -spectra of the same 5 ml natural groundwater sample. The spectrum in Fig. 3 has been counted one day after sample preparation. Fig. 4 represents the same  $\alpha$ -source counted after 10 days, illustrating the time-dependent ingrowth of  $^{225}\text{Ac}$ , with main  $\alpha$ -lines at 5.829 and 5.792 MeV.  $^{225}\text{Ac}$  is associated directly with short-lived  $^{221}\text{Fr}$  ( $T_{1/2} = 4.9$  m),  $^{217}\text{At}$  ( $T_{1/2} = 32.3$  ms), and  $^{213}\text{Po}$  ( $T_{1/2} = 4.2$   $\mu$ s). The first well resolved daughter is  $^{217}\text{At}$  at 7.067 MeV which thus can be used to determine  $^{226}\text{Ra}$  even if problems occur resulting from low resolution due to high barium content of the sample matrix. The measured chemical yield is  $94 \pm 9\%$ . Only 5 ml groundwater are necessary to achieve sufficient counting statistics with uncertainties lower

than 5 %. Source to detector distance was chosen as 16 mm in order to avoid serious detector contamination. In cases of Ra concentration on the order of mBq/l, the sample volume can be enlarged. Volumes of up to 5 liters are suitable and can easily be assayed. The detection limit of the method is 0.2 mBq reached during a counting time of 250,000 s.

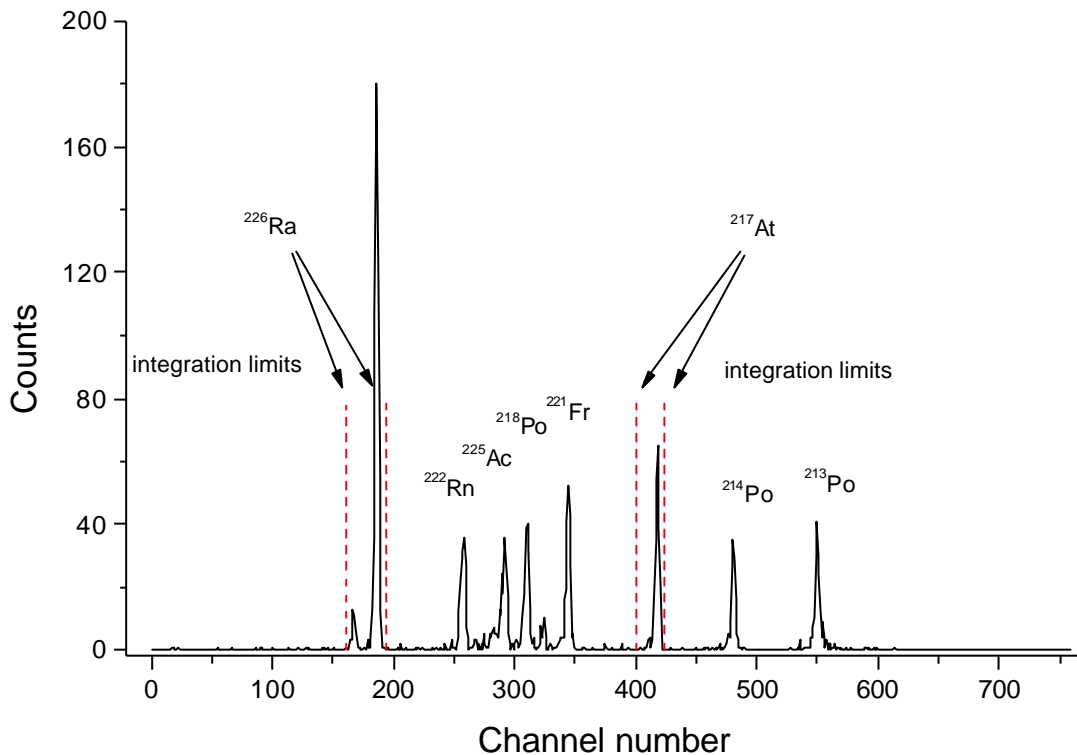


Fig. 3: Typical  $\alpha$ -spectrum of a groundwater sample counted one day after sample preparation. After flaming, peak resolution is 35 keV (FWHM). Regions of interest, marked by dashed lines, are well separated and allow  $^{226}\text{Ra}$  determination even when a difficult sample matrix causes resolution problems.

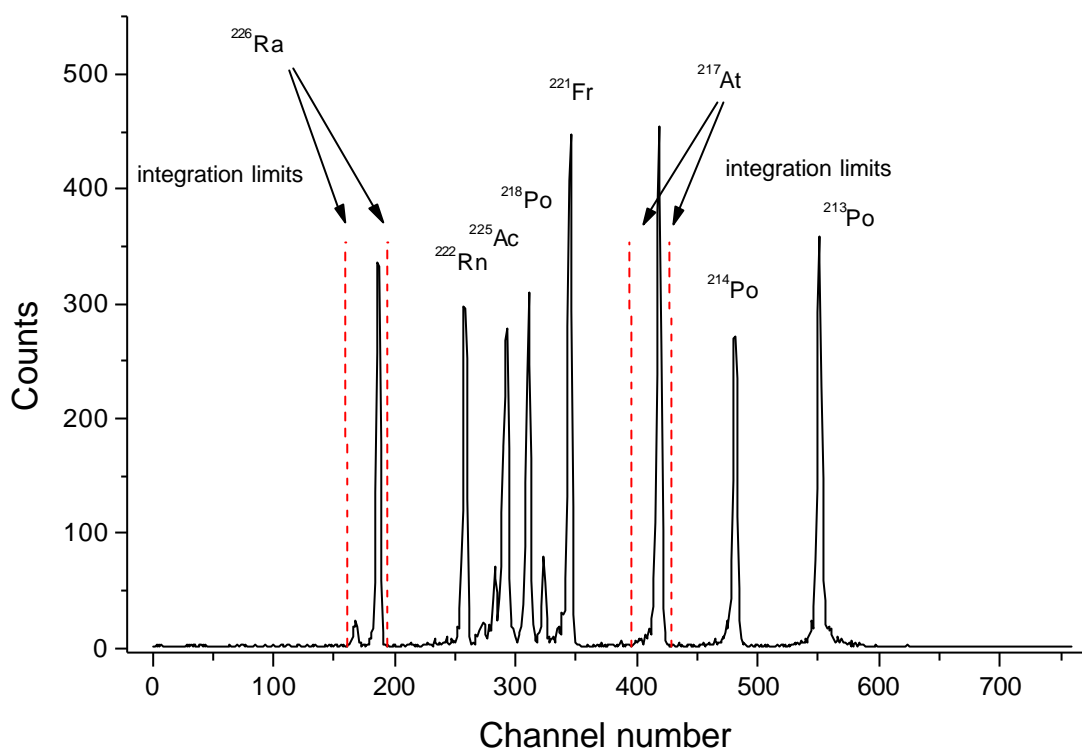


Fig. 4: Same sample, counted 10 days after preparation illustrating the time-dependent ingrowth of  $^{225}\text{Ac}$  and daughters. Regions of interest are marked by dashed lines.

### 3. Results and Discussion

#### 3.1. Separation of Ra from Th

The effectiveness of the separation of  $^{229}\text{Th}$  is determined by analysing the decay of its daughter on the extractive disk, as illustrated in Fig. 5. The upper half of the figure depicts a  $\gamma$ -spectrum of a  $^{225}\text{Ra}$ -loaded membrane counting starting one day after sample preparation, wherein a background-corrected counting rate of  $123.0 \pm 1.6 \text{ h}^{-1}$  is observed for  $^{225}\text{Ra}$ . In contrast, the lower half, taken 71 days after sample preparation, shows a counting rate of only  $5.1 \pm 0.5 \text{ h}^{-1}$ , indicating that a high amount of unsupported Ra must have been present.

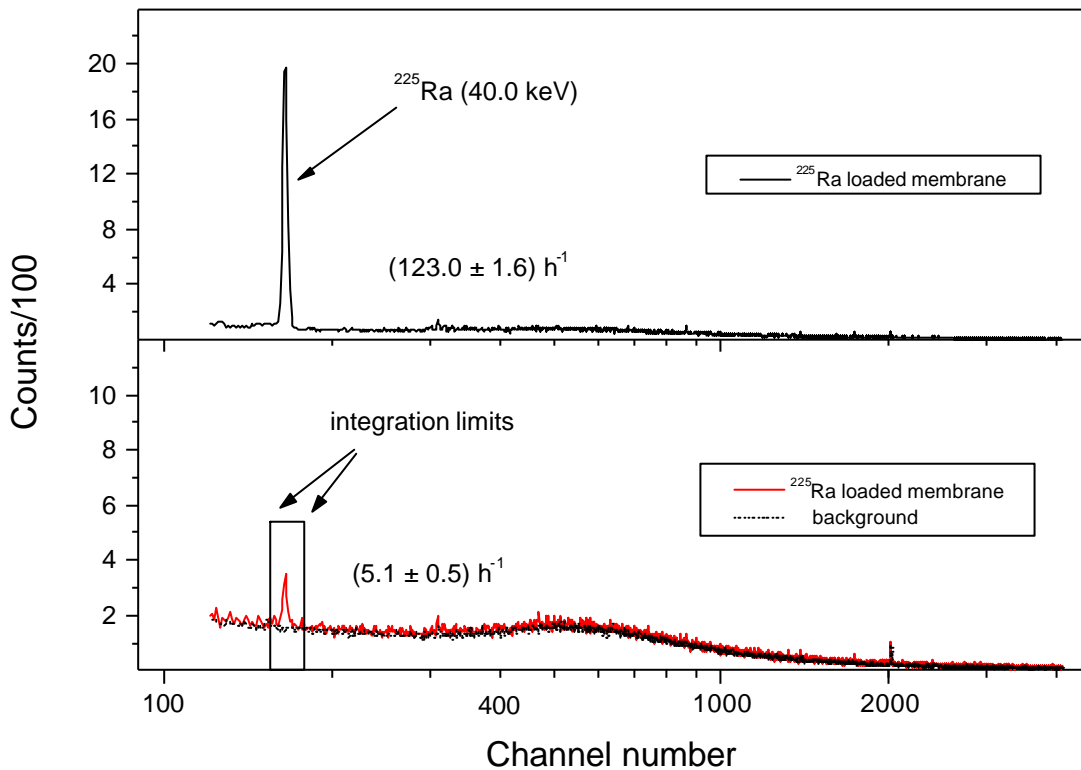


Fig. 5: Upper half of figure:  $\gamma$ -spectrum of a  $^{225}\text{Ra}$ -loaded membrane where counting was started one day after sample preparation. Lower half: same, started 71 days after sample preparation, indicating that a high amount of unsupported Ra must have been present.

The amount of Th remaining on the disk can be calculated by using the fitted parameters  $A = 0.03654 \pm 0.00030 \text{ s}^{-1}$  and  $B = 0.03633 \pm 0.00036 \text{ s}^{-1}$ , (Fig.6). The initial total Ra activity  $A_{Ra}^0$  is given by parameter A and unsupported Ra activity at time  $t_0$   $A_{Ra,us}^0$  is given by B. By using equation (5), the initial activity ratio of  $^{229}\text{Th}$  and  $^{225}\text{Ra}$  at time  $t_0$  after sample extraction results in  $A_{\text{Th}}/A_{Ra}^0 = (5 \pm 18)/1000$ . Latter value corresponds to a separation factor of about 200.

The  $\alpha$ -spectrometric assay of the Th fraction that passes through the membrane agrees well with these results. The recovery of Th in the eluat was  $104 \pm 8 \%$ .

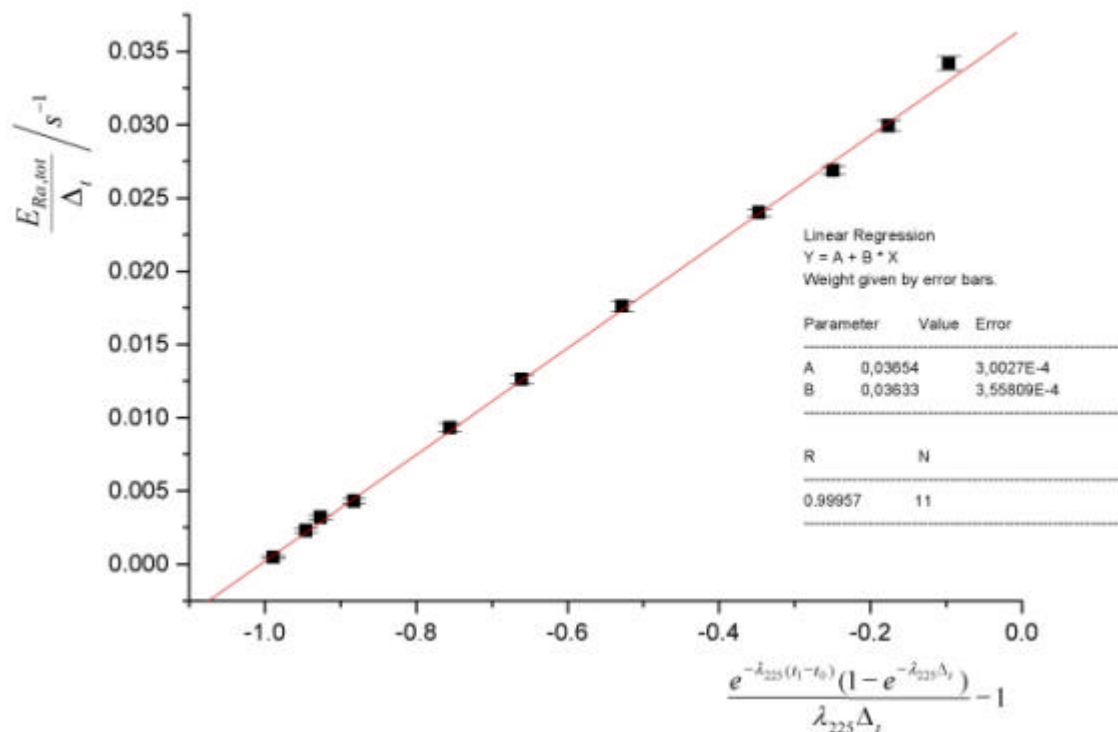


Fig. 6:  $\gamma$ -spectrometric assay of  $^{225}\text{Ra}$  loaded membrane. Experimental data are plotted according to equation (4). A and B are fitting parameters.

### 3.2. Intercomparison of Ra Measurements

$^{226}\text{Ra}$ -containing groundwater assayed by an international laboratory intercomparison is used as reference material in order to verify the membrane approach in combination with  $^{225}\text{Ra}$  as yield tracer. The mean value of the intercomparison is  $c_{\text{Ra}} = 22.4 \text{ Bq/l}$ . Excluding two outliers (42.5 Bq/l and 10.5 Bq/l), the mean value is given as  $c_{\text{Ra}} = 21.9 \text{ Bq/l}$  (L. Salonen, personal communication).

Tab. 1 shows the results of two  $\alpha$ -spectrometric Ra-analyses. Samples 1a-1f are measurements carried out in succession. Due to subsequent  $^{225}\text{Ac}$  ingrowth, uncertainties given as  $1\sigma$  decrease with time after separation. The measured weighted mean value  $c_{\text{Ra}} = 20.6 \pm 0.5 \text{ (n = 2)}$  is in good agreement with the given mean value  $c_{\text{Ra}} = 21.9 \pm 2.9 \text{ (n = 18)}$  of the laboratory intercomparison.

Tab. 1: Comparison of  $^{226}\text{Ra}$  concentrations measured by the present method with reference material [12].

Sample	Volume v/ml	$^{225}\text{Ac}$ ingrowth $(t_2-t_1)/\text{s}$	Counting period $D_t/\text{s}$	$^{226}\text{Ra}$ concentration $c_{\text{Ra}}/\text{Bq l}^{-1}$
1a	5	67410	129271	$20.5 \pm 1.5$
1b	5	196681	163775	$19.8 \pm 1.0$
1c	5	360456	141157	$19.4 \pm 1.0$
1d	5	501613	173182	$21.4 \pm 1.0$
1e	5	674795	255607	$20.2 \pm 0.7$
1f	5	930402	261792	$20.4 \pm 0.7$
1	5	67410	1124785	$20.4 \pm 0.4$
2	10	21720	482820	$21.8 \pm 1.0$
Mean value (n)				$20.6 \pm 0.5 \text{ (2)}$
Reference (n)				$*21.9 \pm 2.9 \text{ (18)}$

\*Uncertainty is given by  $1\sigma$  standard deviation of 18 reported values(15 laboratories), neglecting uncertainties of measurements performed with different methods in each laboratory.

## 4. Summary and Conclusions

The solid-phase extraction method allows the rapid and easy to accomplished preconcentration, desired for Ra analysis in environmental samples. The use of the stipulated yield tracer offers broad adaptability as well as guaranteed accurate measurements even if the analyte is present in difficult matrices and in low concentrations. Effective separation of  $^{225}\text{Ra}$  from the parent  $^{229}\text{Th}$  within a single step reduces complicated and time-consuming sample preparation and minimises the number of chemical operations.

In addition to  $^{226}\text{Ra}$  long lived Th isotopes,  $^{230}\text{Th}$  and  $^{232}\text{Th}$  as well as U isotopes  $^{234}\text{U}$  and  $^{238}\text{U}$  also can be determined by using a  $^{236}\text{U}/^{229}\text{Th}/^{225}\text{Ra}$  mixed tracer. The retention of thorium and U [11] is negligible due to the high selectivity of the Ra extractive disks. Following the procedure for eluat processing, by using Reversed-Phase-Material Chromabond NO<sub>2</sub> impregnated with TOPO, the U and Th fractions could be analysed separately via  $\alpha$ -spectrometric analysis.

$\gamma$ -spectrometric measurements indicate that the percentage of Th remaining on the disk is much lower than 2%. This also allows the usage of  $^{224}\text{Ra}$  as an internal yield tracer added as daughter of an equilibrated  $^{232}\text{U}$  standard solution. Due to the short half life of  $^{224}\text{Ra}$  ( $T_{1/2} = 3.66 \text{ d}$ ), the sample should be processed as fast as possible. Nevertheless, recently collected aqueous samples can contain high amounts of  $^{224}\text{Ra}$  and thus have to be stored for about 20 days before chemical analysis. Using an aged  $^{232}\text{U}$  standard solution becomes attractive because it provides  $^{232}\text{U}$ ,  $^{228}\text{Th}$  and  $^{224}\text{Ra}$  in radioactive equilibrium. Such a tracer can then be applied without complicated calibration and mixing procedures. Regarding importance for radiation protection, simultaneous  $\alpha$ -spectrometric determination of long lived U, Th and Ra isotopes are likewise possible using one single spike.

## References

- [1] H. Jiang and R.B. Holtzman, *Health Phys.* 57 (1989) 167.
- [2] G.J. Hancock and P. Martin, *Int. J. Appl. Radiat. Isot.* 42 (1991) 63.
- [3] H. Surbeck, *Int. J. Appl. Radiat. Isot.* 53 (2000) 97.
- [4] D.F. Reid, R. M. Key and D.R. Schink, *Earth Planet. Sci. Lett.* 43 (1979) 223.
- [5] V.F. Hodge and G. A. Laing, *Radiochim. Acta* 64 (1994) 211.
- [6] R. Chiarizia, M.L. Dietz, E.P. Horwitz, W.C. Burnett and P.H. Cable, *Sep. Sci. Technol.* 34 (1999) 931.
- [7] G.L. Goken, R.L. Bruening, K.E. Krakowiak, and R.M. Izatt, In: *Metal-Ion Separation and Preconcentration: Progress and Opportunities*, A.H Bond, M.L Dietz, R.D Rogers (Eds.), ACS Symposium Series 716, Washington, D.C., 1999, pp. 251-259.
- [8] R.M. Izatt, J.S. Bradshaw and R.L. Bruening, *Pure Appl. Chem.*, 68 (1996) 1237.
- [9] D.C. Seely and J. A. Osterheim, *J. Radioanal. Nucl. Chem. Art.* 236 (1998) 175.
- [10] A. Durecova, *J. Radioanal. Nucl. Chem. Art.* 223 (1997) 225.
- [11] L.L. Smith, J.S. Alvarado, F.J. Markun, K.M. Hoffmann, D.C. Seely and R.T. Shannon, *Radioac. Radiochem.* 8 (1997) 30.
- [12] L. Salonen and T. Ilus, LSC 2001, International Conference on Advances in Liquid Scintillation Spectrometry, Karlsruhe, 2001.
- [13] R. Weber, R.A. Esterlund and P. Patzelt, *Int. J. Appl. Radiat. Isot.* 50 (1999) 929.
- [14] F.V. Tome and A.M. Sanchez, *Int. J. Appl. Radiat. Isot.* 42 (1991) 135.
- [15] L. Hallstadius, *Nucl. Instrum. Methods Phys. Res.* 223 (1984) 266.

## **Kapitel II. Neue analytische Methoden Teil 2**

# **A Rapid Method for $\alpha$ -Spectrometric Analysis of Radium Isotopes in Natural Waters Using Ion-Selective Membrane Technology**

**Stefan Purkl and Anton Eisenhauer**

## Abstract

A  $\alpha$ -spectrometric method for the rapid determination of all four naturally occurring Radium isotopes ( $^{223}\text{Ra}$ ,  $^{224}\text{Ra}$ ,  $^{226}\text{Ra}$ ,  $^{228}\text{Ra}$ ) in environmental samples is presented. Using Empore<sup>TM</sup> Radium Rad Disks complete separation of the target nuclide from the sample matrix is achieved. High separation factors for Thorium (Th) allow the straightforward use of  $^{225}\text{Ra}$  as a yield tracer. The chemical procedure can be accomplished within 5 hours with a chemical yield of up to  $92\pm9\%$ . The prepared  $\alpha$ -sources show energy resolution in the range of typically 26 to 40 keV (FWHM). Despite the minimal thickness of the sources no significant Radon (Rn) losses could be observed. The good Rn-retention is achieved by a protective film most likely consisting of deposited Platinum (Pt).

## 1. Introduction

The use of ion-selective membrane technology (Goken et al., 1999) combines the easy handling of column chromatography with the high selectivity and rapid extraction kinetics of solvent extraction chromatography. Previous studies (Smith et al., 1997, Seely and Osterheim, 1998) using Empore<sup>TM</sup> Radium Rad Disks with high enrichment factors for Ra. However, none of these methods use internal standards to control the chemical yield of the whole chemical procedure prior to radiometric or mass-spectrometric (Joannon and Pin, 2001) measurement.

Furthermore, if in addition to  $^{226}\text{Ra}$  also  $^{228}\text{Ra}$  has to be determined the applied methods require time consuming procedures like precipitation, centrifugation, filtration and redissolution in order to obtain the requested purity for  $\beta$ -spectrometry. Improved background characteristic of Liquid scintillation counting (LSC) (Schönhöfer and Wallner, 2001) allows determination of  $^{228}\text{Ra}$  even in mBq quantities. Nevertheless, poor energy resolution of LSC results in extensive peak overlapping in  $\alpha$ - and  $\beta$ -window and thus making identification of interfering radio nuclides remaining in the prepared source, difficult.

In contrast, high resolution  $\alpha$ -spectrometry allows simultaneous determination of all four naturally occurring Ra isotopes, including short lived isotopes  $^{223}\text{Ra}$  and  $^{224}\text{Ra}$  on a single  $\alpha$ -source. The selectivity of the new analytical method presented here allows straightforward use of  $^{225}\text{Ra}$  as internal standard and furthermore combines sensitivity of high resolution  $\alpha$ -spectrometry with easy handling, high selectivity and advantageous extraction kinetics of solid phase extraction disks, making the procedure very rapid and sensitive.

## 2. Chemical Procedures

### 2.1. Flow Diagram for Sample Preparation

Fig. 1 is a flow diagram which is given for the purpose of clarifying the chronological sequence of the individual steps involved in the preparation of  $\alpha$ -counting samples. Details for each step are given in the appropriate boxes.

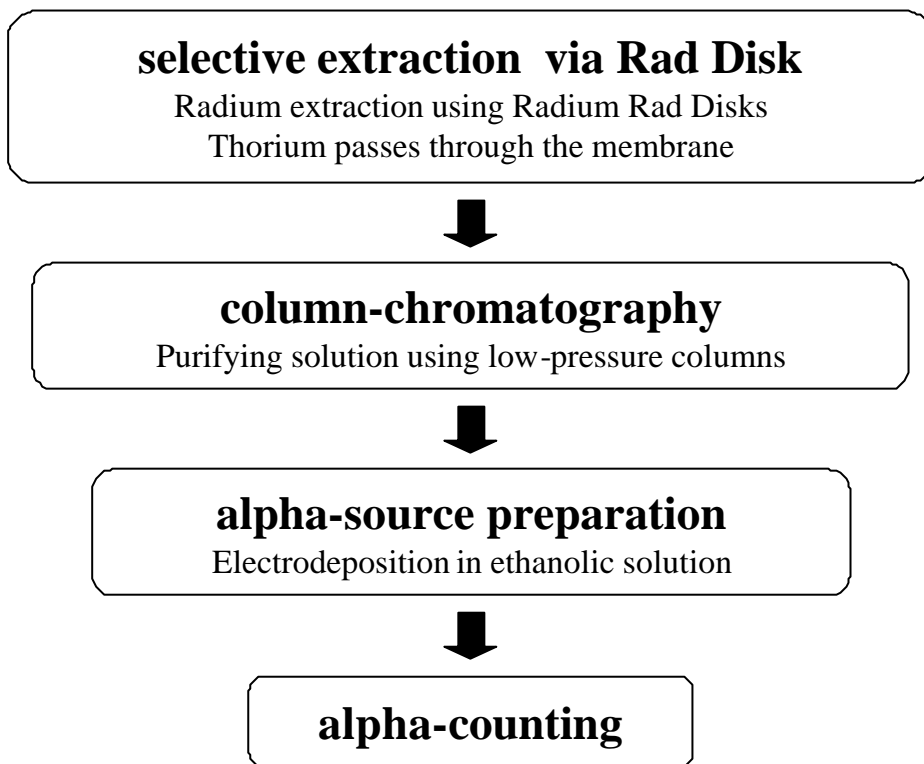


Fig. 1: Flow chart illustrating sample preparation procedure for simultaneous determination of all four naturally occurring Ra isotopes on a single  $\alpha$ -source.

### 2.2. Procedure for Ion-Selective Extraction of Ra via Membrane Technology

#### 2.2.1. Preparation of Aqueous Samples

If necessary the collected aqueous samples are prefiltered through a  $0.45\text{ }\mu\text{m}$  Filter. Subsequent to exact measurement of the sample volume, which optimally should contain an analyte activity of about 2 to 500 mBq, sufficient concentrated  $\text{HNO}_3$  is added to raise the  $\text{HNO}_3$  concentration to 2 N. The amount of  $^{229}\text{Th}$  and  $^{225}\text{Ra}$  tracer activities added should correspond to analyte

activity levels expected in the sample volumes to be analysed. The prepared sample is stirred vigorously for several times in order to assure a completely equilibrated distribution of tracer activities.

### **2.2.2. Rapid and Selective Ra Enrichment Using Membrane Technology**

Prior to the sample processing the Radium Rad disk is conditioned using 20 ml of 2 N HNO<sub>3</sub> under a gentle vacuum. The sample is extracted in a 47 mm diameter vacuum filter apparatus (Roth, Karlsruhe) adjusting the flow rate to 50 ml/min. Afterwards the membrane is washed with three 20 ml aliquots of 2 N HNO<sub>3</sub> to remove any remnants of the processed solution. Like the target nuclides the added internal yield tracer <sup>225</sup>Ra is retained on the membrane whereas <sup>229</sup>Th passes through. Time t<sub>0</sub> of Ra extraction has to be noted. For sample sizes widely exceeding one liter, note start t<sub>B</sub> and endpoint t<sub>E</sub>. Do not allow the disk to go dry.

### **2.2.3. Quantitative Ra Elution**

Elution of the Ra loaded membrane is accomplished using 3 ml of 0.25 N EDTA/1.7 N ammonium acetate in 6 N NH<sub>4</sub>OH which is directly mounted onto the extractive disk, followed by a wash of 16 ml 0.01 N EDTA previously adjusted to about pH 10 using NH<sub>4</sub>OH as well. The EDTA wash solution is added continuously using gravity flow or if necessary by applying a gentle vacuum. Flow rate of 1 ml/min is well suited. The obtained eluats are combined and semi concentrated HNO<sub>3</sub> is added to achieve a pH of 4.5. Now sample volume corresponds to about 22 ml.

## **2.3. Low Pressure Column-Chromatography**

### **2.3.1. Conditioning**

A low pressure cation exchange column (Bio-Rad AG50W-X12, 200-400 mesh, 7 mm in diameter) is prepared and converted in the ammonium form by washing with 15 ml 1.5 N ammonium acetate, followed by 15 ml 0.25 N ammonium acetate solution previously adjusted to pH = 4,5 (Hancock and Martin, 1991). Resulting column height is 75 mm. For the purposes of rapid and unhindered separation gravity flow is not recommended. Applying a gentle pressure the required continuously stable flow rate of 1.0 - 1.2 ml/min could be provided during the whole separation procedure.

### 2.3.2. EDTA Removal and Ingrowth of Actinium (Ac)

The eluat obtained from Ra extraction, is passed through the column. By washing with 50 ml 1.5 N ammonium acetate in 0.1 N HNO<sub>3</sub>, disturbing EDTA matrix is eluted, avoiding formation of precipitates and thus painstaking filtering processes afterwards. Residual actinides are complexed and likewise eluted. After ammonium acetate wash <sup>225</sup>Ac starts to build-up. The time t<sub>i</sub> of the end of EDTA removal has to be noted.

### 2.3.3. Separation of Ba and Elution of Ra

About 54 ml of 2.5 N HCl are used to remove Barium (Ba). Then by adding another 25 ml of 6 N HNO<sub>3</sub> the retained Ra fraction is eluted. The separation of Ba from Ra has to be verified because it is crucial for later electroplating. The solution is evaporated in a PFA beaker in order to remove HNO<sub>3</sub> although complete evaporation to dryness has to be avoided.

## 2.4. Electrodeposition from Ethanolic Solution

After the selective enrichment, removal of interfering elements and separation from complexing agents the analyte is electrodeposited onto a polished stainless steel disc for  $\alpha$ -spectrometric assay. Prior to electrodeposition planchettes have to be cleaned with acetone to remove any oil to ensure that the analyte solution is in uniform contact with it all over its surface.

The evaporated residue is dissolved in 0.5 ml 0.1 M HNO<sub>3</sub> and the beaker is successively flushed with 1 ml 0.05 M HCl (Hancock and Martin, 1991). Combined solutions are transferred together with 9 ml ethanol into a electrodeposition cell. Distance between the electrodes is adjusted to 7 mm in order to attain a homogenous electrical field. The shape and material of the anode are crucial and consist of a plane surface with laser welded Pt-rings. Very low oxidation potential assures that it does not appreciably corrode during the electrodeposition. However, a small amount of platinum dissolves (Ferrero Calabuig et al., 1998) and serves as a carrier (Weber et al., 1999). Electroplating is performed for 1 h at a current of 120 mA and a voltage of about 90 to 100 V. About 1 min before the end of electrodeposition 1 ml NH<sub>4</sub>OH is added to the solution in order to prevent redissolution of Ra once the electrical current is turned off.

After deposition the disc is cautiously rinsed either with ethanol or acetone. The brownish film appearing after volatilisation of acetone is most likely consisting of deposited Pt. During a final flaming to glow of the prepared  $\alpha$ -source, hydroxides are converted to oxides and the analyte is permanently affixed to the disc.

The electrodeposition cell (Fig. 2) is a Teflon coated scintillation vial fitting into a copper mounting. Sealing of the system is reached by affixing a clamp onto commonly used vacuum coupling components. Tightening of the copper modules leads to sealing between vial and stainless steel disc. The deposition cell is coolable via a integrated peletier element ( $P = 123.5 \text{ W}$ ) ventilator unit. The system provides conveniently adjustable cooling of the electrolyte solution down to  $1.5 \text{ }^{\circ}\text{C}$ . Distance between the cathode and the anode can be adjusted attaining an improved homogenous electrical field. A distance between 7 and 10 mm is ideally suited and allows operating of four cells in parallel using one single 400 V power supply.

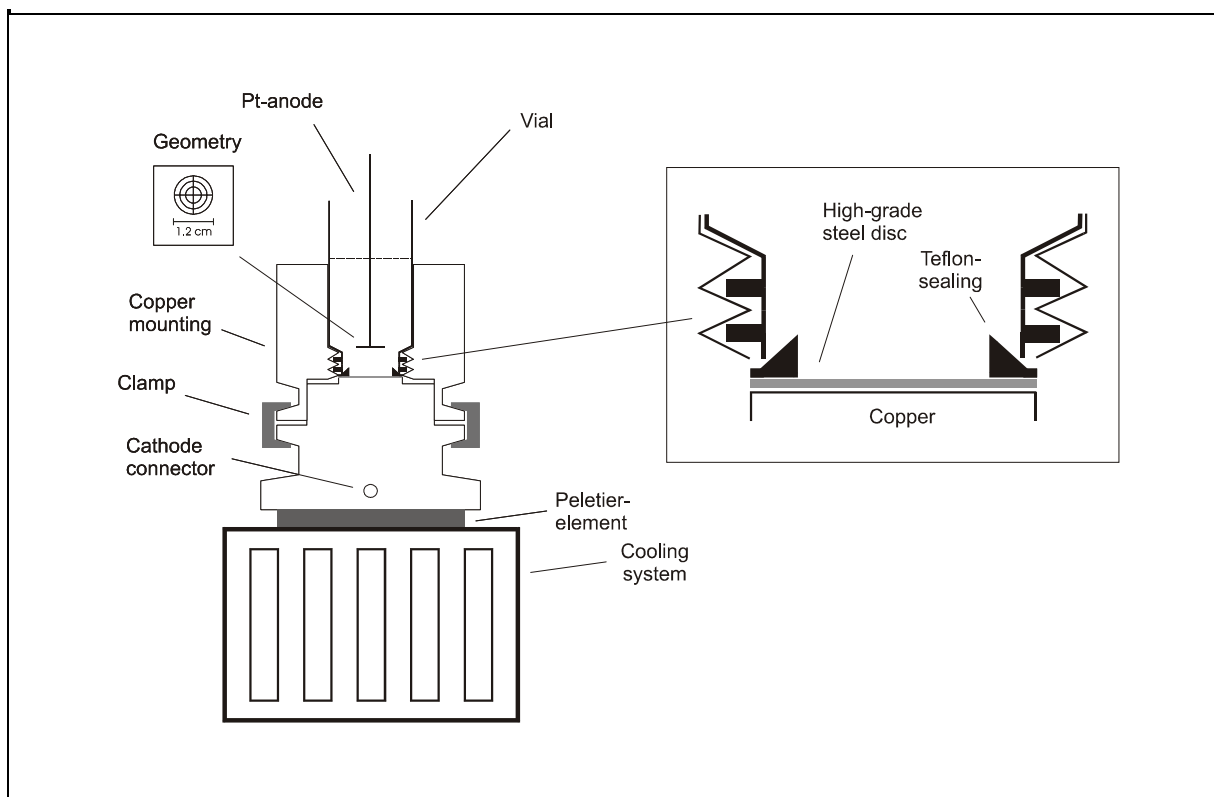


Fig. 2: Coolable electrodeposition cell used for the effective production of uniform and thin deposits.

## 1.1. **$\alpha$ -Spectrometric Analysis**

### 1.1.1. **Instrumentation**

The  $\alpha$ -particle spectroscopy system used consists of an octal  $\alpha$ -spectrometer, OCTÈTE<sup>TM</sup> PC (EG&G ORTEC, Oak Ridge) and eight independent ion implanted silicon ULTRA<sup>TM</sup>  $\alpha$ -detectors with  $450 \text{ mm}^2$  active area, guaranteed resolution of 20 keV (FWHM) and especially low background of 1-6 counts/d. Applied detector bias is 50 V. The operating pressure correspond to values in between 1 and 4 Pa. Source to detector distance varied depending on analyte activity expected in the sample and is set in between 4 and 16 mm.

### 2.5.2. Yield Calculation

The yield is determined by using the peak of  $^{217}\text{At}$  which is an  $\alpha$ -emitting daughter of  $^{225}\text{Ra}$ .

From the initial tracer activity  $A_{^{225}\text{Ra}}^0$  maximal detectable counts ( $E_{\max}$ ) are calculated by considering the decay of unsupported  $^{225}\text{Ra}$  after extraction ( $t_0$ ) as well as build-up of  $^{225}\text{Ac}$  ( $T_{1/2} = 10.0$  d) starting after ammonium acetate wash ( $t_1$ ) and integrating over the counting periode time  $\Delta_t$ .

Time  $t_2$  marks start of  $\alpha$ -counting. Measured counts ( $E_{\text{me}}$ ) observed in the  $^{217}\text{At}$  peak region are detected with an efficiency  $\epsilon$  (geometry factor) via a energy calibrated semiconductor  $\alpha$ -detector.

Ingrowth of  $^{225}\text{Ac}$  is directly associated with short lived progenies  $^{221}\text{Fr}$  ( $T_{1/2} = 4.9$  m),  $^{217}\text{At}$  ( $T_{1/2} = 32.3$  ms), and  $^{213}\text{Po}$  ( $T_{1/2} = 4.2$   $\mu\text{s}$ ). Still equilibrated, the first well separated daughter is  $^{217}\text{At}$  at 7067 keV and allowing correction for losses arising throughout the whole chemical procedure.

$E_{\max}$  is given by:

$$E_{\max} = \epsilon F(\Delta_{ft}) A_{^{225}\text{Ra}}^0 e^{-\lambda_{^{225}\text{Ra}}(t_1-t_0)} \frac{\lambda_{^{225}\text{Ac}}}{\lambda_{^{225}\text{Ac}} - \lambda_{^{225}\text{Ra}}} \int_{t_2}^{t_2+\Delta_t} (e^{-\lambda_{^{225}\text{Ra}}(t-t_1)} - e^{-\lambda_{^{225}\text{Ac}}(t-t_1)}) dt \quad (1)$$

$E_{\max}$  =maximal detectable counts in the  $^{217}\text{At}$  peak region

$\epsilon$  =geometrical efficiency of the  $\alpha$ -detector

$A_{^{225}\text{Ra}}^0$  =initial  $^{225}\text{Ra}$  activity (Bq)

$\lambda_{^{225}\text{Ra}}$  =decay constant of  $^{225}\text{Ra}$  ( $\text{s}^{-1}$ )

$\lambda_{^{225}\text{Ac}}$  =decay constant of  $^{225}\text{Ac}$  ( $\text{s}^{-1}$ )

$t_0$  =time of separation from  $^{229}\text{Th}$  (s)

$t_1$  =time of  $^{225}\text{Ac}$  build-up(s)

$t_2$  =start of counting (s)

$\Delta_t$  =counting period (s)

$F(\Delta_{ft})$  =Factor corrects for decay of  $^{225}\text{Ra}$  during time  $\Delta_{ft}$ , needed for Ra extraction. Can be set as one, if sample volume does not exceeds 1 litre by far.

Comparing measured counts ( $E_{\text{me}}$ ), in the  $^{217}\text{At}$  peak region with calculated counts  $E_{\max}$  ( $k = E_{\text{me}}/E_{\max}$ ), the chemical yield ( $k$ ) is given by:

$$k = \frac{E_{\text{me}}}{\epsilon F(\Delta_{ft}) A_{^{225}\text{Ra}}^0 e^{-\lambda_{^{225}\text{Ra}}(t_1-t_0)} \frac{\lambda_{^{225}\text{Ac}}}{\lambda_{^{225}\text{Ac}} - \lambda_{^{225}\text{Ra}}} \int_{t_2}^{t_2+\Delta_t} (e^{-\lambda_{^{225}\text{Ra}}(t-t_1)} - e^{-\lambda_{^{225}\text{Ac}}(t-t_1)}) dt} \quad (2)$$

### 2.5.3. Simultaneous Determination of $\alpha$ -Emitting Ra Isotopes

For absolute determination of Ra isotopes the knowledge of the geometrical factor  $\epsilon$ , assuming homogeneous source distribution (uncertainty  $\delta\epsilon/\epsilon \approx 10\%$ ) is not necessary. By analysing  $^{217}\text{At}$  peak at 7067 keV, counting efficiency is substituted by the more accurate ratio  $E_{\text{me}}/E_{\text{max}}$ , reflecting overall yield including counting efficiency and correction for chemical losses.

Direct determination of  $^{226}\text{Ra}$  is accomplished using  $\alpha$ -peaks at 4602 keV ( $I_\alpha = 0.0555$ ) and 4784 keV ( $I_\alpha = 0.9445$ ), showing no peak overlapping. In contrast to the well separated  $^{226}\text{Ra}$  peaks, the overlapping 5200-5900 keV region includes activities of  $^{223}\text{Ra}$ , 5283-5872 keV and  $^{224}\text{Ra}$ , 5445 keV ( $I_\alpha = 0.050$ ), 5686 keV ( $I_\alpha = 0.950$ ), as well as ingrowing  $^{222}\text{Rn}$ , 5490 keV and  $^{225}\text{Ac}$  5286-5829 keV accompanied with daughter  $^{213}\text{Bi}$  ( $I_\alpha = 0.022$ ), 5549-5869 keV. Grown into secular equilibrium via  $^{219}\text{Rn}$  ( $T_{1/2} = 4$  s), well separated  $^{215}\text{Po}$  ( $T_{1/2} = 4$  s) peak at 7368 keV is used for determination of  $^{223}\text{Ra}$ .

Due to 100%  $^{220}\text{Rn}$  ( $T_{1/2} = 56$  s) retention,  $^{216}\text{Po}$  ( $T_{1/2} = 0.15$  s) peak at 6779 keV could be used likewise for  $^{224}\text{Ra}$  determination, but it has to be taken into account that counts resulting from overlapping peak of  $^{219}\text{Rn}$  6812 keV, must be stripped according to measured  $^{215}\text{Po}$  activity at 7386 keV in the relevant energy region.

Compared to  $^{224}\text{Ra}$  observed  $^{223}\text{Ra}$  activities are much lower. Thus, applying spectrum stripping technique accompanied with generally derogated accuracy, uncertainty for  $^{224}\text{Ra}$  determination only suffers significantly if storage time of prepared  $\alpha$ -source exceeds mean life time (5 days) for  $^{224}\text{Ra}$  by far.

### 3. Discussion

#### 3.1. Ra Determination Using a $^{229}\text{Th}/^{225}\text{Ra}$ Standard Solution

Previous studies showed that in cases where Ra extraction involves sample processing of several litres and high interference levels, less than 95% recovery may occur (Seely and Osterheim, 1998). Including an appropriate internal standard, that mimics the analyte's interaction with the disc leads to more accurate and reliable results. By measuring analyte and standard simultaneously, the number of reiterate calibrations involved is reduced all the same.

To compensate for losses during sample pre-treatment chemically identical  $^{225}\text{Ra}$  suits perfectly. An advantage is its absence in environmental samples and furthermore allowing measurement of all naturally occurring Ra isotopes on a single source directly after sample collection.  $\alpha$ -emitters could be determined without delay.

Recognising ionic radius, shape and electrical charge of the target ion, membrane approach requires no milking of  $^{225}\text{Ra}$  from a  $^{229}\text{Th}$  stock solution prior use. Acidified with nitric acid to 2 M, extraction of aqueous sample, leads to a selective enrichment of the analyte on the membrane. Simultaneously complete separation from disturbing matrix elements can be achieved. Spiked with tracer system  $^{225}\text{Ra}/^{229}\text{Th}$ ,  $^{225}\text{Ra}$  remains on the Radium Rad Disks, whereas  $^{229}\text{Th}$  passes through. The time of  $^{225}\text{Ra}/^{229}\text{Th}$  separation  $t_0$ , has to be noticed and marks the beginning decrease of  $^{225}\text{Ra}$  activity. Accordingly yield calculations must include correction for decay of unsupported  $^{225}\text{Ra}$ . Sample volumes up to 1 litre, require extraction times of 20 min or less. In such cases it is appropriate to define centre of the time slice between start  $t_B$  and endpoint  $t_E$  as time of  $^{225}\text{Ra}/^{229}\text{Th}$  separation  $t_0$ . For larger sample volumes a correction factor  $F(\Delta_{ft})$  is included and given by:

$$F(\Delta_{ft}) = \frac{1 - e^{-\lambda_{^{225}\text{Ra}} \Delta_{ft}}}{\lambda_{^{225}\text{Ra}}} \quad (3)$$

$\Delta_{ft}$  = time slice between filtration start  $t_B$  and endpoint  $t_E$

Formula regards that unsupported  $^{225}\text{Ra}$  activity still decays during accumulation onto the disk. Filtration endpoint  $t_E$  is now set as  $t_0$ .

The procedure for Ra enrichment described here was applied to a wide range of different water types. Using sample volumes between 0.005 and 5 litres,  $^{226}\text{Ra}$  activities were in the range of 0.002 to about 20 Bq/l. The activity of  $^{223}\text{Ra}$  is in generally much lower compared to  $^{226}\text{Ra}$  and typical  $^{223}\text{Ra}/^{226}\text{Ra}$  activity ratios vary between about 0.071 to about 0.166. In contrast, measured  $^{224}\text{Ra}$  activity in groundwater samples (Fig. 3) may exceed those of  $^{226}\text{Ra}$  up to about 2.33 (this study).

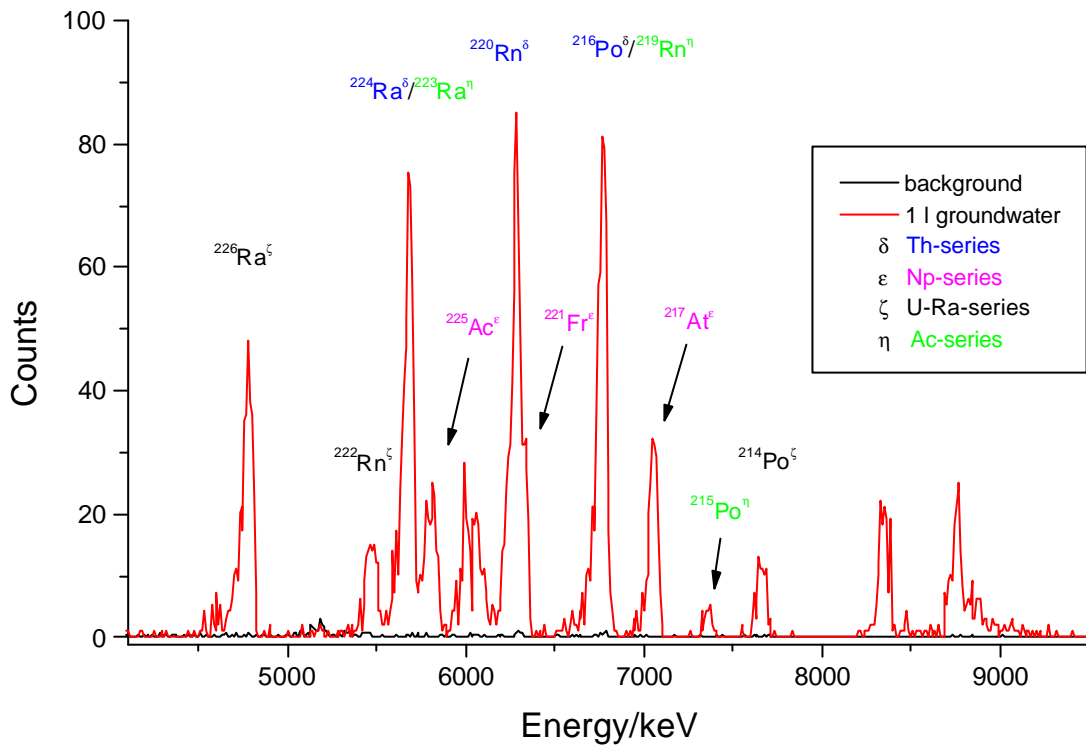


Fig. 3: Typical groundwater sample, measured 12 h after sample collection. Obtained after flaming, high energy resolution (FWHM) of 30 keV, allows straightforward determination of all  $\alpha$ -emitting Ra isotopes in presence of  $^{225}\text{Ra}$  used as yield tracer. Figure depicts the presence of high quantities of short lived isotopes in freshly prepared groundwater samples. Starting the measurement about 12 h after sample collection measured  $^{224}\text{Ra}$  activity exceeds those of  $^{226}\text{Ra}$ .  $^{223}\text{Ra}$  activity can be accurately analysed via the corresponding  $^{215}\text{Po}$  peak. Presence of  $^{225}\text{Ra}$  is indicated by the  $^{217}\text{At}$  activity.

In particular for analysing seawater the use of ion-selective membrane technology allows a rapid and effective enrichment of Ra from highly saline matrices, containing  $^{226}\text{Ra}$  activities in the order of about 2 mBq/l. To determine short lived  $^{224}\text{Ra}$  with a statistical uncertainty of about 5 to 10 % sample volumes can be enlarged to about 5 litres.

## 1.2. Ra Stripping Using Adapted EDTA-Mixtures

For a straightforward assay of Ra loaded onto a membrane it is important to avoid lengthy analytical techniques for Ra stripping. Ensuing eluat should be suited to allow a separation of extraneous matrix components without further pre-treatment. Complete destruction of the disk (Joannon and Pin, 2001) or high amounts of alkaline EDTA (Schönhofer and Wallner, 2001, 3M Test Method Ra-395, 1995) have to be avoided. By using adapted EDTA-mixtures in a specially designed extraction apparatus Ra is effectively stripped and sample pre-treatment involving volume reduction, precipitation or wet ashing are not necessary.

Accurately adjustable conditions are required for quantitative elution of Ra. So the transfer of the disks into better suitable smaller extraction device is recommended. By using the extraction apparatus shown in Fig. 4 a quick and easy insertion of the Ra loaded disk is possible without replacement from underlying filter support and thus avoiding chemical losses caused by embedded air and minimising the risk of membrane destruction. The construction allows the elution of Ra under specific conditions, accurately defined elution volumes, easily controllable pH values and optimally adjustable flow rates. The ensuing eluate is adjusted to pH 4.5 using HNO<sub>3</sub> (semi concentrated). The solution can be transferred to a cation exchange column without further sample pre-treatment.

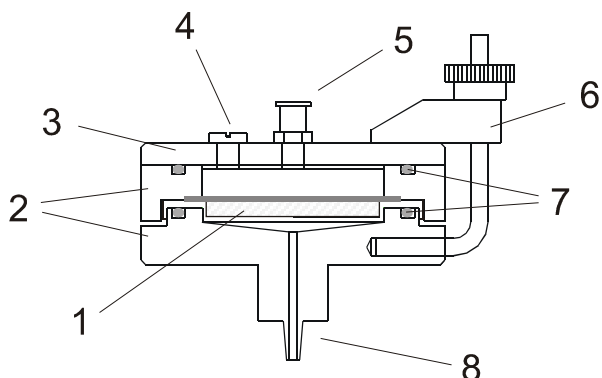


Fig. 4: Extraction device allows easy transfer of Ra loaded disk and stripping of the analyte under controlled conditions. The membrane and underlying filter support (1) are inserted into the extraction device. 3 vices (6) affix Teflon filter mountings (2), transparent polyethylene cap and withal surrounds the filter support. Sealing (7) is appropriately designed to allow elution using gravity flow or a gentle vacuum. Connected via luer adapter (5), syringes are used as reservoir and thus enabling a permanent and controllable flow of extractive reagents. By opening ventilation valve (4) 3 ml of 0.25 N EDTA/1.7 N ammonium acetate in 6 N NH<sub>4</sub>OH are directly mounted onto the extractive disk. After sealing, the reservoir is filled up with 16 ml 0.01 N EDTA/pH 10. The analyte is completely stripped during this wash using a flow rate of 1 ml/min. The second luer adapter (8) is only needed, if a peristaltic pump is used for elution study purpose.

### **3.3. Separation of Disturbing Matrix Composition Using Low Pressure Column-Chromatography**

The separation principle is based on low complexation ability of alkaline earth elements. Ra shows no capability to form EDTA complexes at pH 4.5 and regarding its small hydrate shell is similar to Ba strongly adsorbed on the top of the cation exchange column. Disturbing EDTA-matrix passes through and is completely washed out of the column by using ammonium acetate. This treatment was reported by Hancock and Martin (1991) to elute lead carrier but it is also perfectly suited to prevent formation of EDTA precipitates on the column. Interfering Th, Ac (Durecova, 1997) and uranium (Smith et al., 1997) are not retained on the Radium Rad Disks and thus should not be present on the column. However residual actinides that may have remained are complexed and completely removed (Khopkar and De, 1960).

Separation procedure requires highly cross linked 200-400 mesh cation exchange resins to achieve a sufficient separation of Ra and Ba. Denoted amounts of resin (Hancock and Martin, 1991) are usually adequate to achieve sufficient Ba separation, resulting in excellent  $\alpha$ -spectrum resolution. But flow rates, obtained by gravity flow, are too low for our purpose and even degreased with time. By using low pressure column chromatography flow rates are stable and can be adjusted to 1.0-1.2 ml/l. Convenient handling of the separation procedure described in this paper allows parallel processing of 8 to 10 samples within 5 hours. The chemical procedure could be easily automated via computer-controlled valves and pumps and operator time could be minimised furthermore.

### **3.4. Production of Homogenous $\alpha$ -Sources in Presence of Ba**

Electrochemical parameters, such as ionic strength (Tome and Sanchez, 1991), deposition time, distance between the cathode and the anode, pH-value (Lee and Pimpl, 1999) and temperature (Talvity, 1972) are important factors in achieving a thin and uniform deposit, their influences are well studied in the effective production of actinide sources. In contrast to the quantitative plating of actinides from hot aqueous solutions, sufficient deposition of Ra could not be achieved under similar conditions. Optimised conditions allow deposition from aqueous solution (Roman, 1984), but suffer from long plating time. Plating from organic solutions (Koide and Bruland, 1974, Short, 1986) allows adequate Ra deposition with improved energy resolution and reduced deposition time.

In the case of minimal Ba contamination of several  $\mu\text{g}$  observed energy resolution shows no strong dependence of chosen distance between electrodes. After flaming FWHM-values are in

the range of 26-40 keV. In environmental samples complete separation of Ba and Ra is difficult and not given for groundwater samples, that contain Ba in quantities exceeding 1 mg by far. After chemical preparation a Ba residual remains in the final Ra fraction and a critical value of 100 µg may be exceeded. Avoiding renewed chemical processing,  $\alpha$ -spectrometric assay becomes more robust to the presence of Ba by increasing the distance between the electrodes during electrolysis. Thus, in the case of higher aerial mass an improved homogeneity of the electrical field guarantees optimal spectrum resolution and allows uniform plating of Ra and Ba likewise. Self absorption in the prepared source is brought to a minimum. Evaporation of the volatile electrolyte composition is negligible and refilling is not necessary due to compensation of increased heat dissipation. More over cooling of the deposition cell enhances deposition yield.

In a series of experiments efficient plating of the analyte has been tested by the behaviour of Ba, acting as a carrier. Equilibrium between the deposition of bariumhydroxyd ( $\text{Ba(OH)}_2$ ) and its redissolution is controlled by the temperature of the solution. Accordingly, improved plating efficiency of easily soluble Ba and Ra can be attained in a cooled electrolyte solutions.

Fig. 5a-c show three scans of  $^{133}\text{Ba}$  sources deposited onto stainless steel disks and illustrates the influence of varying distances between electrodes and the effect of varying temperature. Electrodeposition is carried out for 1 h applying an electrical current fixed to about 120 mA. A distance of 2 mm (Fig. 5a) results in a chemical yield of about 89 % which is sufficient for Ra plating. However, the deposited material is not homogeneously distributed on the surface of the planchette. Extending the distance to 7 mm (Fig. 5b) a homogenous field and material deposition is achieved. However, warming of the solution resulted in a low deposition yield of only about 76 %. Plating efficiency is optimised maintaining a distance of about 7 mm between anode and cathode while cooling down the deposition cell (Fig. 5c) to about 1.5°C. In the latter case the obtained deposition yield is about 98 %.

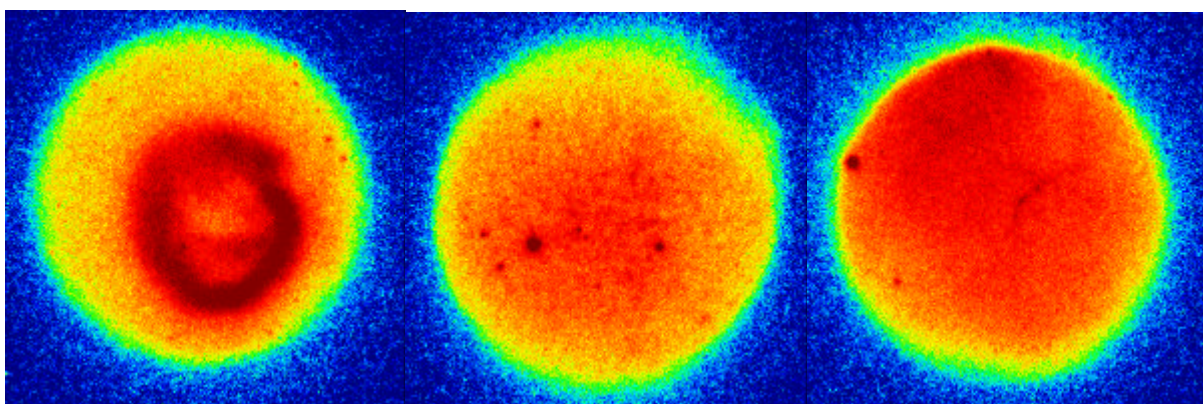


Fig.5:  $^{133}\text{Ba}$ -sources, assayed using Fuji BAS-1800 Bio-Imaging Analyser from Raytest, a) non uniform deposit, obtained using 2 mm distance between electrodes, b) reduced recovery due to warming of the electrolyte, using 7 mm distance, c) effective production of uniform deposits due to the use of a coolable cell, maintaining 7 mm distance.

Conditions and results of the deposition study are listed in Tab.1.

Tab. 1: Conditions and results obtained in a coolable deposition cell, using identical electrolyte composition solution and a fixed current of 120 mA.

<sup>133</sup> Ba source	Distance/mm	Voltage/V	Final temp./°C	Uniformity	Yield/%
a	2	25-35	52	insufficient	89
b	7	70-80	65	improved	76
c	7	90-100	31	improved	98

### 3.5. High Rn Retention in thin Deposits

Studying the effect of radon emanation from thin Ba free  $\alpha$ -sources, prepared in organic solution and accomplished according to methods proposed by Hancock and Martin (1991) and by Witehead et al. (1992), Juardo Vargas et al. (1996 a) observed significant <sup>222</sup>Rn diffusion. Reaching equilibrium after 19 days resulting the <sup>222</sup>Rn/<sup>226</sup>Ra ratio is 0.5. Introducing a diffusion coefficient D Authors were able to describe time dependent behaviour of the radon activity according to equation:

$$\frac{A_{222}Rn(t)}{A_{226}Ra} = \frac{\lambda_{222}Rn}{\lambda_{222}Rn - \lambda_{226}Ra + D} (1 - e^{-(\lambda_{222}Rn - \lambda_{226}Ra + D)t}) \quad (4)$$

$A_{222}Rn$  =activity of <sup>222</sup>Rn (Bq)

$A_{226}Ra$  =activity of <sup>226</sup>Ra (Bq)

$\lambda_{222}Rn$  =decay constant of <sup>222</sup>Rn ( $s^{-1}$ )

$\lambda_{226}Ra$  =decay constant of <sup>226</sup>Ra ( $s^{-1}$ )

$\lambda_{222}Rn$  =decay constant of <sup>222</sup>Rn ( $s^{-1}$ )

D =diffusion coefficient ( $s^{-1}$ )

Determined diffusion coefficient  $D = 2.060 \times 10^{-6} s^{-1}$  is in the order of the decay constant  $\lambda_{222}Rn = 2.098 \times 10^{-6} s^{-1}$  and decreases, if Ba is added to the solution (Juardo Vargas et al., 1996 a). Coherently, calculating related systems <sup>219</sup>Rn/<sup>223</sup>Ra and <sup>220</sup>Rn/<sup>224</sup>Ra, assuming similar diffusion coefficients for <sup>219</sup>Rn and <sup>220</sup>Rn, but considering that decay constants are orders of magnitudes higher, resulting ratios are practicable one likewise. For the system <sup>220</sup>Rn/<sup>224</sup>Ra the <sup>220</sup>Rn retention is calculated to be 0.99997 (Juardo Vargas et al., 1996 b). To explain reported <sup>220</sup>Rn losses, corresponding to measured <sup>220</sup>Rn/<sup>224</sup>Ra ratios in the range of 0.569-0.771 (Hancock and Martin, 1996), an improved model (Juardo Vargas, 2000) with a remarkably high diffusion coefficient  $D = 0.01-0.1 s^{-1}$  on the surface is used. Applying the improved model, all the same activity ratios of <sup>219</sup>Rn/<sup>223</sup>Ra and <sup>220</sup>Rn/<sup>224</sup>Ra must exceed those of <sup>222</sup>Rn/<sup>226</sup>Ra.

Thus, quantitative  $^{222}\text{Rn}$  retention will guarantee complete sealing for  $^{219}\text{Rn}$  and  $^{220}\text{Rn}$ . Consequently this will simplify  $^{223}\text{Ra}$  and  $^{224}\text{Ra}$  determination and, without further calibration, allow their straightforward determination via their daughters. Indeed, using recommended electrochemical parameters to prepare  $\alpha$ -sources and heating to glow to affix the deposit, a quantitative  $^{222}\text{Rn}$  retention is observed. Without a diffusion term and taking into account  $\lambda_{^{222}\text{Rn}} \gg \lambda_{^{226}\text{Ra}}$ , Fig. 6 shows time dependent behaviour of  $^{222}\text{Rn}$  according to commonly used ingrowth equation:

$$\frac{A_{^{222}\text{Rn}}(t)}{A_{^{226}\text{Ra}}} = 1 - e^{-(I_{^{222}\text{Rn}})t} \quad (5)$$

During six measurements (53a – 53f, Tab. 2), accomplished in succession, the activity ratio  $^{222}\text{Rn}/^{226}\text{Ra}$  is determined. After integration of equation (5) over time of measurement  $\Delta_t$  and rearranging, detected counts  $E_{222}$ ,  $E_{226}$  in the  $^{222}\text{Rn}$  and  $^{226}\text{Ra}$  peak region are analysed according to the resulting equation:

$$\ln \left\{ \left( \frac{E_{222}}{E_{226}} - 1 \right) \frac{I_{^{222}\text{Rn}} \Delta_t}{e^{-I_{^{222}\text{Rn}} \Delta_t} - 1} \right\} = I_{^{222}\text{Rn}} (t_1 - t_0) \quad (6)$$

$t_0 - t_1$  =time slice between flaming,  $t_0$ , and start of counting,  $t_1$ .

From a linear approximation of the measured data a decay constant for  $^{222}\text{Rn}$  of  $\lambda_{^{222}\text{Rn}} = 2.13 \pm 0.13 \cdot 10^{-6} \text{ s}^{-1}$  can be calculated. Latter value is in agreement with literature data of  $\lambda_{^{222}\text{Rn}} = 2.0982 \cdot 10^{-6} \text{ s}^{-1}$  (<http://iaeand.iaea.or.at/nudat/radform.html>). The perfect agreement of both values clearly proofs that the diffusive loss of  $^{222}\text{Rn}$  and hence of  $^{220}\text{Rn}$  and  $^{219}\text{Rn}$  is minor to negligible.

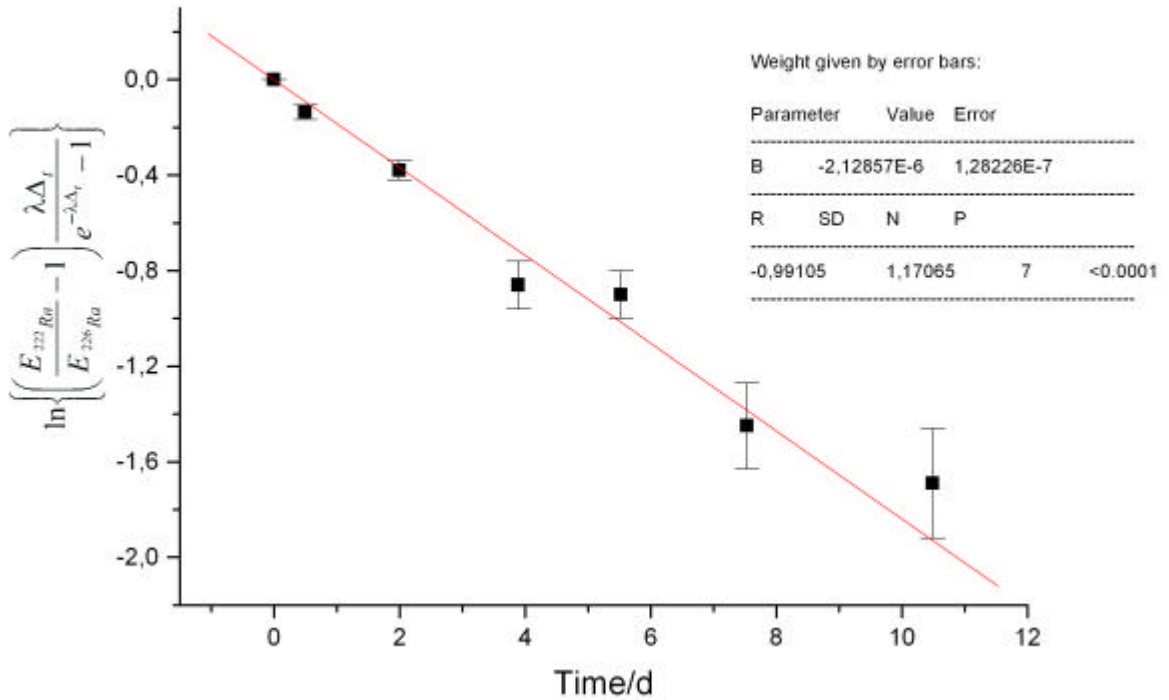


Fig. 6: Fitted decay constant  $\lambda_{^{222}\text{Rn}} = 2.13 \pm 0.13 \cdot 10^{-6} \text{ s}^{-1}$  is in perfect agreement with literature data. The influence of Radon diffusion is minimal and thus allows description of time dependent behaviour of  $^{222}\text{Rn}$  according to commonly used ingrowth equation (5).

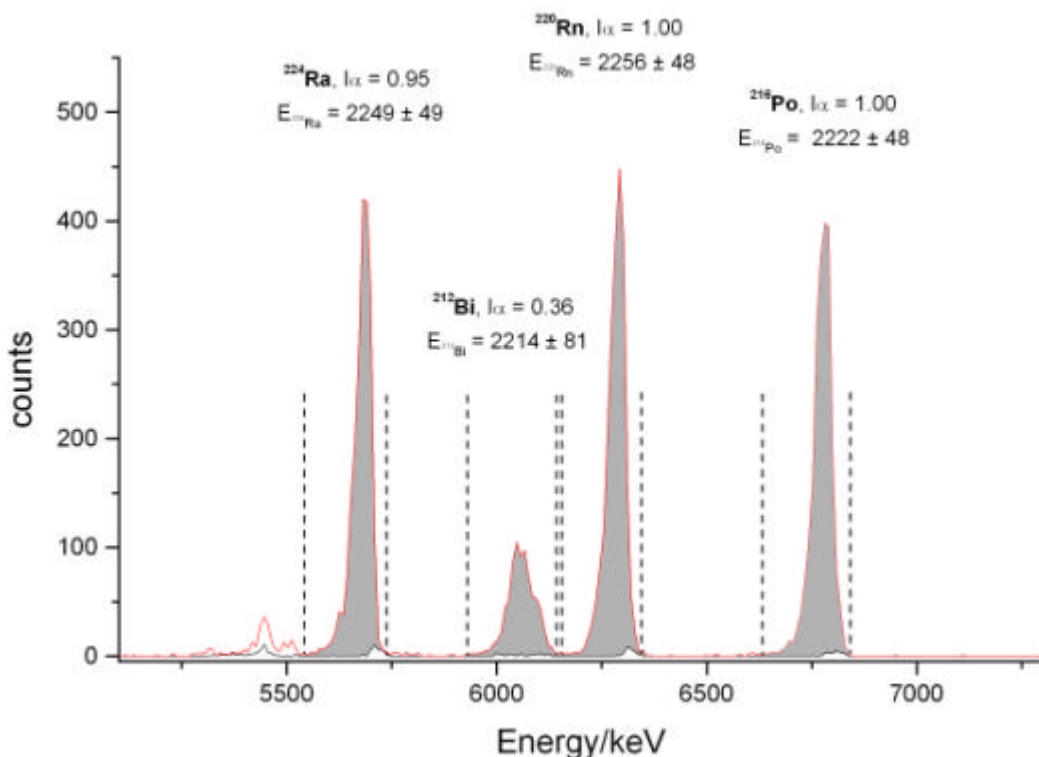
The summation of detected counts acquired during overall time of measurement (Tab. 2: sample 53a-f) results in a total activity ratio  $^{222}\text{Rn}/^{226}\text{Ra} = 0.653 \pm 0.013$ . Using constant diffusion model, described by equation (4) obtained diffusion coefficient is  $D \leq 6 \cdot 10^{-8} \text{ s}^{-1}$ .

In consistence with both approaches quantitative  $^{222}\text{Rn}$  retention is shown even in thin  $\alpha$ -sources.. Due to minimal  $^{222}\text{Rn}$  losses, equilibrium is reached after one month, resulting in an observed activity ratio of  $^{222}\text{Rn}/^{226}\text{Ra} \geq 0.97$ .

Tab. 2.  $^{222}\text{Rn}/^{226}\text{Ra}$  ratios acquired from six successional accomplished measurements.

sample	time $t_0-t_1/d$	time $D_t/d$	activity ratio $^{222}\text{Rn}/^{226}\text{Ra}$
53	0	-	0
53a	0.5000	1.4962	$0.235 \pm 0.020$
53b	1.9962	1.8955	$0.421 \pm 0.025$
53c	3.8917	1.6338	$0.634 \pm 0.036$
53d	5.5255	2.0114	$0.659 \pm 0.033$
53e	7.5299	2.9584	$0.819 \pm 0.032$
53f	10.488	3.0300	$0.858 \pm 0.032$
53a-f	0.5000	13.0183	$0.653 \pm 0.013$

Confirming the complete sealing for short lived isotopes  $^{219}\text{Rn}$  and  $^{220}\text{Rn}$ , Fig. 7 illustrates, within given uncertainties (1  $\sigma$ ), radioactive equilibrium, between  $^{224}\text{Ra}$ , its direct progeny  $^{220}\text{Rn}$  and  $\alpha$ -emitting daughters. Analysed  $\alpha$ -source is maintained following the given procedure for the preparation from an equilibrated  $^{232}\text{U}$ -standard solution (DAMRI, Gif-sûr-Yvette: product-code 015685, U232-ELSA45, No4571) and counted 10 min after flaming to assure equilibration. After background subtraction, given counts E are acquired from detected counts  $E_{\text{me}}$  in marked regions of interest and calculated according to specified  $\alpha$ -radiation intensity  $I_\alpha$ .

Fig. 7: Source maintained from a  $^{232}\text{U}$ -standard solution. Spectrum shows  $^{224}\text{Ra}$  and equilibrated  $\alpha$ -emitting progenies. According to given uncertainties no significant  $^{220}\text{Rn}$  losses are observed

Radon losses may occur during long storage times due to possible alterations in the nature of the protective film. Nevertheless the  $\alpha$ -spectrum in Fig. 8 shows that the diffusive characteristics of the surface could ensure quantitative radon retention, even in aged samples. The source, was prepared from Baltic seawater and, after being analysed for short lived Ra isotopes, was stored for several months allowing ingrowth of  $^{228}\text{Th}$  and determination of  $^{228}\text{Ra}$  via its  $\alpha$ -emitting daughters. Avoiding a second flaming procedure, source was counted without further treatment.

Analysing system  $^{224}\text{Ra}$  and progenies according to marked regions of interest (Fig. 8) resulting activity ratios are  $^{220}\text{Rn}/^{224}\text{Ra} = 0.982 \pm 0.044$  and  $^{216}\text{Po}/^{224}\text{Ra} = 0.995 \pm 0.044$  respectively. Within uncertainties, the activity of each particular progeny equals that of  $^{224}\text{Ra}$  and thus confirming a closed system with negligible losses of  $^{220}\text{Rn}$ .

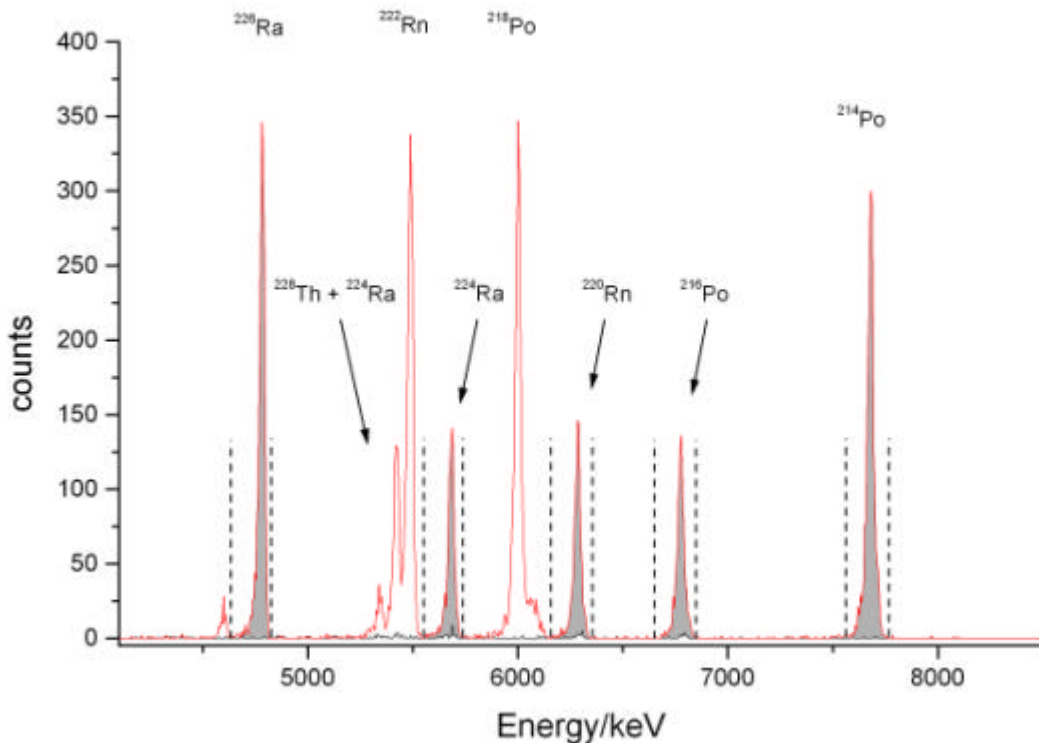


Fig. 8:  $\alpha$ -spectrum to illustrate the excellent energy resolution attained from a Baltic seawater sample. Source to detector distance was 4 mm. Despite storage of several months quantitative radon retention was observed. Dashed lines mark regions of interest.

## 4. Summary

High selectivity of solid phase extraction disks allows effective Ra enrichment in presence of a  $^{225}\text{Ra}$  yield tracer, added in radioactive equilibrium with its parent  $^{229}\text{Th}$ . By simply sucking the aqueous sample through the membrane a rapid preconcentration of all Ra isotopes is achieved where as  $^{229}\text{Th}$  and main fraction of disturbing elements are removed simultaneously within in one single step. The use of an optimally adapted ion exchange procedure further on reduces the number of chemical operations involved and prevents lengthy and time consuming sample preparation. Effective separation from inactive matrix components enables the production of thin and uniform counting samples, via electrodeposition, in which the energy loss of  $\alpha$ -particles through self-absorption is very low. Accompanied by  $^{225}\text{Ra}$ , all four naturally occurring Ra isotopes are affixed simultaneously onto a single disc.  $\alpha$ -emitting  $^{223}\text{Ra}$ ,  $^{224}\text{Ra}$  and  $^{226}\text{Ra}$  can be determined directly without any ingrowth time. Despite of minimal thickness radon losses from the prepared  $\alpha$ -source were not observed. Thus, procedure proposed here allows the determination of Ra isotopes via ingrowth of short-lived daughters, leading to simplified spectrum analysis and allows furthermore determination of  $^{223}\text{Ra}$  and  $^{224}\text{Ra}$  with improved accuracy.

If focus is on the short lived isotope  $^{224}\text{Ra}$  time is a vital factor and counting should be performed as soon as possible. Preparing a recently collected aqueous sample, chemical procedure takes 5 hours and thus substantial losses due to radioactive decay can be avoided. In hydrological tracer studies, using long and short live Ra isotopes, the number of samples could be analysed for  $^{224}\text{Ra}$  in one campaign is primarily limited to its mean life time of about 5 Days. Simplified accomplishment and reduction of operator time enabling the convenient preparation of 8 - 10 samples simultaneously. Due to low-costs of  $\alpha$ -spectrometry systems (compared to  $\gamma$ -spectrometry and LSC) a number of  $\alpha$ -detectors is commonly available. Despite the counting times of 1 to 3 days, ordinarily used in  $\alpha$ -spectrometric analysis (resulting in a detection limit of 0.2 mBq), operating in parallel, thus leads to the required high sample through put.

## References

- Durecova, A., 1997. Contribution to the simultaneous determination of  $^{228}\text{Ra}$  and  $^{226}\text{Ra}$  by using 3M's Empore<sup>TM</sup> Radium Rad Disks, *J. Radioanal. Nucl. Chem. Art.* 223, 225.
- Ferrero Calabuig, J.L., Martín Sánchez, A., Roldán García, C., Vera Tome, F., Da Silva, M.F., Soares, J.C., Juanes Barber, D., 1998. Semipermeable membrane to retain platinum atoms in the electrodeposition process of alpha spectrometry sources, *Int. J. Appl. Radiat. Isot.* 49, 1269.
- Goken, G.L., Bruening, R.L., Krakowiak, K.E., Izatt, R.M., 1999. In Metal-ion separation and preconcentration: Progress and opportunities, Bond, A.H., Dietz, M.L., Rogers, R.D., (Eds.), pp. 251-259, ACS Symposium Series 716, Washington, D.C..
- Joannon, S., Pin, C., 2001. Ultra-trace determination of  $^{226}\text{Ra}$  in thermal waters by high sensitivity quadrupol ICP-mass spectrometry following selective extraction and concentration using radium-specific membrane disks, *J. Anal. At. Spectrom.* 16, 32.
- Juardo Vargas, M., Fernández de Soto, F., 1996a. A study of  $^{222}\text{Rn}$  emanation in electrodeposited sources of  $^{226}\text{Ra}$  with barium, *Nucl. Instrum. Methods Phys. Res. A*368, 488.
- Juardo Vargas, M., Fernández de Soto, F., 1996b. On the determination of  $^{223}\text{Ra}$  and  $^{224}\text{Ra}$  from their daughter products in electrodeposited sources of radium, *Int. J. Appl. Radiat. Isot.* 47, 129.
- Jurado Vargas, M., 2000. A model to explain simultaneously the  $^{222}\text{Rn}$  and  $^{220}\text{Rn}$  emanation from thin electrodeposited sources; *Nucl. Instrum. Methods Phys. Res. A*447, 608.
- Hancock, G.J., Martin, P., 1991. Determination of Ra in environmental samples by  $\alpha$ -particle spectrometry, *Int. J. Appl. Radiat. Isot.* 42, 63.
- Hancock, G.J., Martin, P., 1996. Reply to Vargas and de Soto: On the determination of  $^{223}\text{Ra}$  and  $^{224}\text{Ra}$  from their daughter products in electrodeposited sources of radium, *Int. J. Appl. Radiat. Isot.* 47, 131.
- Khopkar, S.M., De, A.K., 1960. Cation-exchange behaviour of barium on Dowex 50W-X8, *Analytica Chimica Acta* 23, 441.
- Koide, M., Bruland, K.W., 1974. The electrodeposition and determination of radium by isotopic dilution in sea water and in sediments simultaneously with other natural radionuclides; *Analytica Chimica Acta* 75, 1.
- Lee, M.H., Pimpl, M., 1999. Development of a new electrodeposition method for Pu-determination in environmental samples, *Int. J. Appl. Radiat. Isot.* 50, 851.
- Roman, D., 1984. Electrodeposition of radium on stainless steal from aqueous solutions, *Int. J. Appl. Radiat. Isot.* 35, 990.

- Tome, F.V., Sanchez, A.M., 1991. Optimizing the parameters affecting the yield and energy resolution in the electrodeposition of uranium. *Int. J. Appl. Radiat. Isot.* 42, 135.
- Schönhöfer, F., Wallner, G., 2001. Very rapid determination of  $^{226}\text{Ra}$ ,  $^{228}\text{Ra}$  and  $^{210}\text{Pb}$  by selective adsorption and liquid scintillation spectrometry, *Radioac. Radiochem.* 12, 33.
- Seely, D.C., Osterheim, J.A., 1998. Radiochemical analyses using Empore<sup>TM</sup> Disk Technology, *J. Radioanal. Nucl. Chem. Art.* 236, 175.
- Short, S.A., 1986. Measurement of all radium isotopes at environmental levels on a single electrodeposited source; *Nucl. Instrum. Methods Phys. Res. B* 17, 540.
- Smith, L.L., Alvarado, J.S., Markun, F.J., Hoffmann, K.M., Seely, D.C., Shannon, R.T., 1997. An evaluation of radium-specific, solid phase extraction membranes, *Radioac. Radiochem.* 8, 30.
- Talvitie, N.A., 1972. Electrodeposition of actinides for alpha spectrometric determination, *Anal. Chem.* 44, 280.
- Weber, R., Esterlund, R.A., Patzelt, P., 1999. On the energy resolution of  $\alpha$ -sources prepared by electrodeposition of uranium, *Nucl. Instrum. Methods Phys. Res. A* 423, 468.
- Whitehead, N.E., Ditchburn, R.G., McCabe, W.J., Van der Raaij, R., 1992. Factors affecting the electrodeposition of  $^{226}\text{Ra}$ . *J. Radioanal. Nucl. Chem. Art.* 160, 477.
- 3M Test Method Ra-395, 1995. Rapid determination of radium-226 in water using Empore<sup>TM</sup> Radium Rad Disks, [www.3m.com/empore/Library/PDFS/RAD/Ra\\_395.pdf](http://www.3m.com/empore/Library/PDFS/RAD/Ra_395.pdf)
- Radiation retrieval parameters, <http://iaeand.iaea.or.at/nudat/radform.html>.

### **Kapitel III. Radium und Radon als natürliche Tracer**

## **Determination of Radium Isotopes and $^{222}\text{Rn}$ in a Groundwater Affected Coastal Area of the Baltic Sea and the Underlying Sub-Sea Floor Aquifer**

**Stefan Purkl and Anton Eisenhauer**

## Abstract

All four naturally occurring radium isotopes ( $^{223}\text{Ra}$ ,  $^{224}\text{Ra}$ ,  $^{226}\text{Ra}$ ,  $^{228}\text{Ra}$ ) and  $^{222}\text{Rn}$  in the groundwater affected Eckernförder Bay (EB) of the Baltic Sea (Germany) were measured using optimal adapted analytical methods for their extensive field surveillance.

Dispersive physical mixing acting over time scales in the order of days is responsible for the distribution of  $^{223}\text{Ra}$ ,  $^{224}\text{Ra}$  and  $^{222}\text{Rn}$  in EB. The distribution of these natural tracers is controlled by the strength of the sedimentary source, the influence of direct groundwater input, the dispersive mixing coefficient in the water column and their own radioactive decay. Using a one-dimensional transport model, distribution of  $^{224}\text{Ra}$  in the deep water can be described suggesting a horizontal dispersivity in the range between  $10^0$  to  $5 \times 10^1 \text{ m}^2\text{s}^{-1}$ .

From the inventory of  $^{222}\text{Rn}$  ( $72.4 \pm 7.4 \text{ Bqm}^{-2}$ ) in the EB the obtained groundwater discharge rate can be estimated to be  $1.7 \pm 0.3 \text{ m}^3\text{s}^{-1}$ . In order to balance the inventory of  $^{223}\text{Ra}$  ( $0.52 \pm 0.22 \text{ Bqm}^{-2}$ ) and  $^{224}\text{Ra}$  ( $6.46 \pm 2.6 \text{ Bqm}^{-2}$ ) a source other than groundwater seepage has to be responsible for almost all of the  $^{224}\text{Ra}$  and  $^{223}\text{Ra}$  inventory of the EB. Diffusion from sediments seems to be the major source for short-lived Ra isotopes in the lower water column of EB.

## 1. Introduction

Ra (Bollinger and Moore, 1993; Rama and Moore, 1996) and Rn (Cable et al., 1996) are ideal suited natural tracers to analyse mixing processes between ground- and near coastal seawater. In seawater the generally low Ra and Rn concentrations (in the order of  $\text{mBql}^{-1}$ ) are related to the insolubility of thorium (Th) being the parent (grandparent) nuclide of Ra and Rn, respectively (Fig. 1). A major source for Ra in seawater is diffusion out of the marine sediments (Li, 1977) and the riverine input including both, dissolved and sedimentary load (Hancock and Murray, 1996). However, there is a third important source being the direct input of Ra enriched groundwaters into the coastal zone which has recently been recognised and emphasized by Moore (1996). During the percolation of groundwater through the geological structure the fluid becomes enriched in Rn and Ra. High concentrations (in the order of  $\text{Bql}^{-1}$ ) are mainly related to their easy solubility but also controlled by their adsorptive behaviour. For short-lived isotopes enrichment via  $\alpha$ -recoil mechanisms (Krishnaswami et al., 1982) have to be taken in consideration. The discharge of these natural tracers into the depleted water column, provides a time information due to their radioactive decay. The spectrum of half-lives ( $T_{1/2}$ ) (Fig. 1) allows

to study mixing processes on different length scales. Large scale mixing can be monitored using long lived radium isotopes  $^{226}\text{Ra}$  and  $^{228}\text{Ra}$  (Schmidt and Reyss, 1996).

To analyse near coastal mixing processes between ground- and seawater in the range of about  $10^0$  to  $10^3\text{ m}$  there is need for short-lived radio tracers, having half-lives in the order of days (Moore, 2000). But, recently applied methods for the determination of short-lived  $^{224}\text{Ra}$  ( $T_{1/2}=3,66\text{ d}$ ), and  $^{223}\text{Ra}$  ( $T_{1/2}=11,43\text{ d}$ ) need an elaborated counting equipment (Moore and Arnold, 1996) and are sensitive to the water content (Sun and Torgersen, 1998) of the counted manganese fibers (Moore and Reid, 1973). Other techniques suffer from very time consuming chemical preparation prior to radiometric measurement (Elsinger et al., 1982) also restricting the broad application of these natural tracers.

In order to overcome these problems we apply a radium-specific membrane technique and use  $^{225}\text{Ra}$  as an internal standard. Simultaneous measurement of all radium isotopes on one single source allows their determination via  $\alpha$ -spectrometry in  $\text{mBq}^{-1}$  quantities. Without the need for complicated and painstaking sample preparation the chemical procedure is accomplished within 5 hours. Simplified accomplishment and the reduction of operator time enabling the convenient preparation of 8 to 10 samples simultaneously.

In an attempt to extend our study we applied liquid scintillation (LS) counting in order to determine the  $^{222}\text{Rn}$  ( $T_{1/2}=3.82\text{ d}$ ) concentrations of seawater samples directly on board of a research vessel.  $^{222}\text{Rn}$  concentrations are measured using "Triathler", a portable, single tube liquid scintillation spectrometer (Haaslahti et al., 2000), which allows sensitive  $\alpha$ -counting of Rn activities down to a concentration of about 2.5  $\text{mBq}$ .

Both new methods were applied to the measurement of  $^{228}\text{Ra}$ ,  $^{226}\text{Ra}$ ,  $^{224}\text{Ra}$ ,  $^{223}\text{Ra}$  and  $^{222}\text{Rn}$  in Eckernförde Bay (EB), Germany (Fig. 2). This bay is known to be affected by submarine groundwater discharge (Bussmann and Suess, 1998). The goal of this study is to analyse the parameters influencing the distribution of Ra and Rn in the water column and the underlying sub-sea floor aquifer and further on to provide an estimate for rates of ground water discharge.

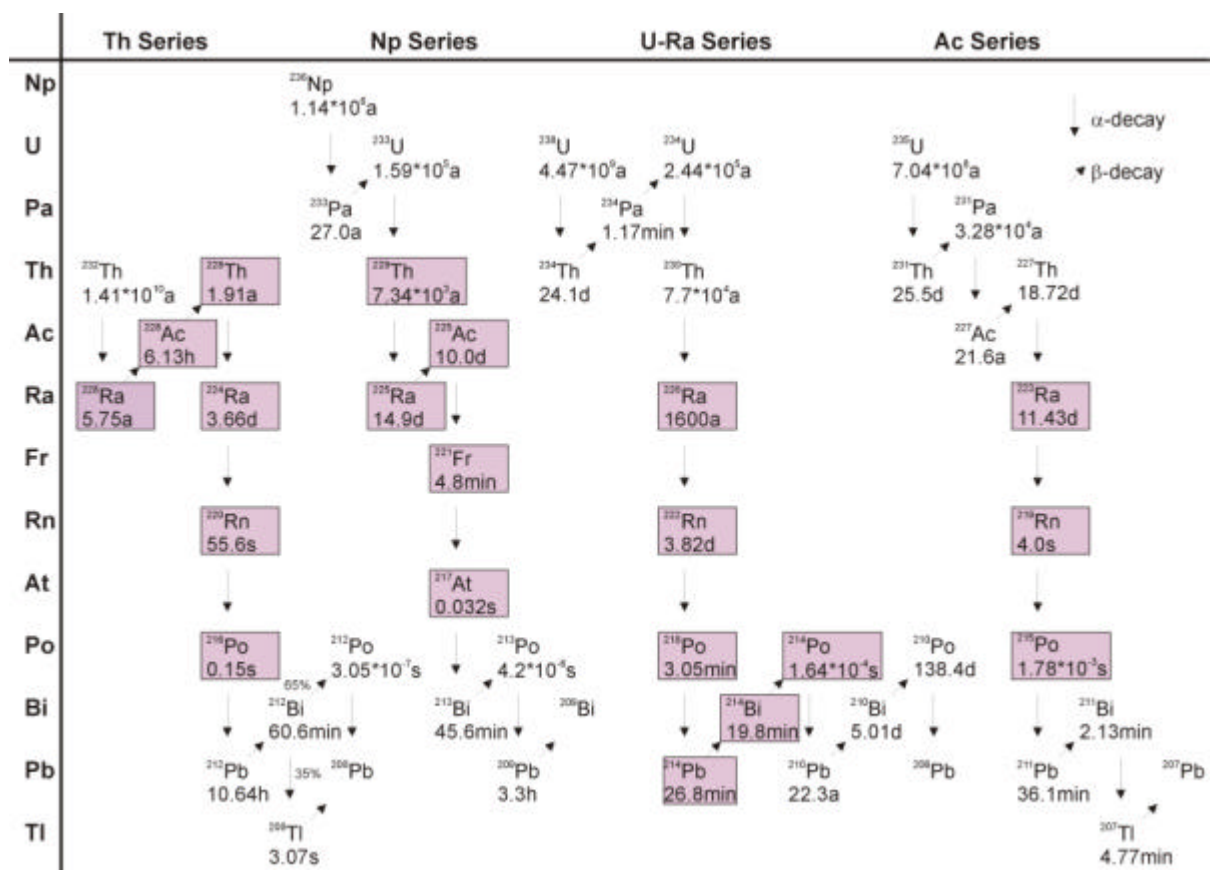


Fig.1: Nuclides of the four decay chains including their half-lives, and decay characteristics. Boxes indicate nuclides involved in the analytical methods presented in this study.

## 2. Location and Sampling

Morphology of EB was largely created during the Scandinavian ice sheet retreat. Main groundwater aquifers consist of layers of high hydraulic conductivity deposited during the Pleistocene and the Holocene. The upper boundary of the studied aquifer lies only 4 to 5 meters below the sea floor (Sauter et al., *in press*). Within the framework of the EU project SUB-G.A.T.E. (Submarine Groundwater-fluxes and Transport-processes from methane-rich coastal sedimentary Environments) diffusive submarine freshwater seepage was mainly observed near the coast. In bowl-shaped bottom depressions ((pockmarks), (Edgerton et al., 1966) (Hovland and Judd, 1988)), also observed in greater distance from the shore (Whiticar and Werner, 1981), salinity decreases downwards to freshwater values as a function of the sediment depth representing the increasing influence of the groundwater input.

EB water profiling and groundwater monitoring was carried out during seven cruises between Mai 2000 and September 2001. The deeper water column was sampled at several depths. For high resolution sampling a horizontal 5 litre water sampler was applied. Standard oceanographic profiles were taken using a CTD sensor. Typically, the thermocline is observed between 7 and 11 m water depth (not observed in February 2001). In general, the deeper water is poorly stratified indicating a well mixed water column. During two weeks before sampling no considerable changes in hydrographic conditions are observed. All Sites are shown in Fig. 2 together with a well onshore, sampled in August 2000.

Pre-investigating the underlying aquifer (1 km off shore), a temporary well was deployed at P2. The deploying technique is based on a modified sediment vibro corer system, described in detail by Sauter et al. (*in press*). The groundwater obtained 4-6 m below the sea floor, was pure freshwater, indicated by a salinity of 0.2 ‰. For the following long term monitoring a stationary well was drilled at the same site in November 2000. For both wells a Grundfos<sup>TM</sup> MP1 submersible pump had been used for groundwater collection.

For Ra analysis sea- and groundwater was pre-filtered through Nuclepore<sup>TM</sup> polycarbonate filters (diameter  $\phi = 142$  mm,  $0.4\text{ }\mu\text{m}$  nominal pore width) and directly transferred into five litre PP-canisters (seawater) and one litre PE-bottles (groundwater) respectively. A certain amount of nitric acid ( $w = 65\text{ \%}$ ) has to be added until, as to achieve a final concentration of about  $c(\text{HNO}_3) = 2\text{ mol}^{-1}$ . After adding a defined amount of a  $^{229}\text{Th}/^{225}\text{Ra}$  standard solution, the sample is shaken vigorously several times assuring complete equilibration. Radium analysis is carried out as described in chapter 3.

For  $^{222}\text{Rn}$  determination in seawater, one litre of the sample is carefully transferred into an extraction apparatus by continuously flushing the system with four aliquots of the applied volume. While completely sealed, 22 ml of a water-immiscible scintillation cocktail MaxiLight (Hidex Oy, Turku) is added. By shaking the sample vigorously,  $^{222}\text{Rn}$  becomes enriched in the organic phase. This phase is transferred in a low diffusive LS-vial and set aside for three hours to improve the  $\alpha$ -counting efficiency. Analysis by LS-counting is carried out as described in chapter 4.

For  $^{222}\text{Rn}$  determination in groundwater, extraction is accomplished directly in a 7 ml frosted glass vial. 3.5 ml MaxiLight are carefully sublayered with 3.5 ml of the un aerated water sample, capped and shaken vigorously. After waiting three hours, the sample is analysed by LS-counting as described in chapter 4.

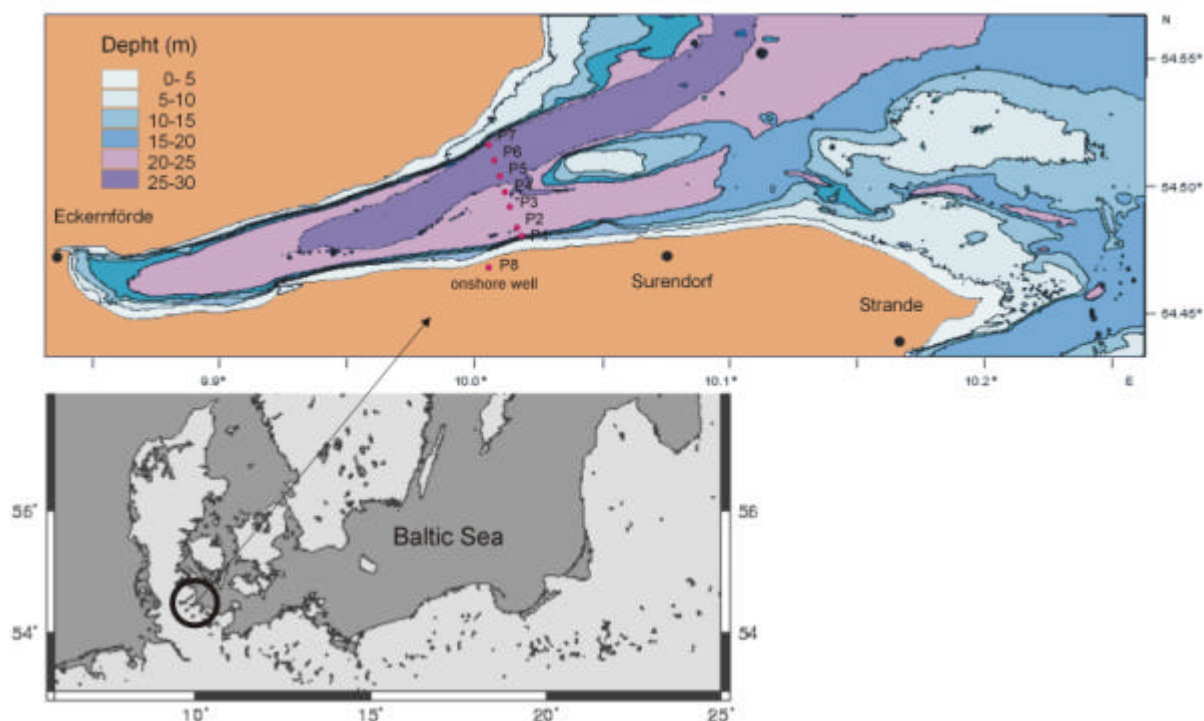


Fig. 2: Sample locations in the EB.

### 3. Simultaneous Determination of Ra Isotopes

Using 3M Empore<sup>TM</sup> Radium Rad Disks a rapid enrichment of the analyte can be achieved. Based on the selectivity of macrocyclic ligands, this solid phase extraction disks simultaneously allow a quantitative separation from extraneous matrix components. In earlier studies Smith et al. (1997) applied this effective enrichment procedure, resulting in recoveries of 95 % or better for one litre aqueous samples.

For the processing of up to five litres Baltic seawater addition of a  $^{225}\text{Ra}$  spike allows correction for chemical losses. The Ra fraction can be stripped from the disk using EDTA/ammonium acetate in alkaline solution. Low pressure column chromatography is used to eliminate the EDTA. The ensuing eluate is ideally suited for electrodeposition.  $\alpha$ -spectrometric analysis (Fig. 3) allows the direct determination of  $^{226}\text{Ra}$  via  $\alpha$ -lines at 4602 keV and 4784 keV and the indirect determination of  $^{224}\text{Ra}$  and  $^{223}\text{Ra}$  via the  $^{216}\text{Po}$  peak at 6779 keV and  $^{215}\text{Po}$  at 7368 keV.  $\beta$ -emitting  $^{225}\text{Ra}$  is identified by its decay products. Following the ingrowth of  $^{225}\text{Ac}$  yield can be determined using the  $^{217}\text{At}$  peak at 7067 keV. After storing for several months, to allow sufficient  $^{228}\text{Th}$  ingrowth,  $\beta$ -emitting  $^{228}\text{Ra}$  can be measured on the same  $\alpha$ -source.

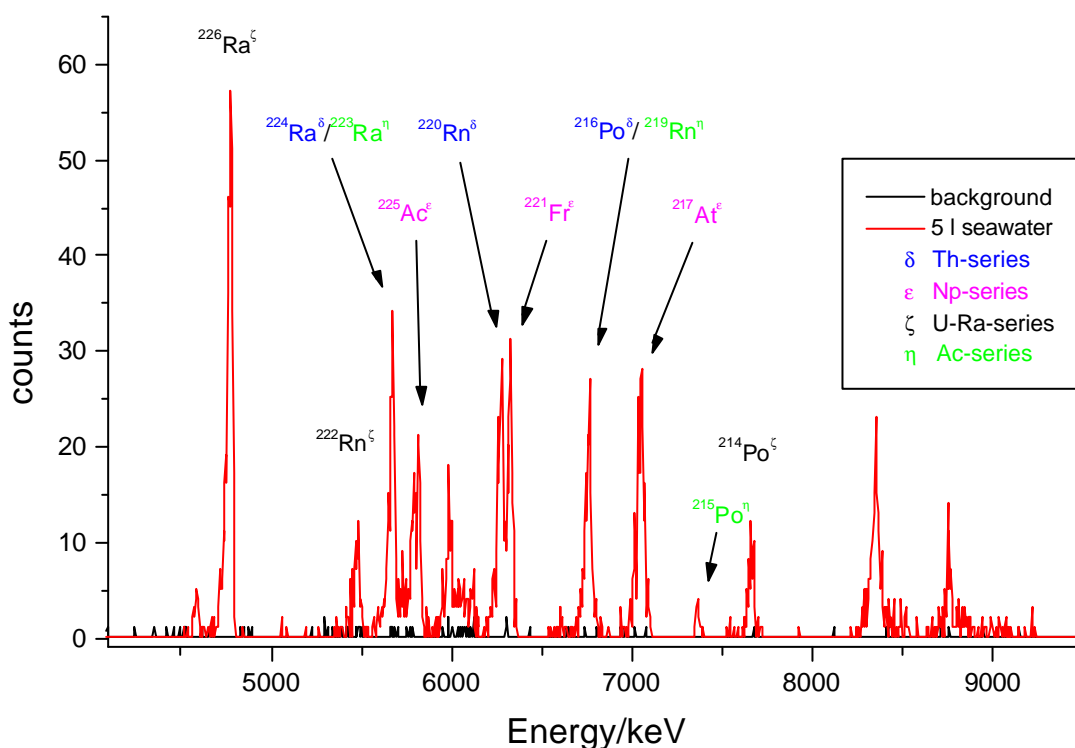


Fig. 3: Spectrum illustrates presence of short lived radium isotopes in Baltic seawater. The use of an internal yield tracer allows extraction from 5 litre sample volume.

## 4. $^{222}\text{Rn}$ Measurement Using a Portable LS-Counter

### 4.1. Principle

For ship based Rn measurements we used a portable, single tube LS-counter (Triathler). In LS-cocktails  $\alpha$ -particles generate pulses with longer duration than  $\beta$ -particles, the high  $\beta$ -background (also include counts resulting from chemoluminescence cosmic-rays and  $\gamma$ -radiation) can be electronically discriminated using a multi channel analyser (MCA) for this purpose (Oikari et al., 1987). By means of a standard computer software the  $\alpha/\beta$ -separation performance can be visualised allowing the convenient adjustment of the system to find optimal settings. In a three dimensional (3 D) plot the x-axis represents the pulse amplitude, the y-axis its duration and the z-axis detected decay events accumulated during time of measurement (Fig. 4). Due to their longer pulses,  $\alpha$ -particles have greater y-coordinates than  $\beta$ -particles with the same amplitude (x-coordinates). Thus, excluding  $\beta$ -particles, a region only occupied by  $\alpha$ -particles can be selected, resulting in the required low  $\alpha$ -background of  $2.5\text{--}0.5 \times 10^{-3}$  counts per second.

For the measurement of  $^{222}\text{Rn}$  in both, ground- and seawater the analyte is extracted into a water-immiscible LS cocktail. The scintillator (MaxiLight) used is a non-evaporating cocktail with di-isopropyl naphtalene solvent, forming a biphasic extraction system.  $^{222}\text{Rn}$  has a much higher affinity to organic solvents and is therefore quantitatively extracted from large volumes of water. The sample is shaken vigorously with the cocktail and the system is set aside for three hours. During this time  $\alpha$ -emitting daughters  $^{218}\text{Po}$  and  $^{214}\text{Po}$  equilibrates with  $^{222}\text{Rn}$  (half-lives of relevant  $\beta$ - and  $\alpha$ -progenies are shown in (Fig.1.). After phase separation the organic phase is counted with efficiency of about 270 % at most.

The excess radon concentration  $^{222}\text{Rn}_{\text{ex}}$  is determined via a second extraction of the sample one month after sample collection when  $^{222}\text{Rn}$  is equilibrated with its parent nuclide  $^{226}\text{Ra}$ . Excess radon concentration is defined as:

$$^{222}\text{Rn}_{\text{ex}} = ^{222}\text{Rn} - ^{226}\text{Ra} \quad (1)$$

$^{222}\text{Rn}_{\text{ex}}$  = excess radon concentration ( $\text{mBq l}^{-1}$ )

$^{222}\text{Rn}$  = concentration of supported and unsupported  $^{222}\text{Rn}$  ( $\text{mBq l}^{-1}$ )

$^{226}\text{Ra}$  = concentration of  $^{226}\text{Ra}$  ( $\text{mBq l}^{-1}$ )

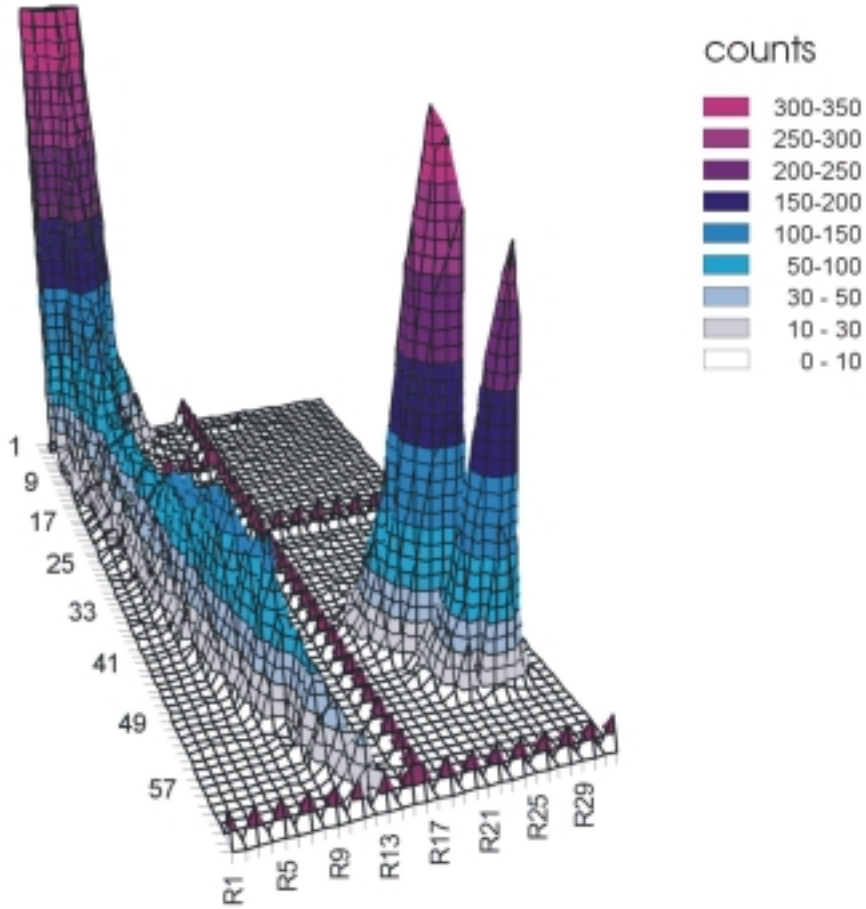


Fig.2: 3 D LS-spectrum of a  $^{222}\text{Rn}$  containing sample. The figure illustrates the excellent  $\alpha/\beta$ -separation performance. Counted 3 hours after sample preparation, the  $\alpha$ -region (to the right) includes a major peak resulting from  $\alpha$ -decay of  $^{222}\text{Rn}$  and  $^{218}\text{Po}$  and a minor peak resulting from  $^{214}\text{Po}$  (following the ingrowth of  $\beta$ -emitting  $^{214}\text{Pb}$  and  $^{214}\text{Bi}$ ).

## 1.1. Analytical Procedure

Samples from the sub-sea floor aquifer containing high  $^{222}\text{Rn}$  activities in the order of some  $\text{Bq l}^{-1}$  allow the direct counting without any pre-concentration procedure. 3.5 ml scintillator are carefully sublayered with 3.5 ml of the unaerated water sample, capped and shaken vigorously. Direct counting of the two phase system results in a reduced counting efficiency of about 203 %. Counting period for the samples is 3.5 hours, resulting in a lower limit of detection (LLD) of  $150 \text{ mBq l}^{-1}$  for the given procedure. Blank vial was counted for 9.3 hours.

For seawater samples containing lower  $^{222}\text{Rn}$  activities (some  $\text{mBq/l}$ ), the analyte has to be enriched from larger sample volumes. For this purpose an extraction apparatus was designed for processing of 1 litre sample material. Sealing and connectors (luer fittings) allow extraction of  $^{222}\text{Rn}$  under exactly defined conditions. Easy handling guarantees rapid and accurate phase separation in combination with a high scintillator recovery of 89 %. After transferring the

organic phase in a 20 ml Teflon® coated low-diffusive LS-vial the overall efficiency of the proposed method is determined to be 98 %. Using the same periods of counting, as mentioned above the lower limit of detection (LLD) is 2.5 mBql<sup>-1</sup>.

## 5. Results

Results from seawater samples, analysed for Ra isotopes and <sup>222</sup>Rn, are shown in Tab. 1. The groundwater sample taken during the May 2000 cruise was collected from the deployed temporary well 1 km off shore (P2). Results between July and September 2001 are obtained from the later installed stationary well. Tab. 1. also includes the analysis of an onshore well (P8). Ranges of Ra isotope concentration in seawater are <sup>226</sup>Ra = 0.71-7.5 mBql<sup>-1</sup>, <sup>228</sup>Ra = 3.0-7.4 mBql<sup>-1</sup>, <sup>224</sup>Ra = 0.2-2.7 mBql<sup>-1</sup>, and <sup>223</sup>Ra = 0.02-0.23 mBql<sup>-1</sup>. <sup>222</sup>Rn concentrations are in the range of 3.8 to 21.5 mBql<sup>-1</sup>.

Tab. 1: Ra isotope and <sup>222</sup>Rn data for seawater samples of the EB.

Date dd.mm.yy	Site	Water depth/m	Sample depth/m	A <sub>226</sub> Ra /mBql <sup>-1</sup>	A <sub>228</sub> Ra /mBql <sup>-1</sup>	A <sub>224</sub> Ra /mBql <sup>-1</sup>	A <sub>223</sub> Ra /mBql <sup>-1</sup>	A <sub>222</sub> Rn /mBql <sup>-1</sup>	A <sub>228</sub> Ra /A <sub>226</sub> Ra	A <sub>224</sub> Ra /A <sub>226</sub> Ra	A <sub>224</sub> Ra /A <sub>223</sub> Ra
11.05.00	P2	25.5	18.0	2.61±0.25	n/a	0.53±0.10	0.02±0.01	n/a	n/a	0.20±0.04	27±16
11.05.00	P2	25.5	22.0	2.73±0.30	n/a	0.84±0.17	0.04±0.02	n/a	n/a	0.31±0.06	23±12
11.05.00	P2	25.5	24.0	3.38±0.43	n/a	2.72±0.50	0.23±0.07	n/a	n/a	0.80±0.14	12±4
11.05.00	P2	25.5	25.0	2.39±0.21	n/a	1.82±0.23	0.11±0.03	n/a	n/a	0.76±0.09	16±2
09.08.00	P1	20.5	19.0	2.10±0.11	3.96±0.28	0.9±70.10	0.05±0.01	n/a	1.88±0.09	0.46±0.04	18±4
09.08.00	P2	24.0	22.5	3.40±0.17	7.35±0.47	1.38±0.14	0.12±0.02	n/a	2.16±0.09	0.41±0.04	12±2
09.08.00	P3	23.5	22.0	3.21±0.16	6.98±0.46	1.28±0.14	0.15±0.02	n/a	2.18±0.09	0.40±0.04	9±1
09.08.00	P4	25.5	24.0	2.48±0.15	5.16±0.37	0.84±0.13	0.10±0.02	n/a	2.09±0.09	0.34±0.05	8±2
09.08.00	P5	25.0	23.5	2.99±0.14	6.68±0.45	0.84±0.10	0.05±0.01	n/a	2.23±0.10	0.28±0.03	17±4
09.08.00	P6	27.0	25.5	2.94±0.16	6.83±0.51	1.05±0.17	0.14±0.02	n/a	2.32±0.12	0.36±0.05	8±2
09.08.00	P7	26.0	24.5	2.92±0.15	5.94±0.40	1.08±0.14	0.11±0.02	n/a	2.03±0.09	0.37±0.04	10±2
26.02.01	P2	25.0	10.0	1.94±0.11	3.01±0.23	0.29±0.08	0.02±0.01	n/a	1.55±0.08	0.15±0.04	13±4
26.02.01	P2	25.0	10.0	1.81±0.11	2.97±0.25	0.20±0.09	0.01±0.01	n/a	1.64±0.10	0.11±0.05	14±6
26.02.01	P2	25.0	18.0	2.63±0.14	4.83±0.33	0.10±0.06	0.01±0.01	n/a	1.84±0.08	0.04±0.02	7±4
26.02.01	P2	25.0	21.0	2.44±0.12	4.78±0.28	1.17±0.13	0.06±0.01	n/a	1.96±0.07	0.48±0.05	19±2
26.02.01	P2	25.0	24.0	2.48±0.13	4.66±0.31	0.88±0.13	0.06±0.01	n/a	1.88±0.07	0.36±0.05	14±2
02.08.01	P2	22.5	13.0	0.77±0.06	n/a	0.17±0.04	0.01±0.01	4.0±1.2	n/a	0.23±0.06	13±7
02.08.01	P2	22.5	15.0	1.19±0.09	n/a	0.46±0.08	0.03±0.01	4.8±1.3	n/a	0.39±0.07	17±8
02.08.01	P2	22.5	17.0	2.72±0.24	n/a	0.33±0.10	0.03±0.02	7.1±1.5	n/a	0.12±0.03	11±7
02.08.01	P2	22.5	19.0	4.67±0.40	n/a	0.67±0.16	0.11±0.03	15.5±2.0	n/a	0.14±0.03	6±2
02.08.01	P2	22.5	20.0	6.44±0.43	n/a	1.18±0.15	0.11±0.02	10.1±1.7	n/a	0.18±0.02	11±2
02.08.01	P2	22.5	21.0	6.46±0.43	n/a	1.29±0.16	0.10±0.02	13.0±2.0	n/a	0.20±0.02	13±3
02.08.01	P2	22.5	22.0	5.76±0.40	n/a	2.03±0.22	0.15±0.03	20.5±2.3	n/a	0.35±0.03	14±3
02.08.01	P6	26.5	13.0	0.71±0.08	n/a	0.32±0.09	0.02±0.01	3.8±1.1	n/a	0.45±0.12	17±11
02.08.01	P6	26.5	17.0	2.79±0.20	n/a	0.27±0.09	0.06±0.02	6.0±1.3	n/a	0.10±0.03	5±2
02.08.01	P6	26.5	20.0	5.98±0.42	n/a	0.89±0.15	0.11±0.02	11.5±1.6	n/a	0.15±0.02	8±2
02.08.01	P6	26.5	23.0	7.15±0.47	n/a	2.28±0.22	0.15±0.03	12.6±1.7	n/a	0.32±0.02	15±3
02.08.01	P6	26.5	24.0	6.12±0.38	n/a	1.93±0.19	0.16±0.03	16.1±1.9	n/a	0.31±0.03	12±2
02.08.01	P6	26.5	25.0	6.57±0.43	n/a	2.02±0.21	0.15±0.03	21.5±2.1	n/a	0.31±0.03	13±2
02.08.01	P6	26.5	26.0	7.50±0.52	n/a	2.18±0.22	0.14±0.03	16.5±1.9	n/a	0.29±0.02	15±3

Ra isotopes and  $^{222}\text{Rn}$  concentrations in the underlying sub-sea floor aquifer are shown in Tab. 2. Groundwater concentrations generally exceed those measured in the water column. Results range from  $^{226}\text{Ra} = 5.1\text{-}8.5 \text{ mBql}^{-1}$ ,  $^{228}\text{Ra} = 9.3\text{-}15.5 \text{ mBql}^{-1}$ ,  $^{224}\text{Ra} = 9.8\text{-}13.1 \text{ mBql}^{-1}$  and  $^{223}\text{Ra} = 0.47 \text{ to } 0.64 \text{ mBql}^{-1}$ .  $^{222}\text{Rn}$  concentrations are in the range of 5900 to 6900  $\text{mBql}^{-1}$ .

Tab. 2: Ra isotope and  $^{222}\text{Rn}$  data for groundwater samples of the sub-sea floor aquifer.

Date dd.mm.yy	Site	$A_{226}\text{Ra}$ /mBql <sup>-1</sup>	$A_{228}\text{Ra}$ /mBql <sup>-1</sup>	$A_{224}\text{Ra}$ /mBql <sup>-1</sup>	$A_{223}\text{Ra}$ /mBql <sup>-1</sup>	$A_{222}\text{Rn}$ /mBql <sup>-1</sup>	$A_{228}\text{Ra}$ $A_{226}\text{Ra}$	$A_{224}\text{Ra}$ $A_{226}\text{Ra}$	$A_{224}\text{Ra}$ $A_{223}\text{Ra}$
<b>12.05.00</b>	P2	$7.19\pm0.32$	$11.3\pm0.5$	$9.8\pm0.6$	$0.61\pm0.05$	n/a	$1.57\pm0.03$	$1.36\pm0.07$	$16.1\pm1.5$
<b>09.08.00</b>	P8	$8.54\pm0.34$	$15.5\pm0.7$	$12.4\pm1.0$	$0.64\pm0.08$	n/a	$1.82\pm0.03$	$1.38\pm0.05$	$19.5\pm1.9$
<b>26.02.01</b>	P2	$5.59\pm0.25$	$13.2\pm0.7$	$11.4\pm0.6$	$0.54\pm0.05$	n/a	$2.36\pm0.07$	$2.04\pm0.09$	$21.1\pm2.0$
<b>26.02.01</b>	P2	$6.19\pm0.28$	$15.1\pm0.8$	$12.8\pm0.7$	$0.53\pm0.05$	n/a	$2.43\pm0.07$	$2.06\pm0.08$	$24.0\pm2.2$
<b>17.07.01</b>	P2	$5.85\pm0.25$	$14.0\pm1.0$	$13.1\pm0.7$	$0.62\pm0.06$	$6520\pm470$	$2.39\pm0.13$	$2.25\pm0.11$	$21.0\pm2.1$
<b>17.07.01</b>	P2	$6.08\pm0.25$	$14.9\pm0.9$	$13.1\pm0.7$	$0.60\pm0.05$	$6940\pm500$	$2.44\pm0.12$	$2.16\pm0.10$	$22.0\pm2.1$
<b>04.05.01</b>	P2	$5.35\pm0.25$	$11.3\pm0.8$	$12.2\pm0.7$	$0.47\pm0.07$	$6640\pm410$	$2.12\pm0.12$	$2.28\pm0.12$	$26.1\pm3.9$
<b>04.05.01</b>	P2	$5.48\pm0.38$	$12.0\pm1.0$	$10.7\pm0.8$	$0.53\pm0.09$	$6020\pm380$	$2.18\pm0.11$	$1.95\pm0.13$	$20.1\pm3.4$
<b>06.09.01</b>	P2	$5.10\pm0.57$	$9.3\pm1.2$	$11.9\pm1.4$	$0.52\pm0.14$	$5940\pm400$	$1.83\pm0.13$	$2.33\pm0.25$	$22.9\pm6.0$
<b>06.09.01</b>	P2	n/a	n/a	n/a	n/a	$6060\pm400$	$1.92\pm0.14$	n/a	n/a

Belonging to the same decay series (Fig.1),  $^{224}\text{Ra}$  and  $^{228}\text{Ra}$  activities in groundwater within statistical uncertainty are in radioactive equilibrium, indicating that  $^{224}\text{Ra}$  is slowly (relative to its half-life) transported within the percolating groundwater front. In contact with the  $^{228}\text{Th}$  bearing solid phase  $^{224}\text{Ra}$  remains close to radioactive equilibrium. The  $^{222}\text{Rn}$  concentrations exceed those measured for  $^{224}\text{Ra}$  by a factor of 500. Analysing their adsorption/desorption in groundwater from Connecticut, USA Krishnaswami et al. (1982) explained similar observations by differing adsorption behaviour. Both short-lived nuclides are supplied into the aqueous phase mainly via  $\alpha$ -recoil mechanisms. Whereas adsorption for the noble gas  $^{222}\text{Ra}$  is negligible, the residence time for  $^{224}\text{Ra}$  in solution is in the order of minutes and does not migrate far from the injection point.

$^{223}\text{Ra}$ ,  $^{224}\text{Ra}$ , and  $^{222}\text{Rn}$  concentrations in the water column decrease with distance from the sea floor (Fig. 5). This reflects the input of these nuclides from their sources being the sedimentary pore water, fine-grained bottom sediments and the groundwater seepage. Within the water column support is negligible for  $^{223}\text{Ra}$  and  $^{224}\text{Ra}$  due to high particle reactivity of their parent nuclides. Only for  $^{222}\text{Rn}$  significant supply comes from the decay of the easily soluble parent  $^{226}\text{Ra}$ . Neglecting scavenging losses, observed gradients of short-lived  $^{223}\text{Ra}$ ,  $^{224}\text{Ra}$ , and  $^{222}\text{Rn}_{\text{ex}}$  are the result of their dispersive physical mixing away from the source and the unsupported decay within the water column.

According to their longer half-lives  $^{228}\text{Ra}$ , and  $^{226}\text{Ra}$  display mixing processes on scales far exceeding dimensions of the contemplated water body. As illustrated in Fig. 5 their concentrations do not vary much within the water column. Results are consistent with earlier findings of Turekian et al. (1996) for dissolved  $^{226}\text{Ra}$  in Long Island Sound. Nevertheless, during the August 2001 cruise unusual  $^{226}\text{Ra}$  distributions were measured in the water column at two sites of EB. Whereas usual concentrations within the deeper water column are 2 to 3 mBq $^{-1}$ , the near bottom value then exceeded 6 mBq $^{-1}$  and decreases rapidly with distance from the sea floor to 0.7 mBq $^{-1}$  measured at 13 m water depth (Fig. 6). This observation indicates that the geochemical processes involved must also have a similar influence on the behaviour of the other Ra species. Thus, studies of disperse physical mixing possesses using short-lived isotopes must include a correction for their geochemical behaviour. An adequate approach is to use the activity ratio normalised to the measured  $^{226}\text{Ra}$  concentration (see chapter 6).

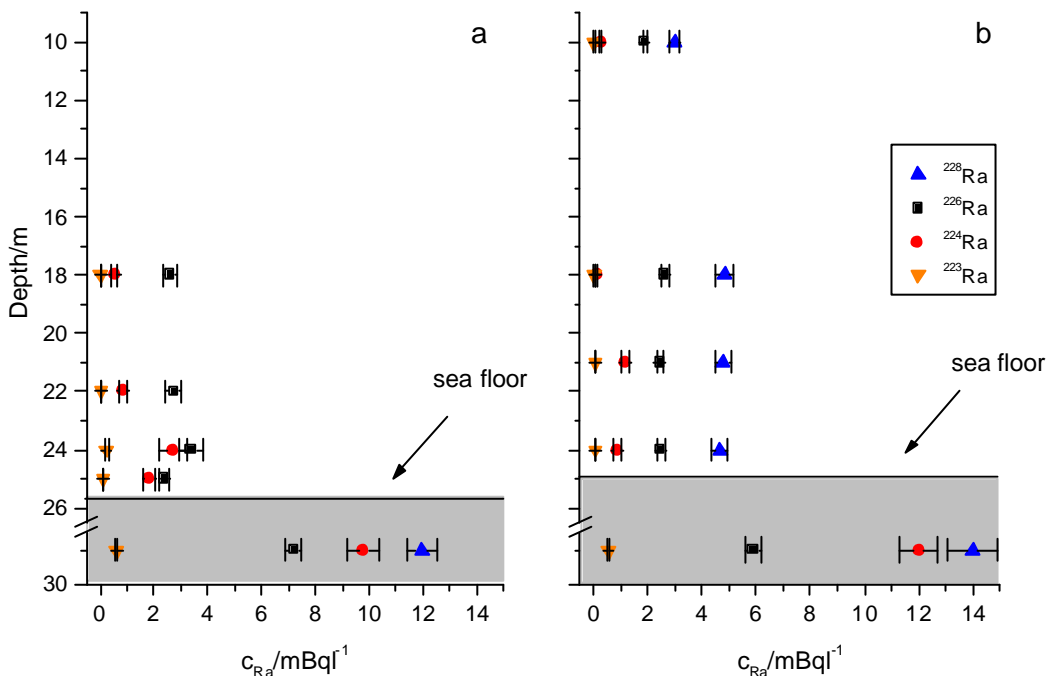


Fig. 5: Radium isotopes in the water column and the underlying aquifer for site P2 on May 2000 (a) and February 2001 (b). Groundwater concentrations generally exceed those within the water column.  $^{228}\text{Ra}$  and  $^{226}\text{Ra}$  activities do not vary much with depth.

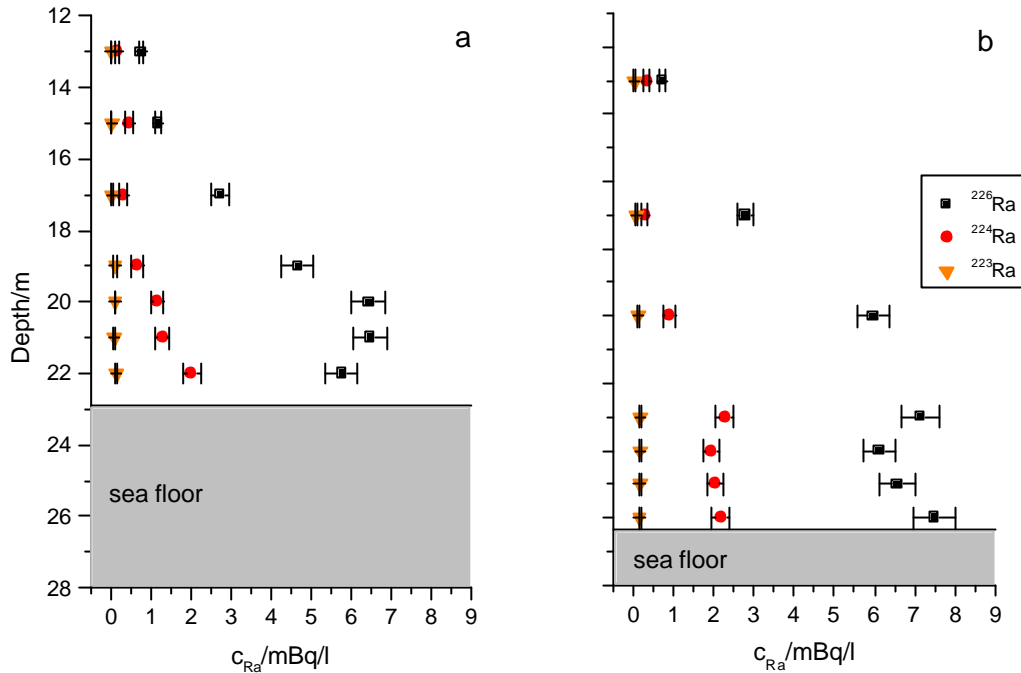


Fig. 6: Ra isotopes in the water column on August 2001 for site P2 (left half of figure) and for site P6 (right half of figure). Likewise the short-lived Ra isotopes the  $^{226}\text{Ra}$  activity varies strongly with depth.

## 6. Analysis of Small-Scale Coastal Mixing Processes

### 6.1. Modelling of Vertical Dispersive Mixing

Assuming one-dimensional vertical transport in the water column, neglecting advective transport and correcting for geochemical processes by the use of the normalised  $^{224}\text{Ra}/^{226}\text{Ra}$  activity ratio, the behaviour of  $^{224}\text{Ra}$  below the thermocline can be described as:

$$D_z \frac{\partial^2 r}{\partial z^2} - \lambda_{\text{Ra}} r = -P \quad (2)$$

- $D_z$  = coefficient of vertical eddy dispersion ( $\text{m}^2\text{s}^{-1}$ )
- $r$  =  $^{224}\text{Ra}/^{226}\text{Ra}$  activity ratio
- $\lambda_{\text{Ra}}$  = decay constant for  $^{224}\text{Ra}$  ( $\text{s}^{-1}$ )
- $P$  = production term ( $\text{s}^{-1}$ )
- $z$  = height above sea floor (m)

Highest activity ratios are observed at the sediment/water interface which can be expressed by the boundary condition:

$$r(z=0) = r_0$$

The differential equation is simplified by neglecting the production term P which is justified by the depletion of  $^{228}\text{Th}$  within the water column.

Then, the activity ratio  $r(z)$  is:

$$r = r_0 e^{-\sqrt{\frac{\lambda_{\text{Ra}}}{D_z}} z} \quad (3)$$

Fig. 7a illustrates for site P2 that field data are in good agreement with these model assumptions. However, a gradient measured at site P6 (deepest region of the Bay) shows the influence of  $^{228}\text{Th}$  containing suspended particles near the sea floor (Fig. 7b).

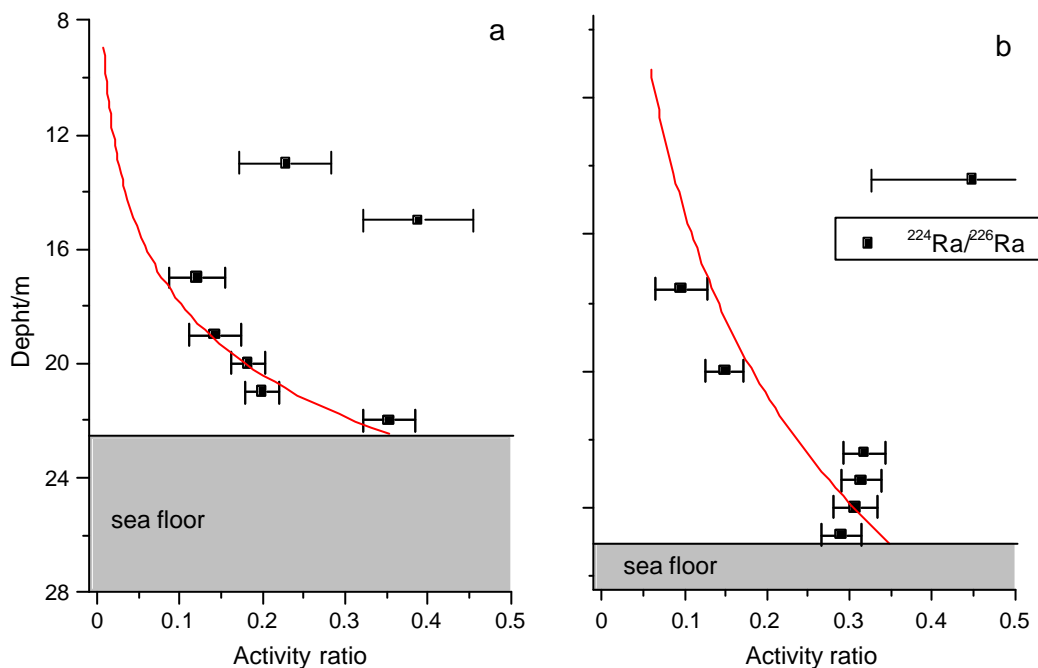


Fig. 7: Normalised  $^{224}\text{Ra}$  in the water column on August 2001 for site P2 (a) and for site P6 (b). Solid line represents the exponential curve fit according to equation (3). A deviation from theoretical expectations is observed at P6. Most likely, this gradient shows the influence of suspended particles near the sea floor on the  $^{224}\text{Ra}$  record.

The behaviour of  $^{222}\text{Rn}_{\text{ex}}$  (Fig. 8) can also be described with the same theoretical approach. Measured data fits adequately with obtained expression:

$$c = c_0 e^{-\sqrt{\frac{\lambda_{\text{Rn}}}{D_z}} z} \quad (4)$$

- $c$  = concentration of  $^{222}\text{Rn}_{\text{ex}}$  ( $\text{mBql}^{-1}$ )
- $c_0$  = concentration of  $^{222}\text{Rn}_{\text{ex}}$  at sediment/water interface ( $\text{mBql}^{-1}$ )
- $\lambda_{\text{Rn}}$  = decay constant for  $^{222}\text{Rn}$  ( $\text{s}^{-1}$ )
- $D_z$  = coefficient of vertical eddy dispersion ( $\text{m}^2\text{s}^{-1}$ )
- $z$  = height above sea floor (m)

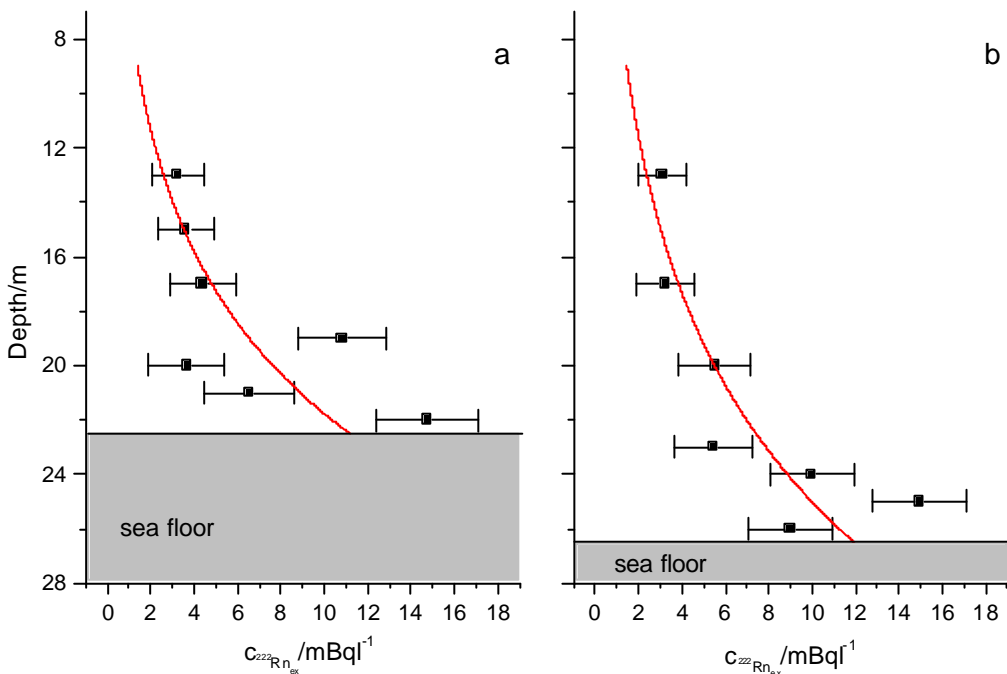


Fig. 7:  $^{222}\text{Ra}$  in the water column on August 2001 for site P2 (a) and for site P6 (b). Data are fitted according to equation (4).

The discussion above clearly shows that Ra and Rn tracer studies provide an estimate for the coefficient of vertical eddy dispersion. The coefficient calculated from fitting parameters of normalised  $^{224}\text{Ra}$  data results in  $\bar{D}_z = 4.9 \pm 1.2 \cdot 10^{-5} \text{ m}^2\text{s}^{-1}$  (weighted mean,  $n=3$ ). Although the value calculated from  $^{222}\text{Rn}$  data should be similar, the obtained coefficient for radon  $\bar{D}_z = 11.0 \pm 4.1 \cdot 10^{-5} \text{ m}^2\text{s}^{-1}$  (weighted mean,  $n=2$ ) is a factor of about 2 higher. The larger value may be explained by a synergetic methane ( $\text{CH}_4$ ) and  $^{222}\text{Rn}$  gas transport. Formation of gas bubbles is a known phenomenon in the study area (Dando et al., 2000, Anderson et al., 1998).

Thus, it can be supposed that methane gas acting as a carrier and supports a rapid transport of  $^{222}\text{Rn}$  within the water column when compared to the Ra.

## 6.2. Modelling of Horizontal Dispersive Mixing

To provide an estimate of the coefficient  $D_x$  for horizontal diffusive dispersion, field data of the transect through the EB, collected during the August 2000 cruise, are compared to the best fit obtained from solving the general differential equation (2) for horizontal transport in the deep water near the sea floor. Solving the second order inhomogeneous differential equation is simplified using an appropriate co-ordinate system:

- The distance between intersection points of the near coastal 20 m iso-line of water depth and the transect-line are defined as total length of the system (4100 m).
- The centre of the transect is defined as  $x = 0$ .
- The co-ordinate of the southern intersection point is  $x = -L$ .
- The co-ordinate of the northern intersection point is  $x = L$ .

Adequate model assumptions are:

- constant sediment production term,  $\frac{\partial P}{\partial x} = 0$
- influence by groundwater discharge/freshly eroded deposits primarily from the coast
- equal quantities of  $^{224}\text{Ra}$  discharged from both sides of the Bay

Searching for a symmetrical function a promising Ansatz to solve the homogeneous part of the equation is:

$$r_s = Ae^{\sqrt{\frac{\lambda}{D_x}}x} + Be^{-\sqrt{\frac{\lambda}{D_x}}x} \quad (5)$$

Inserting into equation (2) gives the general solution:

$$r = Ae^{\sqrt{\frac{\lambda}{D_x}}x} + Be^{-\sqrt{\frac{\lambda}{D_x}}x} + \frac{P}{\lambda} \quad (6)$$

With the boundary conditions:

$$r(x = \pm L) = r_{\max}$$

$$r(x = 0) = r_{\min}$$

the following equation is obtained describing the horizontal mixing behaviour of  $^{224}\text{Ra}$  near the sea floor:

$$\frac{r_{\max} - r(x)}{r_{\max} - r_{\min}} = \frac{(e^{\sqrt{\frac{\lambda}{D_x}}L} + e^{-\sqrt{\frac{\lambda}{D_x}}L}) - (e^{\sqrt{\frac{\lambda}{D_x}}x} + e^{-\sqrt{\frac{\lambda}{D_x}}x})}{(e^{\sqrt{\frac{\lambda}{D_x}}L} + e^{-\sqrt{\frac{\lambda}{D_x}}L}) - 2} \quad (7)$$

Choosing values of  $r_{\max} = 0.42$  and  $r_{\min} = 0.30$  adapted from measured  $^{224}\text{Ra}/^{226}\text{Ra}$  activity ratios (Tab. 1) and varying the value for  $D_x$  in the range of  $10^{-2} - 5*10^1 \text{ m}^2\text{s}^{-1}$  the quality of obtained fitting results is improved by increasing the values chosen for  $D_x$ . Fig. 9 illustrates that all fits using values of  $D_x \geq 10^0 \text{ m}^2\text{s}^{-1}$  are generally in good agreement with the measured data. As curves for  $D_x = 5*10^0 \text{ m}^2\text{s}^{-1}$  and  $D_x = 5*10^1 \text{ m}^2\text{s}^{-1}$  are already almost identical, the graph also depicts that, due to geological settings, the used model is only sensitive for values of  $D_x \leq 10^0 \text{ m}^2\text{s}^{-1}$ . This leads to the estimate of  $D_x = 10^0 \text{ m}^2\text{s}^{-1}$  as lower-limit value of the coefficient for horizontal eddy dispersion.

Torgersen et al. (1996) analysed the movement of  $^{224}\text{Ra}$  in the deep water of Long Island Sound and observed maximal  $^{224}\text{Ra}$  activities in the centre of the Bay. Different geological settings lead to improved sensitivity for  $D_x \geq 10^0 \text{ m}^2\text{s}^{-1}$ . Thus, the reported upper limit  $5*10^1 \text{ m}^2\text{s}^{-1}$  is certainly a good approximation and can also be considered as conservative estimate regarding horizontal eddy dispersion in the EB.

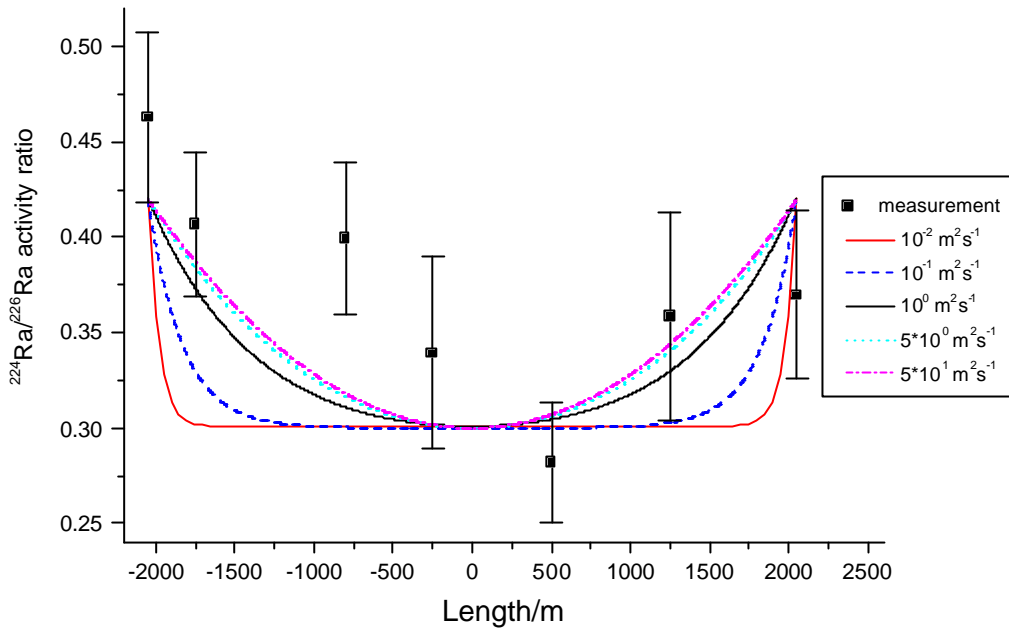


Fig. 9: Normalised  $^{224}\text{Ra}$  in the deep water of EB. Different lines represents predicted values based on horizontal coefficients of eddy dispersivity in the range of  $D_x = 10^{-2}$  to  $5 \cdot 10^{-1} \text{ m}^2 \text{s}^{-1}$ .

### 6.3. Simple Two-Box Model for Groundwater Discharge

Applying a simple two-box steady-state model for EB bottom water and the underlying sub-sea floor aquifer an upper limit for submarine discharge can be estimated.

Groundwater contains short-lived tracers in a concentration  $\bar{c}_g$  and discharges them with a steady flow rate of  $Q$  into the bottom water of the bay with a total area  $A$ . The vertical transport of the tracers within the water column could be described according to diffusion theory. Balancing the resulting inventory  $I$  of  $^{222}\text{Rn}$ ,  $^{224}\text{Ra}$ ,  $^{226}\text{Ra}$  in the water column the only mechanism considered is radioactive decay, other sources and sinks are neglected. The equation for balance is:

$$Q\bar{c}_g = AI\lambda \quad (8)$$

- $Q$  = groundwater flow rate ( $\text{m}^3 \text{s}^{-1}$ )
- $\bar{c}_g$  = tracer concentration (mean) in the aquifer ( $\text{Bq m}^{-3}$ )
- $A$  = total area of the bay ( $\text{m}^2$ )
- $I$  = inventory, calculated by integration of fitted gradients ( $\text{Bq m}^{-2}$ )
- $\lambda$  = decay constant

Tab.3: Groundwater flow rates calculated for each particular tracer isotopes.

Tracer	A/10 <sup>6</sup> m <sup>2</sup>	$\bar{c}_g$ (n = 8) /Bqm <sup>-3</sup>	I/10 <sup>-6</sup> s <sup>-1</sup>	I/Bqm <sup>-2</sup>	Q/m <sup>3</sup> s <sup>-1</sup>
<sup>222</sup> Rn	70±7	6400±400	2.098	72.4±7.4	1.7±0.3**
<sup>223</sup> Ra	70±7	0.55±0.05	0.702	0.52±0.22*	46±21**
<sup>224</sup> Ra	70±7	11.9±1.2	2.189	6.46±2.6	83±36**

\*Calculated, using same coefficient  $\bar{D}_z = 4.9 \pm 1.2 \times 10^{-5} \text{ m}^2 \text{s}^{-1}$  obtained from analysis of <sup>224</sup>Ra gradients

\*\*Uncertainty does not include systematic errors (e.g.: other source or sinks)

Numerical modelling of the hydrology of the catchment area of the EB by Dahmke et al. (2001) using the finite-difference groundwater-simulation-programme MODFLOW (McDonald and Harbaugh, 1988) gives  $Q = 1.93 \text{ m}^3 \text{s}^{-1} (\approx 1.61 \text{ lm}^{-2} \text{d}^{-1})$ . Flow rates were also directly measured by Suess and Linke (2000) at active pockmarks using a seepage meter (Linke et al., 1994). Authors reported higher flow rates in the range of  $Q = 20\text{-}260 \text{ lm}^{-2} \text{d}^{-1}$ . These results support the spatial variability of discharge within the Bay.

Comparing calculated flow rates (Tab.3) with those mentioned above it becomes evident that the more integrated box-modelling approach should be more adequately reflected by numerical modelling of the hydrology than by discrete seepage measurements. Obtained from <sup>222</sup>Rn inventory modelling,  $Q = 1.7 \pm 0.3 \text{ m}^3 \text{s}^{-1}$  is in good agreement with the numerical approach.

Due to a much stronger signal in groundwater and lower particle reactivity <sup>222</sup>Rn seems to fulfil the model assumptions of the simple two box-model more satisfactorily than <sup>224</sup>Ra and <sup>223</sup>Ra. Estimates for groundwater discharge rates obtained from radium isotopes are similar to each other, but in contrast to <sup>222</sup>Rn one to two orders of magnitudes higher. Comparable flow rates  $Q = 46 \pm 21 \text{ m}^3 \text{s}^{-1}$  and  $Q = 83 \pm 36 \text{ m}^3 \text{s}^{-1}$  are related to their identical chemical behaviour. Higher flow rates are indicating a much stronger supplementary source for <sup>223</sup>Ra and <sup>224</sup>Ra in this coastal environment. The radium inventories can be explained by an additional sedimentary supply, responsible for a proportion of >98 % of the total <sup>224</sup>Ra and >96 % of the total <sup>223</sup>Ra within the water column.

## 7. Summary and Conclusion

Analytical methods presented here are ideally suited for the determination of all four natural radium isotopes and  $^{222}\text{Rn}$  in the near coastal marine environment. Samples can be easily processed without delay even on restricted conditions aboard small marine research vessels. By sampling the water column and the underlying sub-sea floor aquifer of EB results demonstrate the use of short lived natural tracers to study small scale mixing processes. Dispersive physical mixing acting over the time scale in the order of days are responsible for the distribution of  $^{223}\text{Ra}$ ,  $^{224}\text{Ra}$  and  $^{222}\text{Rn}$  in the EB. Measured variations in the concentrations depend on the distance from the source. The distribution of the used tracers is controlled by the strength of the sediment source, the influence of the direct groundwater input, the dispersive mixing coefficient in the water column and its own radioactive decay.

In this particular marine environment seepage of pure freshwater with salinity of 0.2‰ promotes adsorption of radium onto sediment particles within the aquifer and thus the tracer does not migrate far from the point of injection. Due to increased mobility  $^{222}\text{Rn}$  provide a much stronger groundwater signal. The obtained  $^{222}\text{Rn}$  discharge rates are in agreement with hydrogeological modelling. To balance measured  $^{223}\text{Ra}$  and  $^{224}\text{Ra}$  inventories, in distinction to radon measurements, there is need for a strong additional source. Based on the calculated flow rate  $Q = 1.7 \pm 0.3 \text{ m}^3\text{s}^{-1}$ , a supply from sediment must be responsible for a proportion of >98 %  $^{224}\text{Ra}$  and >96 %  $^{223}\text{Ra}$ .

## References

- Anderson, A. L., Abegg, F., Hawkins, J. A., Duncan, M. E., Lyons, A. P., 1998. Bubble populations and acoustic interaction with the gassy floor of Eckernförde Bay. *Cont. Shelf Res.* 18, 1807-1838.
- Bollinger, M. S., Moore, W. S., 1993. Evaluation of salt marsh hydrology using radium as a tracer. *Geochim. Cosmochim. Acta* 57, 2203-2212.
- Bussmann, I., Suess, E., 1998. Groundwater seepage in Eckernförde Bay (Western Baltic Sea): effect on methane and salinity distribution of the water column. *Cont. Shelf Res.* 18, 1795-1806.
- Cable, J. E., Burnett, W. C., Chanton, J. P., Weatherly, G. L., 1996. Estimating groundwater discharge into the northeastern Gulf of Mexico using radon-222. *Earth Planet. Sci. Lett.* 144, 591-604.
- Dahmke, A., Piotrowski, J. A., Marczinek, S., 2001. Hydrogeology of the catchment area of Eckernförde Bay. Sub-Gate, Final sum. report. Kiel, Germany, Part B.
- Dando, P.R., Rees, E. I. S., Dando, M. A. Schlüter, M. Sauter, E. J., 2000. Methane venting associated with submarine groundwater discharge in Eckerförde Bucht; Baltic Sea. 6th Int. Conf. on Gas in Marine Sediments-Geology-Chemistry-Mircobiology-Applications, St. Petersburg.
- Edgerton, H., Seibold, E., Vollbrecht, K., Werner, F., 1966. Morphologische Untersuchungen am Mittelgrund (Eckernförde Bucht, westliche Ostsee). *Meyniana* 16, 37-50.
- Elsinger, R. J., King, P. T., Moore, W. S., 1982.  $^{224}\text{Ra}$  in natural waters measured by  $\gamma$ -ray spectrometry. *Anal. Chem. Acta* 144, 227-281.
- Haaslahti, J., Aalto, J., Oikari, T., 2000. A portable liquid scintillation counter for general LSC and high sensitivity alpha-counting applications. *J. Radioanal. Nucl. Chem. Art.* 243, 377-381.
- Hancock, G. J. and Murray, A. S., 1996. Source and distribution of dissolved radium in the Bega River estuary, southeastern Australia. *Earth Planet. Sci. Lett.* 138, 145-155.
- Hovland, M. and Judd, A. G. 1988. Seabed pockmarks and seepages: impact on geology, biology and the marine environment. Graham & Trotman.
- Kandriche, A., Werner, F., 1995. Freshwater-induced pockmarks in Bay of Eckernförde, Western Baltic. Proc. 3rd Marine Geol. Conf. "The Baltic", 155-164.
- Krishnaswami, S., Graustein, W. C., Turekian, K. K., Dowd, J. F., 1982. Radium, thorium and radioactive lead isotopes in groundwaters; application to the in situ determination of adsorption-desorption rate constants and retardation factors. *Water Resour. Res.* 18, 1663-1675.
- Li, Y. H., 1977. The flux of  $^{226}\text{Ra}$  from estuarine and continental shelf sediments. *Earth Planet. Sci. Lett.* 37, 237-241.

- Linke, P., Suess, E., Torres, M., Martens, V., Rugh, W. D., Ziebis, W., Kulm, L. D., 1994. In situ measurement of fluid flow from cold seeps at active continental margins. Deep-Sea Res. 41, 721-739.
- McDonald, M. C., Harbaugh, A. W., 1988. MODFLOW, A modular three-dimensional finite difference ground-water flow model, U.S. Geological Survey, Open-file report 83-875, Chapter A1.
- Moore, W. S., 1996. Large groundwater inputs to coastal waters revealed by  $^{226}\text{Ra}$  enrichments. Nature 380, 612-614.
- Moore, W. S., 2000. Ages of continental shelf waters determined from  $^{223}\text{Ra}$  and  $^{224}\text{Ra}$ . J. Geophys. Res. 105, 22117-22122.
- Moore, W. S., Reid, D. F., 1973. Extraction of Radium from Natural Waters Using Manganese-Impregnated Acrylic Fibers. J. Geophys. Res. 78, 8880-8886.
- Moore, W. S., Arnold, R., 1996. Measurement of  $^{223}\text{Ra}$  and  $^{224}\text{Ra}$  in coastal waters using a delayed coincidence counter. J. Geophys. Res. 101, 1321-1329.
- Oikari, T., Kojola, H., Nurmi, J., Kaihola, L., 1987. Simultaneous counting of low alpha- and beta-particle activities with liquid-scintillation spectrometry and pulse shape analysis. Int. J. Appl. Radiat. Isot. 38 : 875-878
- Rama, Moore, W. S., 1996. Using the radium quartet for evaluating groundwater input and water exchange in salt marshes. Geochim. Cosmochim. Acta 60, 4645-4652.
- Sauter, E. J., Laier, T., Andersen, C. E., Dahlgaard, H., Schlüter, M., (in press) Sampling of sub-sea floor aquifers by a temporary well for CFC dating and natural tracer investigations. J. Sea Res.
- Schmidt, S., Reyss, J. L., 1996. Radium as internal tracer of Mediterranean Outflow Water. J. Geophys. Res. 101, 3589-3595.
- Smith, L. L., Alvarado, J. S., Markun, F. J., Hoffmann, K. M., Seely, D.C., Shannon, R.T., 1997. An evaluation of radium-specific, solid phase extraction membranes, Radioac. Radiochem. 8, 30.
- Suess, E., Linke, P., 2000. Continuous monitoring of fluid flow at vent sites. Sub-Gate, Summary Progress Report (End of year 2). Kiel, Germany, Part B.
- Sun, Y., Torgersen, T., 1998. The effects of water content and Mn-fiber surface conditions on  $^{224}\text{Ra}$  measurement by  $^{220}\text{Rn}$  emanation. Mar. Chem. 62, 299-306.
- Torgersen, T., Turekian, K. K., Turekian, V. C., Tanaka, N., DeAngelo, E., and O'Donnell, J., 1996.  $^{224}\text{Ra}$  distribution in surface and deep water of Long Island Sound; sources and horizontal transport rates. Cont. Shelf Res. 16, 1545-1559.
- Turekian, K. K., Tanaka, N., Turekian, V. C., Torgersen, T., and Deangelo, E. C., 1996. Transfer rates of dissolved tracers through estuaries based on  $^{228}\text{Ra}$ ; a study of Long Island Sound. Cont. Shelf Res. 16, 863-873.
- Whiticar, M., Werner, F., 1981. Pockmarks: Submarine vents of natural gas or freshwater seeps?. Geo Marine Lett. 1, 193-199.

## **Kapitel IV. Neuanmeldung zum Gebrauchsmuster**

# **Vorrichtung zur Extraktion von Stoffen von einer Membran**

**Stefan Purkl und Anton Eisenhauer**

## BOEHMERT & BOEHMERT ANWALTSZOSSIETÄT

Boehmert & Boehmert • Niemannsweg 133 • D-24105 Kiel

**Deutsches Patentamt-  
und Markenamt  
Zweibrückenstr. 12  
80297 München**

DR.-ING. KARL BOEHMERT, PA (1999-197)  
DIPL.-ING. ALBERT BOEHMERT, PA (1902-193)  
WILHELM J. H. STAHLBERG, RA, Bremen  
DR.-ING. WALTER HOORMANN, PA\*, Bremen  
DIPL.-PHYS. DR. HEINZ GODDAR, PA\*, München  
DR.-ING. ROLAND LIESEGANG, PA\*, München  
WOLF-DIETER KUNTZE, RA, Bremen, Alicante  
DIPL.-PHYS. DR. ROBERT MUNZHUBER, PA (1933-1992)  
DR. LUDWIG KOUKER, RA, Bremen  
DR. (CHEM.) ANDREAS WINKLER, PA\*, Bremen  
MICHAEL HÜTHNER, RA, Bremen  
DIPL.-PHYS. DR. MARION TÖNHARDT, PA\*, Düsseldorf  
DR. ANDREAS EBERT-WEIDENFELLER, RA, Bremen  
DIPL.-ING. EVA LIESEGANG, PA\*, München  
DR. AXEL NORDEMANN, RA, Berlin  
DIPL.-PHYS. DR. DOROTHEE WEBER-BRULS, PA\*, Frankfurt  
DIPL.-PHYS. DR. STEFAN SCHOHE, PA\*, München  
DR.-ING. MATTHIAS PHILIPP, PA\*, Bielefeld  
DR. MARTIN WITZ, RA, Düsseldorf  
DR. DETMAR SCHÄFER, RA, Bremen  
DR. JAN BERND NORDEMANN, LL. M., RA, Berlin

PROF. DR. WILHELM NORDEMANN, RA, BRP<sup>1</sup>  
DIPL.-PHYS. EDUARD BAUMANN, PA\*, Höhenkirchen  
DR.-ING. GERALD KLOPSCH, PA\*, Düsseldorf  
DIPL.-ING. HANS W. GROENING, PA\*, München  
DIPL.-ING. SIEGFRIED SCHIRMER, PA\*, Bielefeld  
DIPL.-PHYS. LORENZ HANEWINCKEL, PA\*, Paderborn  
DIPL.-ING. DR. JAN TÖNNIES, PA, RA, Kiel  
DIPL.-PHYS. DR.-ING. UWE MANASSE, PA\*, Bremen  
DR. CHRISTIAN CZYCHOWSKI, RA, Berlin  
DR. CARINA HÜTHNER, RA, Bremen, RA, München  
DIPL.-PHYS. DR. THOMAS A. BITTNER, PA\*, Berlin  
DR. VOLKER SCHMITZ, RA, München  
DIPL.-PHYS. CHRISTIAN W. APPELT, PA\*, München  
DR. ANKE NORDEMANN-SCHIFFEL, PA\*, Potsdam  
KERSTIN MAUCH, LL. M., RA, Potsdam  
DIPL.-Biol. DR. JAN B. KRAUSS, PA, München  
JÜRGEN ALBRECHT, RA, München  
ANKE SIEBOLD, RA, Bremen  
DR. KLAUS TIB. BROCKER, RA, Berlin  
DR. ANDREAS DUSTMANN, LL. M., RA, Potsdam  
DIPL.-ING. NILS T. F. SCHIMID, PA\*, München

In Zusammenarbeit mit/in cooperation with  
DIPL.-CHEM. DR. HANS ULRICH MAY, PA\*, München

Ihr Zeichen  
Your ref.  
Neuanmeldung

Ihr Schreiben  
Your letter of

Unser Zeichen  
Our ref.  
E 5124

Kiel,  
3. 9. 01

Prof. Dr. Anton Eisenhauer  
Granitzer Weg 11, 24226 Heikendorf

Stefan Purkl  
Holtenauer Str. 59, 24105 Kiel

### Vorrichtung zur Extraktion von Stoffen von einer Membran

Die Erfindung betrifft eine Vorrichtung zur Extraktion  
von Stoffen von einer Membran.

1967

Niemannsweg 133 • D-24105 Kiel • Telephon +49-431-84075 • Telefax +49-431-84077

MÜNCHEN - BREMEN - BERLIN - DÜSSELDORF - FRANKFURT- BIELEFELD - POTSDAM - BRANDENBURG - KIEL - PADERBORN - HÖHENKIRCHEN - ALICANTE  
<http://www.boehmert.de> e-mail: postmaster@boehmert.de

## BOEHMERT &amp; BOEHMERT

- 2 -

In der Umweltanalytik muß der Analyt oft aus wässrigen Lösungen und daher großen Probevolumina angereichert werden, um die geforderten Nachweisgrenzen zu erreichen. Ionenselektive Membrane werden dazu bisher in handelsübliche Filtrationseinheiten eingebaut und der Analyt dann mit hoher Extraktionsrate extrahiert.

Üblicherweise muß der Analyt für weitere Analyseschritte von der Membran eluiert werden. Bei der Durchführung der Festphasenextraktion in den für große Probevolumina ausgelegten Filtrationseinheiten treten aber Schwierigkeiten bei der Einstellung der Elutionsbedingungen auf. Der pH-Wert und die Konzentration des Elutionsmittels sowie die Durchflußgeschwindigkeit können in den Filtrationseinheiten nicht exakt eingestellt und kontrolliert werden. Notwendig ist daher der Transfer in einen anderen Filterhalter. Das Ablösen der Membran von der Filterfritte und der Transfer in einen geeigneten Filterhalter mit kleinen Totvolumen gestaltet sich zeitaufwendig, die Gefahr einer Zerstörung der sensiblen Membran ist groß. Die erneute Einbettung der Membran auf eine andere Filterfritte führt oft zu Lufteinschlüssen zwischen Membran und Fritte. Eine vollständige Elution des Analyten ist dann nicht gewährleistet, die Ausbeute des Verfahrens sinkt.

Der Erfindung liegt die Aufgabe zugrunde, eine Vorrichtung zu schaffen, die es ermöglicht, die Elution der Membran unter exakt definierten Bedingungen durchzuführen, ohne daß die Membran abgelöst werden muß.

Erfindungsgemäß wird diese Aufgabe gelöst durch eine Bodenplatte, einen auf der Bodenplatte ruhenden Mantelabschnitt, der mit einem Anschluß für eine Verbindung mit einer Unterdruckquelle versehen ist, eine den Mantelab-

## BOEHMERT &amp; BOEHMERT

- 3 -

schnitt abdeckenden Deckplatte, die mit einer zentral angeordneten Bohrung und einem auf dem Mantelabschnitt aufliegenden Flansch versehen ist, eine Grundplatte, die auf ihrer nach unten weisenden Fläche ein mit einer zentralen Bohrung versehenes Kupplungsstück, das in die Bohrung in dem Deckel einsetzbar ist, aufweist, auf seiner nach oben weisenden Seite mit einer kreisrunden Ausnehmung und an seiner Peripherie mit Klemmbügeln versehen ist, eine mit einer in diese eingepaßte Filterfritte versehene PTFE-Lochscheibe, deren Außendurchmesser dem Innendurchmesser der Ausnehmung in der Grundplatte entspricht und der mit einem Flansch versehen ist, der auf der Grundplatte aufliegt, einen Ring, der auf der Lochscheibe aufliegt und mit einer umlaufenden Schürze versehen ist, die die Lochscheibe umgreift, eine auf den Ring aufgesetzte Abdeckplatte, die eine zentrale, mit einer Bohrung versehenen Nippel und eine seitlichen Gewindebohrung, in die eine Entlüftungsschraube eingesetzt ist, aufweist, auf die Klemmbügel aufgesetzte Klemmblöcke, die auf den Ring verschwenkbar und von Muttern beaufschlagt gegen diesen preßbar sind, wobei die Teile mit einer Mehrzahl von O-Ringen versehen sind, die zusammenwirkenden Teile dichtend gegeneinander abschließen.

Die Unteransprüche geben vorteilhafte Ausgestaltungen der Erfindung an.

Bei der Vorrichtung nach der Erfindung ist ein schneller und einfacher Transfer der Membran in Verbund mit Filterfritte und PTFE-Lochscheibe in die Grundplatte möglich, ein Ablösen der Membran ist vermeidbar.

## BOEHMERT &amp; BOEHMERT

- 4 -

Das Dichtungssystem der Grundplatte gewährleistet die Einstellung einer exakt definierten Elutionsvolumens und reproduzierbare Extraktionsverhältnisse. Die Absaugvorrichtung erlaubt eine die Einstellung hoher Durchflußraten.

Die Teile, die mit aggressiven Lösungen in Kontakt kommen können, sind aus Teflon hergestellt. Die Dichtungen bestehen aus einem chemikalienbeständigen Silikon unterschiedlicher Härte. Erforderliche Metallteile sind aus Titan gefertigt.

gepaßte ... als einen Filterzylinder.  
Lueranschlüsse an Ein- und Ausgang der Vorrichtung gewährleisten eine Systemkompatibilität. Sie erlauben das Aufstecken von Einmalspritzen, die als Reservoir für das Elutionsmittel dienen. Für andere Anwendungen in der Filtrationstechnik können über die Anschlüsse Schlauchsysteme leicht befestigt werden.

Weitere Merkmale der Erfindung ergeben sich aus der beiliegenden Zeichnung. Dabei zeigt

Fig. 1 die einzelnen Elemente der Vorrichtung und

Fig. 2 die montierte Vorrichtung.

Die Vorrichtung besteht aus einer Bodenplatte 10, einem Mantelabschnitt 12, einer diese abdeckenden Deckplatte 16, einer Grundplatte 20, einer Lochscheibe 32, einem Ring 36 und einer Abdeckplatte 40.

Der Mantelabschnitt 12 ist zylindrisch ausgebildet und weist eine seinen Boden bildenden Bodenplatte 10 auf. Der Mantelabschnitt 12 ist mit einem Anschluß 14 zum

## BOEHMERT &amp; BOEHMERT

- 5 -

Anschluß an eine Unterdruckquelle versehen. Die Deckplatte 16, die mit einer zentral angeordneten Bohrung 18 versehen ist, liegt mit einem Flansch 17 auf dem oberen Rand des Aufnahmehbehälters auf. Die Grundplatte 20 ist auf ihrer nach unten weisenden Fläche mit einem mit einer zentralen Bohrung 22 versehenen Kupplungsstück 24 ausgebildet, das in die Bohrung 18 in der Deckplatte 16 einsetzbar ist. Auf seiner nach oben weisenden Seite ist die Grundplatte 20 mit einer kreisrunden Ausnehmung 26 und an seiner Peripherie mit Klemmbügeln 28 versehen. Eine bei Verwendung mit einer in die Ausnehmung 26 eingepaßte, mit einer Filterfritte 34 versehene PTFE-Lochscheibe 32 ist mit einer ersten Schürze 35 versehen, die auf der Grundplatte 20 aufliegt. Der Ring 36, der auf der Lochscheibe 32 aufliegt, ist mit einer umlaufenden zweiten Schürze 38 versehen, die die Lochscheibe 32 umgreift. Die auf den Ring 36 aufgesetzte Abdeckplatte 40 ist mit einer zentralen Gewindebohrung 42 versehen, in die ein mit einer zentralen Bohrung versehener Nippel eingesetzt werden kann. In eine seitlichen Gewindebohrung 36 ist eine Entlüftungsschraube eingesetzt.

Auf die Klemmbügel 28 sind Klemmblöcke 44 aufgesetzt, die auf den Ring 36 verschwenkbar und von Muttern beaufschlagt gegen diesen preßbar sind.

Die genannten Teile mit einer Mehrzahl von Nuten versehen, in die O-Ringe einpaßt sind, die zusammenwirkenden Teile dichtend gegeneinander abschließen.

## BOEHMERT &amp; BOEHMERT

- 1 -

E 5124

ANSPRÜCHE

1. Vorrichtung zur Extraktion von Stoffen von einer Membran, gekennzeichnet durch

eine Bodenplatte (10),

einen auf der Bodenplatte (10) ruhenden Mantelabschnitt (12), der mit einem Anschluß (14) zur Verbindung mit einer Unterdruckquelle versehen ist,

eine den Mantelabschnitt (10) abdeckende Deckplatte (16), die mit einer zentral angeordneten Bohrung (18) und einem auf dem Mantelabschnitt (10) aufliegenden Flansch (17) versehen ist,

eine Grundplatte (20), die auf ihrer nach unten weisenden Fläche ein mit einer zentralen Bohrung (22) versehenes Kupplungsstück (24), das in der Bohrung (18) in der Deckplatte (16) einsetzt, aufweist, auf seiner nach oben weisenden Seite mit einer leicht konischen, kreisrunden Ausnehmung (26) und an seiner Peripherie mit Klemmbügeln (28) versehen ist,

eine mit einer in diese eingepaßten Filterfritte (28) versehene PTFE-Lochscheibe (32), die mit einer ersten umlaufenden Schürze (34) versehen ist, die auf der Grundplatte (20) aufliegt,

BOEHMERT & BOEHMERT

- 2 -

einen Ring (36), der auf der Lochscheibe (32) aufliegt und mit einer zweiten umlaufenden Schürze (38) versehen ist, die die Lochscheibe (32) umgreift,

eine Abdeckplatte (40), die auf den Ring (36) aufgesetzt ist und die einen zentralen, mit einer Bohrung (42) und einer seitlichen Gewindebohrung (46), in die eine Entlüftungsschraube eingesetzt ist, aufweist, und

auf die Klemmbügel (28) aufgesetzte Klemmblöcke (44), die auf den Ring (36) verschwenkbar und von Muttern beaufschlagt gegen diesen preßbar sind, wobei

die Teile mit einer Mehrzahl von O-Ringen versehen sind, die zusammenwirkenden Teile dichtend gegeneinander abschließen.

2. Vorrichtung nach Anspruch 1, dadurch gekennzeichnet, daß das Kupplungsstück (24) mit einem Luer-Anschluß versehen ist.

3. Vorrichtung nach Anspruch 1 oder 2, dadurch gekennzeichnet, daß die Bohrung (42) mit einem Luer-Anschluß versehen ist.

4. Vorrichtung nach einem der Ansprüche 1 bis 3, dadurch gekennzeichnet, daß die Abdeckplatte (40) mit einer zentralen Vertiefung (44) versehen ist, die in den Ring (36) eingreift.

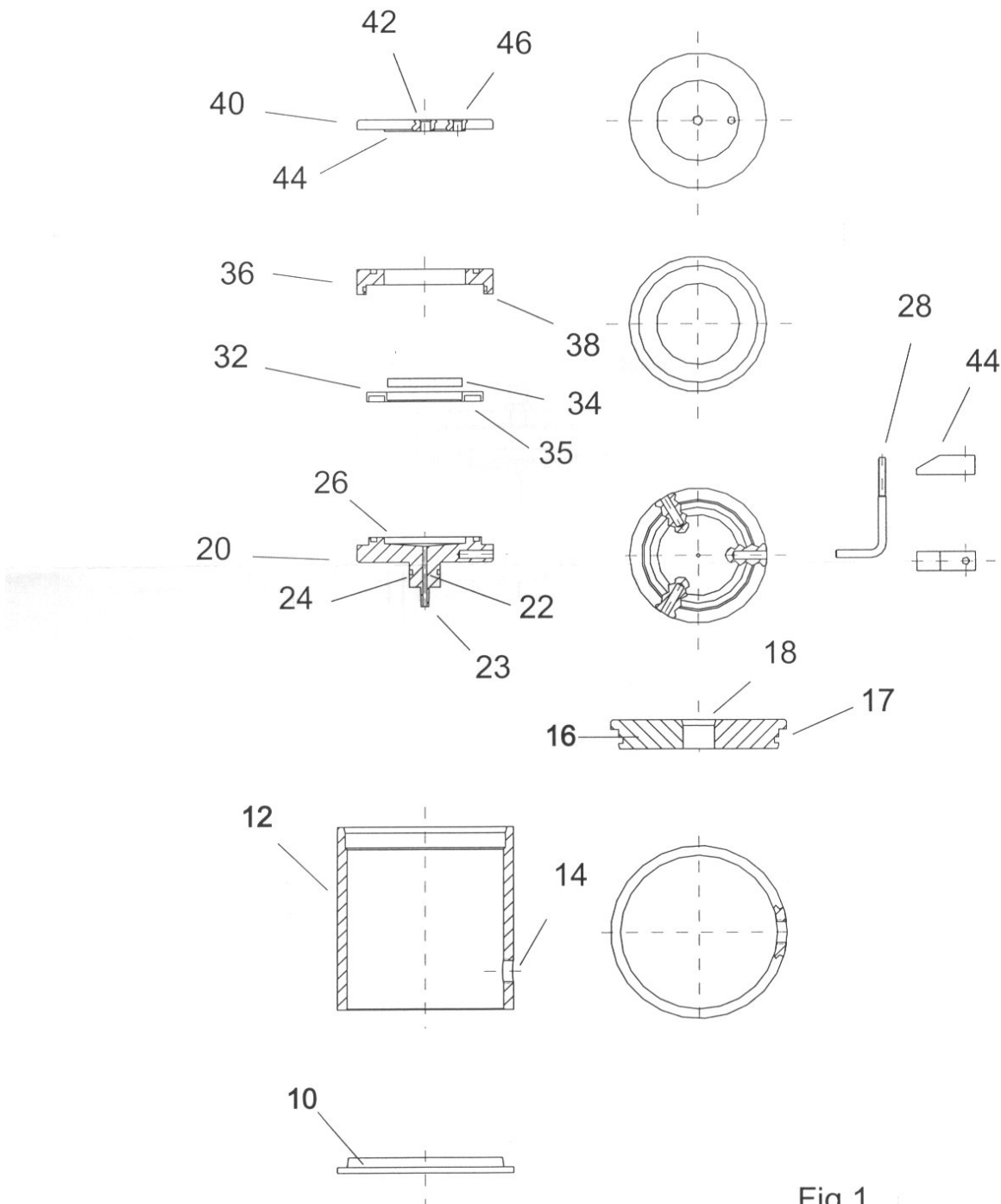


Fig.1

## Zusammenfassung

Diese Arbeit stellt durch die Entwicklung und Anwendung neuer analytischer Methoden zur schnellen Bestimmung von kurzlebigen Radiumisotopen und Radon im grundwasserbeeinflussten Milieu der Ostsee einen Beitrag zur Untersuchung von küstennahen Mischungsprozessen dar.

Die Kombination der ionenselektiven Membrantechnik mit der Sensitivität der  $\alpha$ -Spektrometrie stellt die geforderte einfache Messbarkeit für alle Radiumisotope sicher. Durch die Verwendung von Empore<sup>TM</sup> Radium Rad Disks kann der Analyt sehr effizient angereichert werden. Die durchgeführten  $\alpha$ - und  $\gamma$ -spektrometrischen Untersuchungen zeigen, dass neben anderen störenden Matrixkomponenten auch Thorium nicht auf der Membrane festgehalten wird. Bei der Extraktion von  $^{229}\text{Th}/^{225}\text{Ra}$ -Lösungen werden Separationsfaktoren von etwa 200 erreicht. Damit ergibt sich die einfache Verwendung von  $^{225}\text{Ra}$  als interner Standard zur Radiumbestimmung.

Das neue Verfahren konnte so optimiert werden, dass eine Bestimmung der  $\alpha$ -strahlenden Radiumisotope  $^{223}\text{Ra}$ ,  $^{224}\text{Ra}$  und  $^{226}\text{Ra}$  innerhalb von 5 Stunden Aufarbeitungszeit möglich ist. Die erzielten Ausbeuten betragen mit diesem Verfahren bis zu  $92\pm 9\%$ . Durch die Reduktion zeitaufwendiger Analyseschritte können 8 bis 10 Proben gleichzeitig aufgearbeitet werden. Die Anzahl der vorhandenen  $\alpha$ -Messplätze limitiert den Probendurchsatz, der innerhalb von etwa 5 Tagen (mittlere Lebensdauer von  $^{224}\text{Ra}$ ) zu erreichen ist.

Zusammen mit der Bestimmung von Radon über Flüssigszintillationsmesstechnik konnten die neuen Verfahren erfolgreich für die Analyse von küstennahen Mischungsprozessen eingesetzt werden. Der Einfluss submariner Grundwasseraustritte auf das Verhalten und den Transport von kurzlebigen Radiumisotopen und Radon im küstennahen Bereich wurde am Beispiel der Eckernförder Bucht studiert. Bedingt durch die geringe Mobilität von Radium im betrachteten Grundwasserleiter ist die Hauptquelle für die kurzlebigen Isotope die Freisetzung aus den Sedimenten. Die gewonnenen Felddaten erlauben die Beschreibung der Tracerverteilung von  $^{223}\text{Ra}$ ,  $^{224}\text{Ra}$  und  $^{222}\text{Rn}$  in der Wassersäule über diffusive Modellansätze. In Übereinstimmung mit hydrogeologischen Untersuchungen im Einzugsgebiet der Eckernförder Bucht konnten weiterhin submarine Ausstromraten von  $1,7\pm 0,3 \text{ m}^3\text{s}^{-1}$  quantifiziert werden.

# Anhang

## 1.1. Alpha-Spektrometrie

### 1.1.1. Messprinzip

Das Messprinzip der energieaufgelösten  $\alpha$ -Spektrometrie beruht auf dem Vermögen von  $\alpha$ -Strahlung, in einem Halbleiterdetektor längs des Weges Elektronen-Defektelektronen-Paare zu erzeugen. Durch Anlegen eines äußeren elektrischen Feldes kann so am Arbeitswiderstand des Detektors ein Spannungsimpuls abgegriffen werden. Der Betrag dieses Spannungsimpulses ist von der Menge der erzeugten Ladungsträger und damit von der Energie, der auf die Detektorschicht treffenden Strahlung, abhängig. Wird zudem die Anzahl der Messsignale pro Zeit registriert, kann man eine Nuklidart durch die charakteristische  $\alpha$ -Energie nicht nur identifizieren, sondern anhand der auftretenden Ereignisse auch quantifizieren.

Die Spannungsimpulse, die bei der Absorption von ionisierender Strahlung an einem Halbleiterdetektor abgegriffen werden können, sind sehr klein und werden daher über einen Vor- und einen Hauptverstärker verstärkt. Anschließend wird über einen Vielkanalanalysator jedem Signal entsprechend seiner Pulshöhe ein Kanal zugeordnet. Der Vielkanalanalysator erlaubt in diesem Fall die Aufnahme von  $\alpha$ -Spektren mit bis zu 2048 Kanälen. Eingelesen in einen Personalcomputer können diese Spektren dann abgespeichert und mit dem Programm Origin 5.0 ausgewertet werden (Abb. 1).

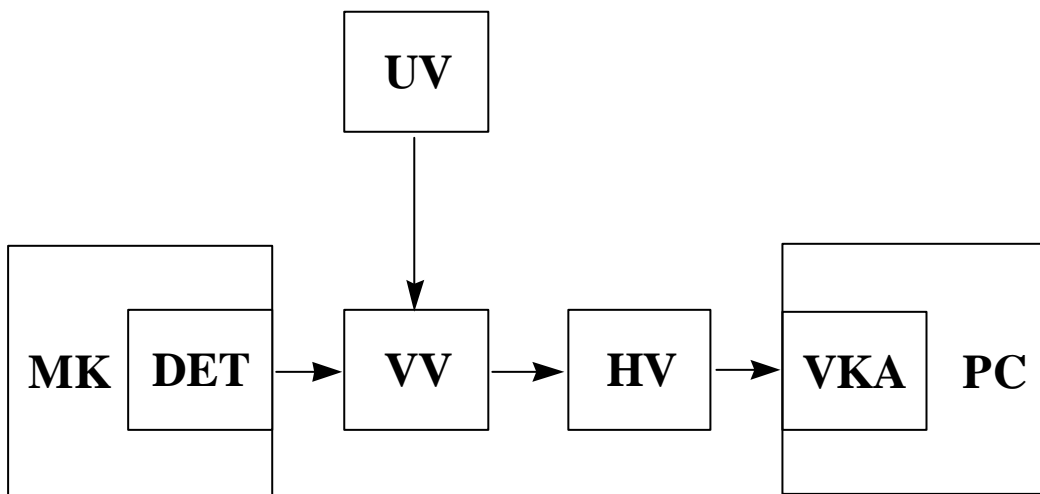


Abb. 1: Blockschaltbild des Messplatzes.

**MK:** Messkammer,    **DET:** Detektor,    **VV:** Vorverstärker,    **UV:** Spannungsversorgung,  
**HV:** Hauptverstärker, **VKA:** Vielkanalanalysator, **PC:** Personalcomputer

### 1.1.2. Energiekalibrierung

Damit die in Kanallagen ausgegebenen  $\alpha$ -Zerfallsenergien einer unbekannten Probe den katalogisierten Radionukliden zugeordnet werden können, muss zunächst eine Energiekalibrierung durchgeführt werden. Dies geschieht über einen Flächenstandard der Firma Amersham-Buchler GmbH & Co. KG, der die drei  $\alpha$ -aktiven Nuklide  $^{239}\text{Pu}$ ,  $^{241}\text{Am}$  und  $^{244}\text{Cm}$  mit bekannten Zerfallsenergien enthält (Abb. 2).

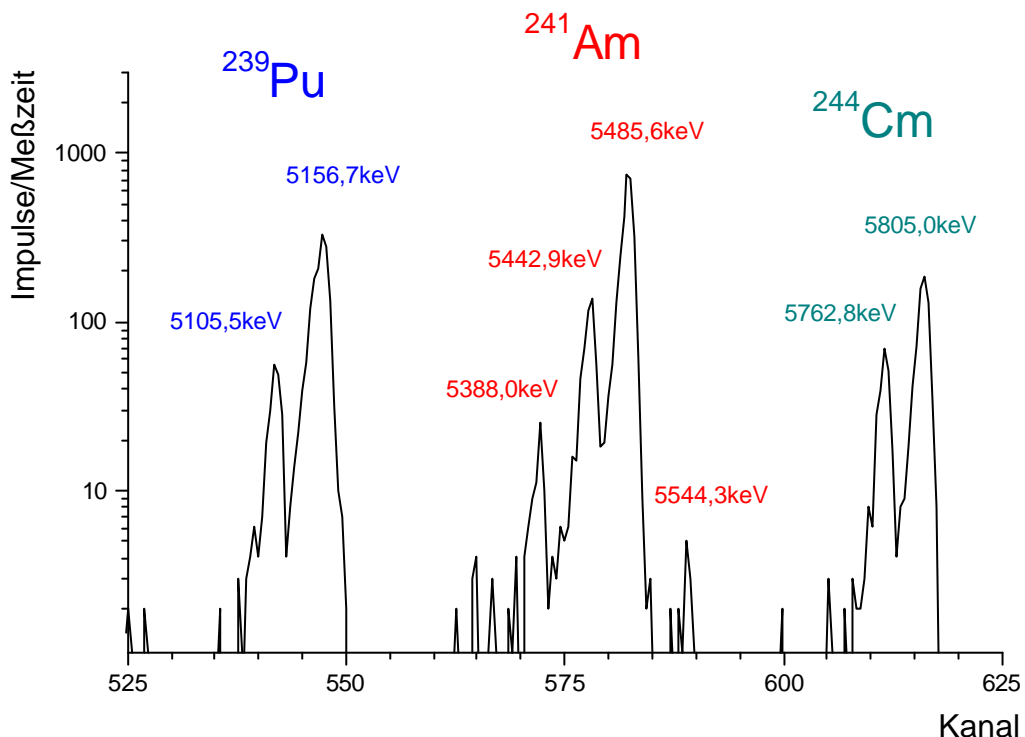


Abb.2: Spektrum eines Standardpräparates; katalogisierte Zerfallsenergien stammen aus [1].

Trägt man nun die Kanallage gegen die zugehörige Zerfallsenergie auf, so wird der lineare Zusammenhang deutlich (Abb. 3).

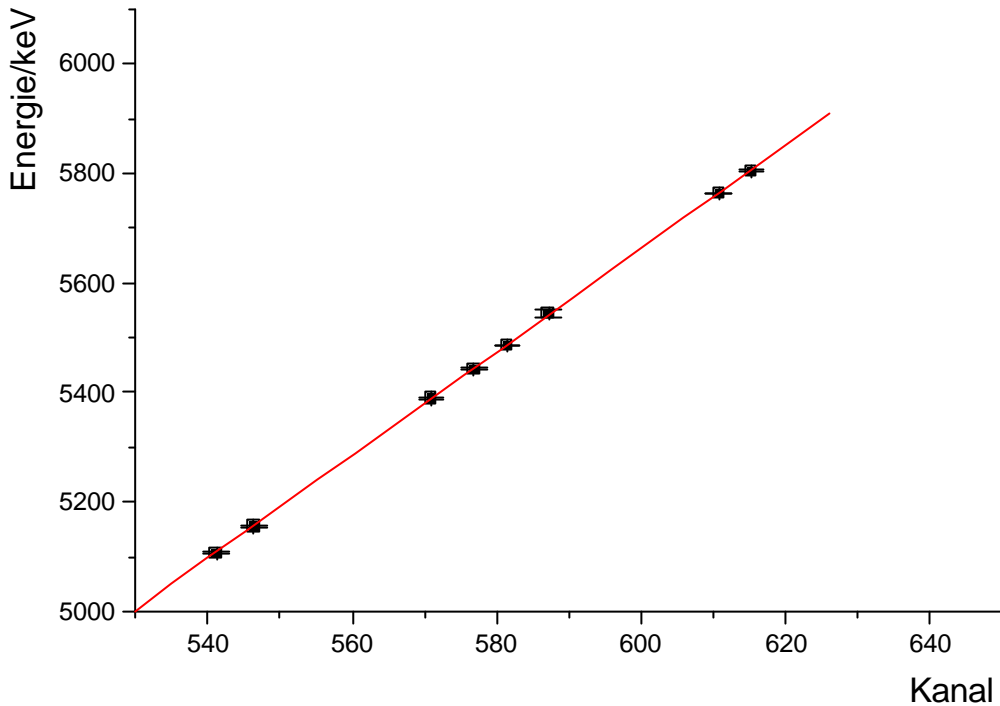


Abb.3: Energiekalibrierung mittels Standardpräparat.

Die ermittelte Geradengleichung erlaubt eine einfache Umrechnung von einer Kanallage in die entsprechende kinetische Energie der registrierten  $\alpha$ -Teilchen.

Es ergibt sich:

$$E = 9,441 \text{ keV} \times K - 4,0 \text{ keV}$$

mit

$E$  = Energie/keV;  $K$  = Kanallage

Damit sind nun qualitative Analysen von unbekannten Proben möglich.

### 1.1.3. Probenpräparation

Die  $\alpha$ -Spektrometrie ist ein sehr sensitives analytisches Werkzeug und damit hervorragend zur Spurenanalyse geeignet, doch stellt sie hohe Anforderungen an die Probenpräparation. Emittierte Heliumkerne wechselwirken aufgrund ihrer hohen Ladung besonders stark mit Materie und verlieren dabei sehr schnell ihre kinetische Energie. Absorption der  $\alpha$ -Strahlung in der Probenmatrix führt dazu, dass Messsignale eines Radionuklides auch bei wesentlich niedrigeren Energien registriert werden. Dieses „low-energy tailing“ kann bei dicken Proben die qualitative/quantitative Auswertung des aufgenommenen Spektrums erschweren, bzw. unmöglich machen. Besondere Maßnahmen sind daher nötig, um dünne Präparate und somit eine ausreichende Energieauflösung zu erreichen. Dies sind z.B.:

- Anreicherung des Analyten
- Abtrennung der inaktiven Probenmatrix
- Abtrennung störender Radionuklide
- Herstellung eines Messpräparates mit homogener Analytverteilung

### 1.1.4. Herstellung des Messpräparats

Es existieren verschiedene Möglichkeiten, Proben mit möglichst dünner und homogener Analytverteilung herzustellen. Ein Maß für die Güte des hergestellten Präparates ist die Breite des Energieintervalls, betrachtet zwischen den beiden Halbwerten der maximalen Zählereignishöhe. Die Energieauflösung wird üblicherweise als FWHM (Full-Width-at-Half-Maximum)-Wert in keV angegeben.

Eine gute Zusammenstellung der angewendeten Techniken zur Herstellung von Messpräparaten findet sich in [2]. Die dargestellten Methoden Vakuumsublimation, Evaporation und Elektrodeposition haben gemeinsam, dass der praktisch gewichtslose Analyt auf ein Substrat mit einer perfekt glatten Oberfläche [3] (meist Platin, Tantal oder polierter Edelstahl) gebracht wird. Für die Analyse von Umweltproben ist die Probenpräparation mittels Elektrodeposition jedoch besonders vorteilhaft, da hier gute Energieauflösungen bei gleichzeitig minimalen Aufarbeitungsverlusten erzielt werden. Durch Anlegen einer Spannung wird in einer meist wässrigen Elektrolytlösung ein pH-Gradient erzeugt. Die Radionuklide scheiden sich dann als Hydroxide auf der Kathode, in der Regel polierter Edelstahl, ab. Es ist zu beachten, dass die Deposition kein Reinigungsschritt ist. Verunreinigungen der Elektrolytlösung mit aktiven und inaktiven Metallionen führen ebenfalls zu deren Abscheidung und damit zu einer erschwerten Auswertung.

### 1.1.5. Interner Standard

Bei der gewählten  $2\pi$  Messgeometrie treffen nie 50% der  $\alpha$ -Partikel die sensitive Oberfläche des Detektors [4]. Die Zählausbeute hängt von der Größe des verwendeten Detektors, der Verteilung des Analyten auf dem Träger, dem gewählten Abstand aber auch von den stattfindenden Rückstoß- und Absorptionsprozessen in der Probe ab. Absolutbestimmungen von Aktivitäten sind daher nur schwer möglich, zumal bei Umweltanalysen durch die notwendige chemische Aufarbeitung immer mit Aktivitätsverlusten zu rechnen ist. Einen Ausweg bietet das Benutzen eines internen Standards (engl. Spike oder Tracer genannt). Als Spike werden manchmal chemisch verwandte Elemente, meist jedoch Radioisotope verwendet, die unter den gegebenen Bedingungen gleiches chemisches Verhalten aufweisen wie der zu bestimmende Analyt. Der interne Standard wird der Probe vor Beginn der Analyse hinzugefügt. Ist die Aktivität des Standards zu diesem Zeitpunkt bekannt, spielen Verluste während der chemischen Aufbereitung und die Abhängigkeit der Zählausbeute von der Geometrie der Messanordnung keine Rolle. Bei der Spektrenauswertung kann durch Vergleich der Peakflächen von eingesetztem, internem Standard zum Analyt dessen absolute Aktivität bestimmt werden.

### 1.1.6. Nulleffekt

Im Gegensatz zu  $\gamma$ -Strahlung ist  $\alpha$ -Strahlung nicht in der Lage, die Wände der Messkammer zu durchdringen. Die trotzdem auftretenden Nulleffektzählraten stammen im wesentlichen von der Kontamination des Detektors und des Kammerinneren aus vorangegangene Messungen. Bei der Probenpräparation ist daher darauf zu achten, dass das Präparat mechanisch stabil ist und keine flüssigen Bestandteile enthält, die beim Anlegen des Vakuums explosionsartig sieden und zum Verspritzen des aktiven Materials führen. Die Proben sollten außerdem in nicht zu geringem Abstand vom Detektor gemessen werden. Zwar ist für kurze Abstände die Zählausbeute höher, doch steigt damit auch die Gefahr einer Detektorkontamination durch Cluster, die beim  $\alpha$ -Zerfall infolge von Rückstoßprozessen aus der Probe herausgeschleudert werden. Eine effektive Dekontamination ist oft nicht möglich, da sowohl saure als auch alkalische Bedingungen zur Zerstörung der empfindlichen Detektoroberfläche führen. Für Messpräparate mit Aktivitäten zwischen 10 mBq und 1 Bq wird ein Abstand von 1,6 cm gewählt. Präparate mit höheren Aktivitäten sollten in größerem Abstand gemessen werden. Die Nulleffektzählrate beeinflusst die Messgenauigkeit. Hohe Zählraten lassen die Nachweisgrenzen ansteigen. Eine über einen langen Zeitraum bestimmte Nulleffektzählrate vergrößert die Sicherheit, registrierte Zählereignisse dem Untergrund zuzuordnen, die Nachweisgrenzen sinken dadurch. Üblicherweise werden Untergrundspektren mit Messzeiten von 3–10 Tagen aufgenommen. Bei der Analyse einer  $\alpha$ -Probe werden die auf die Meßzeit normierten Ereignisse des Nulleffekts von den durch Probe und Untergrund verursachten Impulsen subtrahiert.

### 1.1.7. Erkennungs- und Nachweisgrenzen

Die Berechnung von Nachweis- und Erkennungsgrenzen wird durchgeführt, um die Leistungsfähigkeit des verwendeten Analyseverfahrens zu kennen. Wenn in Messpräparaten z.B. kein Analyt nachgewiesen werden konnte, gelingt mit diesen Grenzwerten eine Abschätzung der maximalen Analytkonzentration in der Probe. Erkennungs- und Nachweisgrenzen für die  $\alpha$ -spektrometrischen Messungen wurden gemäß Literatur [5] berechnet; sie sind auf die DIN-Norm 25482 Teil 1 [6] zurückzuführen. Die folgenden Gleichungen, die auf der Annahme einer Poisson- bzw. Normalverteilung der gemessenen Ereignisse beruhen, stellen für die Praxis brauchbare Näherungen für die Berechnung dar.

#### Erkennungsgrenze

Die Erkennungsgrenze wird berechnet, um feststellen zu können, ob eine gemessene Zählrate neben Untergrundereignissen auch Ereignisse aus der Probe enthält. Die Aussage des Vorliegens eines Probenbeitrags ist bei Anwendung von Gleichung (1) mit der Wahrscheinlichkeit  $a$  falsch. Deswegen muss  $a$  für eine konservative Abschätzung möglichst klein sein.

$$G^* = \varphi_A Z_n^* = \frac{Z_n^*}{\varepsilon I_\alpha} = \frac{k_{1-a}^2}{\varepsilon I_\alpha 2t_0} \left\{ 1 + \sqrt{1 + \frac{4Z_0 t_0}{k_{1-a}^2} \left( 1 + \frac{t_0}{t_m} \right)} \right\} \quad (1)$$

$G^*$  = Erkennungsgrenze (Bq)

$\varphi_A$  = Kalibrierfaktor

$Z_n^*$  = Nettozählrate für die Berechnung der Erkennungsgrenze ( $I s^{-1}$ )

$\varepsilon$  = geometrische Effizienz des verwendeten Messsystems

$I_\alpha$  = Intensität des betrachteten  $\alpha$ -Übergangs

$k_{1-a}$  = Quantil der Normalverteilung; für  $a=1\%$  beträgt der Wert für  $k_{1-a}=2,326$

$Z_0$  = Nulleffektzählrate ( $I s^{-1}$ )

$t_0$  = Messdauer der Nulleffektmessung (s)

$t_m$  = Messdauer der Probe (s)

Für die  $\alpha$ -spektrometrische  $^{226}\text{Ra}$ -Bestimmung mit dem in dieser Arbeit verwendeten Messsystem mussten üblicherweise die folgenden Werte in die Gleichung eingesetzt werden:

$$Z_0 = 13 \cdot 10^{-6} I s^{-1}, \varepsilon = 32\%, I_\alpha = 100\%, t_0 = 1000000, t_m = 250000 \text{ s}, k_{1-a} = 2,326$$

Die angegebene Nulleffektzählrate bezieht sich auf den gesamten Energiebereich, in dem  $\alpha$ -Teilchen des  $^{226}\text{Ra}$  registriert werden können. Durch das Einsetzen der Werte in die Gleichung wird für  $^{226}\text{Ra}$  eine allein auf das Messsystem bezogene Erkennungsgrenze von 0,07 mBq

berechnet. Diese Erkennungsgrenze sinkt sowohl bei einer längeren Messdauer vom Probe- als auch vom Nulleffektspektrum. Im wesentlichen trägt jedoch die Höhe der Nulleffektzählrate zur Höhe der Erkennungsgrenze bei.

### Nachweisgrenze

Ist die Nettozählrate größer als die nach Gleichung (2) berechnete Nachweisgrenze, dann ist die Aussage, dass diese Zählrate von der Probe stammt, mit der Wahrscheinlichkeit  $b$  falsch.

Die Nachweisgrenze gibt daher die geringste Aktivität an, die theoretisch mit dem verwendeten Messsystem in dem Messpräparat gemessen werden kann.

$$G^* = \varphi_A \hat{Z}_n^* = \frac{\hat{Z}_n^*}{\varepsilon I_\alpha} = \varphi_A \left\{ \left( k_{1-a} + k_{1-b} \right) \sqrt{\hat{Z}_0 \left( \frac{1}{t_0} + \frac{1}{t_m} \right)} + \frac{1}{4} (k_{1-a} + k_{1-b})^2 \left( \frac{1}{t_0} + \frac{1}{t_m} \right) \right\} \quad (2)$$

$G$	=Nachweisgrenze (Bq)
$\varphi_A$	=Kalibrierfaktor
$\hat{Z}_n^*$	=Nettozählrate für die Berechnung der Nachweisgrenze ( $I s^{-1}$ )
$\varepsilon$	=geometrische Effizienz des verwendeten Messsystems
$I_\alpha$	=Intensität des betrachteten $\alpha$ -Übergangs
$k_{1-a}$	=Quantil der Normalverteilung; für $a=1\%$ beträgt der Wert für $k_{1-a}=2,326$
$k_{1-b}$	=Quantil der Normalverteilung; für $b=1\%$ beträgt der Wert für $k_{1-b}=2,326$
$\hat{Z}_0$	=Erwartungswert der Nulleffektzählrate ( $I s^{-1}$ ); kann durch $Z_0$ substituiert werden
$t_0$	=Messdauer der Nulleffektmessung (s)
$t_m$	=Messdauer der Probe (s)

Erfolgt die Berechnung der Nachweisgrenze entsprechend Gleichung (2) mit den bereits für die Berechnung der Erkennungsgrenze verwendeten Werten sowie  $k_{1-b}=2,326$ , beträgt sie 0,20 mBq. Damit ist sie ca. um den Faktor 3 höher als die Erkennungsgrenze. Dies lässt sich damit erklären, dass ein Signal für die Quantifizierung wesentlich größer sein muss als die Untergrundsignale. Die Erkennungsgrenze gibt an, ab welcher Zählrate Signale größer als die Untergrundsignale sind. Die Nachweisgrenze hingegen sagt, ab wann solche Signale quantifizierbar größer als der Untergrund sind.

Die hier genannten Erkennungsgrenzen berücksichtigen keine Verluste bei der chemischen Probenpräparation. Sie beziehen sich nur auf das verwendete Messsystem beim  $\alpha$ -spektrometrischen Nachweis von  $^{226}\text{Ra}$

## 1.2 Berechnung von Mittelwerten und Unsicherheiten

### 1.2.1. Zählstatistik

Für den radioaktiven Zerfall gelten die Gesetze der Statistik. Das Messen von Zerfallsereignissen ist also mit einer Unsicherheit behaftet, die um so kleiner ist, je größer die Anzahl der registrierten Zählimpulse ist. Üblicherweise führt man Messungen mehrfach aus und bestimmt so den Mittelwert als wahrscheinlichsten Meßwert. Ist die Anzahl der Messungen genügend groß, so unterscheiden sich, bei Zugrundelegen einer Normal- oder Poissonverteilung, der Mittelwert und der „wahre Wert“ praktisch nicht. Die zugehörige Standardabweichung  $\sigma$  liefert eine Aussage über die Streuung der Meßwerte um den „wahren Wert“.

Für  $\alpha$ -spektrometrische Messungen ist diese Vorgehensweise nicht praktikabel, da die Probenpräparation und anschließende Messung bereits mehrere Tage in Anspruch nimmt. Eine Mehrfachbestimmung ist daher aus Zeitgründen nicht möglich. Unter der Voraussetzung einer ausreichend großen Zahl an registrierten Ereignissen kann die statistische Unsicherheit eines Meßwertes aber mittels Gleichung (3) wie folgt abgeschätzt werden:

$$\sigma = \Delta E = \sqrt{E} \quad (3)$$

- $\sigma$  =Standardabweichung
- $\Delta E$  =Statistische Unsicherheit des Messwertes E
- E =Zahl der registrierten Ereignisse

### 1.2.2. Gauß'sche Fehlerfortpflanzung

Gehen unterschiedliche mit Unsicherheiten behaftete Messgrößen in die Berechnung ein, so wirken sich die Unsicherheiten unterschiedlich auf die zu bestimmende Größe aus.

Mit Hilfe des Gauß'schen Fehlerfortpflanzungsgesetzes können die Auswirkungen statistischer Unsicherheiten in den unabhängig voneinander bestimmten Messgrößen abgeschätzt werden. Es gilt :

$$\Delta G(\Delta g_i) = \sqrt{\sum_{i=1}^n \left[ \frac{\partial G}{\partial g_i} \Delta g_i \right]^2} \quad (4)$$

- $G$  =aus Messgrößen bestimmter Wert
- $\Delta G$  =Unsicherheit von G
- $g$  =Messgröße
- $\Delta g$  =Unsicherheit von g

Gibt man die Unsicherheiten der Messgrößen mit  $\Delta g = \sigma_g$  an, so befindet sich der „wahre Wert“ von G mit 68,3% Wahrscheinlichkeit im Intervall  $G \pm \Delta G$ . Ist eine höhere Wahrscheinlichkeit, mit der der wahre Wert von G innerhalb des angegebenen Fehlerintervalls liegt, gefordert, so gibt man die Unsicherheiten entsprechend mit  $\Delta g = 2\sigma_g$  oder  $3\sigma_g$  an. Die Wahrscheinlichkeit steigt dann auf 95,5% bzw. 99,7%.

In dieser Arbeit werden die für die Radiumbestimmung nötigen Messgrößen mit einer statistischen Unsicherheit  $1\sigma$  angegeben.

### 1.2.3. Gewichtete Mittelwertbildung

Soll aus einer Anzahl von Werten  $x_1, \dots, x_n$ , deren jeweilige Unsicherheit  $\Delta x_i$  beträgt, ein gewichteter Mittelwert gebildet werden, erfolgt dies gemäß [7] nach Gleichung (5) und Gleichung (6)

$$\bar{x} = W \sum_{i=1}^n \frac{x_i}{(\Delta x_i)^2}; \quad (5)$$

- $\bar{x}$  =gewichteter Mittelwert
- $W$  =Wichtungsfaktor (quadratische Wichtung)
- $n$  =Anzahl der Werte
- $x_i$  =i-ter Wert der Werte  $x_1, \dots, x_n$
- $\Delta x_i$  =Unsicherheit der Werte  $x_i$

$$W = \frac{1}{\sum_{i=1}^n \frac{1}{(\Delta x_i)^2}} \quad (6)$$

Bei der Gewichtung der Werte  $x_1$  bis  $x_n$  werden die Quadrate der Unsicherheiten der Werte so berücksichtigt, dass Werte mit großer Unsicherheit die Größe des Mittelwerts nur geringfügig beeinflussen. Bei der Berechnung des Mittelwerts muss darauf geachtet werden, dass die erhaltenen relativen Unsicherheiten der Größe G nicht kleiner werden darf als die relativ betrachtete größte systematische Unsicherheit einer für die Messung wichtigen Größe. Aus diesem Grund werden die systematischen Unsicherheiten erst nach der Mittelwertbildung berücksichtigt.

Die Herstellerfirma des Thoriumtracers gibt z.B.: die Aktivität der  $^{229}\text{Th}$ -Tracerlösung mit einer Unsicherheit von 0,33% an [8]. Nach dem Umfüllen der Lösung wurde die systematische Unsicherheit auf 1% abgeschätzt. Deshalb kann auch bei einer Mehrfachbestimmung einer Radiumaktivität mit diesem Standard die Unsicherheit der Bestimmung nicht kleiner als 1% werden.

Als Unsicherheit des Gewichteten Mittelwerts  $\bar{x}$  wird der größere der beiden nach Gleichung (7) und Gleichung (8) berechneten Werte  $\Delta\bar{x}_{\text{inn}}$  (innere Unsicherheit) oder  $\Delta\bar{x}_{\text{äuß}}$  (äußere Unsicherheit) angegeben. Für die Berechnung der inneren Unsicherheit gemäß Gleichung (7) werden die Unsicherheiten der einzelnen Werte herangezogen. Die Größe dieses Wertes ist daher ein Maß für die Genauigkeit der durchgeföhrtem Messung.

$$\Delta\bar{x}_{\text{inn}} = \sqrt{W} \quad (7)$$

$\Delta\bar{x}_{\text{inn}}$  innere Unsicherheit des Mittelwerts  $\bar{x}$

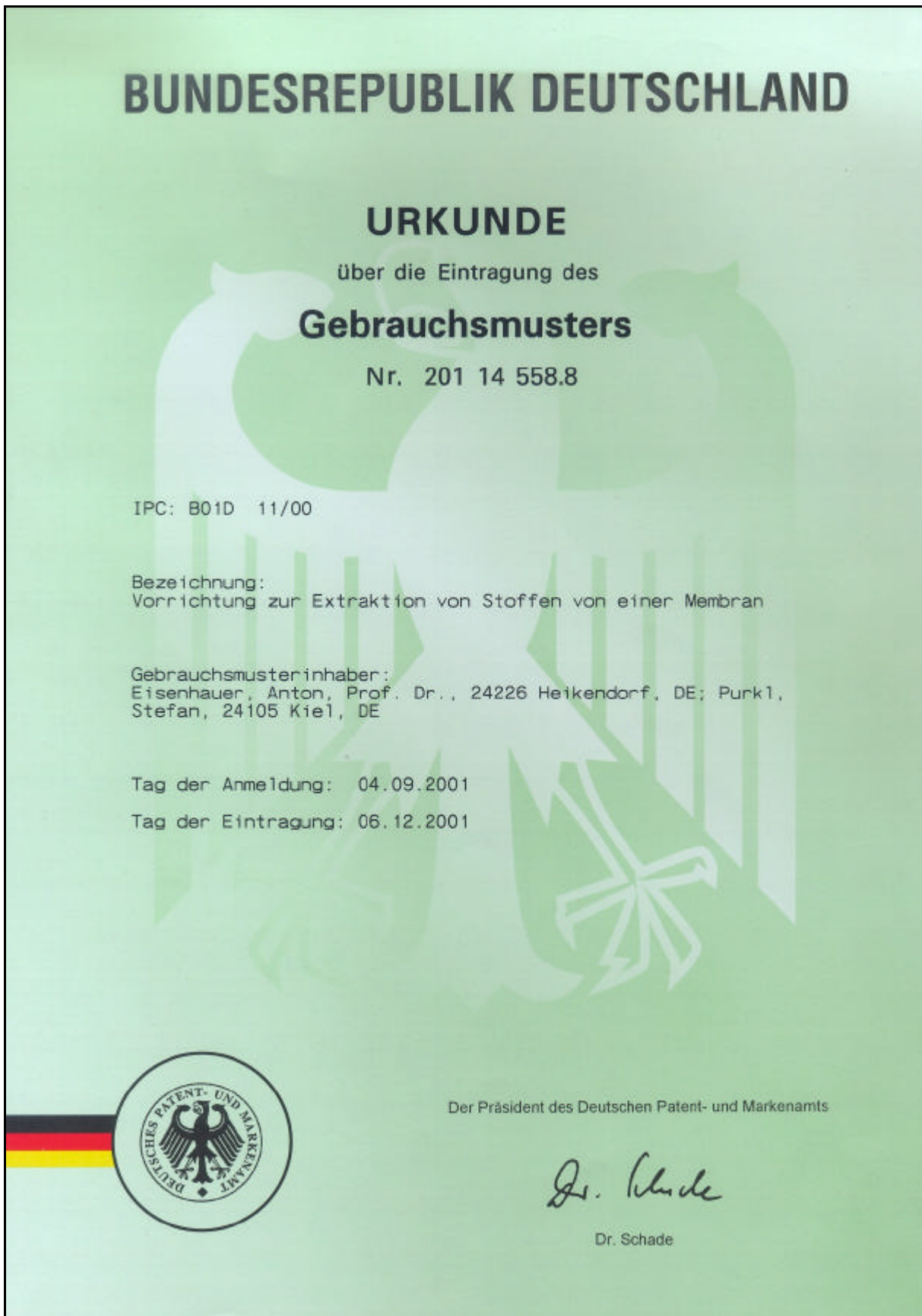
Die äußere Unsicherheit nach Gleichung (8) berücksichtigt die Abweichung der einzelnen Messwerte vom berechneten Mittelwert. Diese Größe gibt Hinweis darauf, wie groß die Streuung der verschiedenen Messwerte um den Mittelwert ist P ist in dieser Gleichung gleich 1, wenn für die Berechnung der äußeren Unsicherheit der nach Gleichung (5) berechnete Mittelwert eingesetzt wird.

$$\Delta\bar{x}_{\text{äuß}} = \sqrt{W \frac{\sum_{i=1}^n \frac{(x_i - \bar{x})^2}{(\Delta x_i)^2}}{n - P}} \quad (8)$$

$\Delta\bar{x}_{\text{äuß}}$  = äußere Unsicherheit des Mittelwerts  $\bar{x}$

P = Anzahl der freien Parameter

### 1.3 Urkunde über die Eintragung des Gebrauchsmusters



## Literatur

- [1] W. Westmeier, A. Merklin; Catalog of Alpha Particles from Radioactive Decay; Physik Daten/Physics Data; Nr. 29-1 (1985)
- [2] P. de Regge, R. Boden; Review of Chemical Separation Techniques applicable to Alpha Spectrometric Measurements; Nuclear Instruments and Methods in Physics Research; **223** (1984) 181-187.
- [3] A.E. Lally, K.M. Glover; Source Preparation in Alpha Spectrometry; Nuclear Instruments and Methods in Physics Research; **223** (1984) 259-265.
- [4] P. Blanco Rodriguez, A. Martín Sánchez, F. Vera Tome; Experimental Studies of Self-absorption and Backscattering in Alpha-particle Sources; International Journal of Applied Radiation and Isotopes; **48** (1997) 1215-1220.
- [5] Der Bundesminister für Umwelt, Naturschutz und Reaktorsicherheit; Messanleitung für die Überwachung der Radioaktivität in der Umwelt und zur Erfassung radioaktiver Emissionen aus kerntechnischen Anlagen; Gustav Fischer Verlag; Stuttgart (1994).
- [6] DIN-Norm 25482 Teil 1: Nachweisgrenze und Erkennungsgrenze bei Kernstrahlungsmessungen-Zählende Messungen ohne Berücksichtigung des Probenbehandlungseinflusses.
- [7] Nuclear Data Sheets, Academic Press, New York and London, „Die Vorschrift zur Berechnung gewichteter Mittelwerte ist in den Policies angegeben.“ (Anmerkung des Autors)
- [8] NIST, Standard-Referenz-Materialnummer: SRM No. 4328B, Referenz-Zeit: 01.07.96, 33,36 Bq  $^{229}\text{Th}$  g $^{-1}$  Lösung, Unsicherheit: 0,33% c(HNO<sub>3</sub>)=1,1 mol/l, Gaithersburg, USA

## **Lebenslauf**

Name: Stefan Purkl  
Anschrift: Holtenauer Str. 59  
24105 Kiel  
Geburtsdatum: 11.08.1973 in Bad Hersfeld  
Nationalität: deutsch

	Studium	Hochschulsemester
1993	Abitur, Jakob-Grimm-Schule	
21.09.1993	Immatrikulation Lehramt L3, Fächer: Physik/Chemie Philipps-Universität Marburg	
21.09.1995	Immatrikulation Geologie/Paläo. Philipps-Universität Marburg	
21.07.1998	Vordiplom Geologie, Gesamtnote „sehr gut“	10
21.06.1999	1. Staatsexamen, Gesamtnote: „mit Auszeichnung“ Exmatrikulation, Philipps-Universität Marburg	12
01.08.1999	Graduiertenkolleg „Dynamik Globaler Kreisläufe“ an der Christian-Albrechts-Universität zu Kiel	12
29.09.1999	Immatrikulation Geologie/Paläo., CAU Kiel	